Chemical Durability Assessment of Glasses for Immobilization of High Level Radioactive Waste

by

VIDYA S. THORAT

(CHEM01201204018 dated 1st September, 2012)

BHABHA ATOMIC RESEARCH CENTRE

A thesis submitted to the
Board of Studies in Chemical Sciences

In partial fulfillment of requirements
For the Degree of

DOCTOR OF PHILOSOPHY
of
HOMI BHABHA NATIONAL INSTITUTE

August 2019

Homi Bhabha National Institute[1]

Recommendations of the Viva Voce Committee

As members of the Viva Voce Committee, we certify that we have read the dissertation prepared by **Smt. Vidya S. Thorat** entitled **"Chemical durability assessment of glasses for immobilisation of high level radioactive waste"** and recommend that it may be accepted as fulfilling the thesis requirement for the award of Degree of Doctor of Philosophy.

Chairman : **Prof. A. Dash**		**Date:** 28/08/2020
Guide / Convener: **Prof. C. P. Kaushik**		**Date:** 28/8/20
Co-guide - (if any) **Prof. A. K. Tyagi**	AKTyagi	**Date:** 28/08/2020
Examiner : **Prof. Tapas K. Mandal**	28/08/20	**Date: 28-08-20**
Member : **Dr. V. Sudarsan**	Sudarsan. V	**Date:** 28/8/2020
Member : **Dr. S. N. Achary**	S. N. Achary	**Date:** 28.08.2020
Invitee : **Dr. P. Sengupta**	P. Sengupta	**Date:** 28/08/2020

Final approval and acceptance of this thesis is contingent upon the candidate's submission of the final copies of the thesis to HBNI.

I/We hereby certify that I/we have read this thesis prepared under my/our direction and recommend that it may be accepted as fulfilling the thesis requirement.

Date: 28/08/2020

Place: BARC, Trombay, Mumbai

(Signature) 28/8/20

Guide

---

[1] This page is to be included only for final submission after successful completion of viva voce.

Version approved during the meeting of Standing Committee of Deans held during 29-30 Nov 2013

STATEMENT BY AUTHOR

This dissertation has been submitted in partial fulfillment of requirements for an advanced degree at Homi Bhabha National Institute (HBNI) and is deposited in the Library to be made available to borrowers under rules of the HBNI.

Brief quotations from this dissertation are allowable without special permission, provided that accurate acknowledgement of source is made. Requests for permission for extended quotation from or reproduction of this manuscript in whole or in part may be granted by the Competent Authority of HBNI when in his or her judgment the proposed use of the material is in the interests of scholarship. In all other instances, however, permission must be obtained from the author.

(Vidya S.Thorat)
Author

DECLARATION

I hereby declare that the investigation presented in the thesis has been carried out by me. The work is original and has not been submitted earlier as a whole or in part for a degree / diploma at this or any other Institution / University.

(Vidya S. Thorat)
Author

List of Publications from PhD

1. **Name of the Student:** Smt Vidya S. Thorat
2. **Name of the Constituent Institution:** Bhabha Atomic Research Centre
3. **Enrolment No.:** CHEM01201204018
4. **Board of Studies:** Chemical Sciences
5. **Title:** Chemical durability assessment of glasses for immobilisation of high level radioactive waste

Journal

1. "Corrosion of Borosilicate glasses subjected to Aggressive test conditions: Structural Investigations", **Vidya S. Thorat,** R.K. Mishra, V. Sudarsan, Amar Kumar, R.K. Vatsa, C.P. Kaushik and A.K. Tyagi, Journal of American Ceramic Society, 99 (2016) 3251–3259.

2. "Leaching studies on borosilicate glasses for immobilization of High Level Radioactive Waste in pellet form subjected to aggressive test conditions", **Vidya S Thorat,** R.K. Mishra, V. Sudarsan, Amar Kumar, A.K. Tyagi and C.P. Kaushik, Bulletin of Materials Science, 42 (2019) 211.

3. "Characterization of High Level Nuclear Waste Solutions from Different Origin", **Vidya S Thorat**, N. Soudamini, A. Sengupta, R.K. Mishra, Amar Kumar, A.K. Tyagi and C.P. Kaushik, Journal of Radioanalytical and Nuclear Chemistry, 320 (2019) 627-631.

Conferences

1. "Studies on the accelerated chemical durability test and its impact on structural changes in borosilicate glass matrix", **Vidya S. Thorat**, P.S. Kadam, R.K. Mishra, V. Sudarsan, Amar Kumar, C.P. Kaushik and A.K. Tyagi presented in symposium NCFGC -2015 held at VNIT NAGPUR, Maharashtra.
2. "Studies on the physico-chemical properties of nuclear waste glasses and its comparison with ISG", **Vidya S Thorat**, A.K. Munshi, R.K. Mishra, V Sudarsan, Amar Kumar, A.K. Tyagi and C.P .Kaushik is presented in 6th Interdisciplinary Symposium on Materials Chemistry (ISMC-2016) held in Mumbai in December 6-10, 2016.
3. "Thermal and structural studies on borosilicate glasses in pellet form subjected to aggressive test conditions", **Vidya S. Thorat**, R.K. Mishra, V. Sudarsan, Amar Kumar, A.K. Tyagi and C.P. Kaushik is presented in 7th Interdisciplinary Symposium on Materials Chemistry (ISMC-2016) held in Mumbai in December 4-8, 2018.

Dedicated to

“ANVI, SHRIYA AND SHRISHTI”

ACKNOWLEDGEMENTS

I am deeply indebted to Dr. C. P. Kaushik, Professor HBNI and Associate Director, Nuclear Recycle Group, BARC who not only introduced me to the subject of nuclear waste management but also encouraged me to do the PhD work on the title topic. He kindly accepted my registration for the PhD programme under his guidance and provided invaluable support and encouragement during the course of this work.

I am extremely grateful to Dr. A. K. Tyagi, Professor HBNI and Associate Director, Chemistry Group, BARC, who accepted me wholeheartedly as his student, without his deep involvement and invaluable guidance, this thesis would have never seen the light of day.

I wish to express my most sincere gratitude to Dr. Amar Kumar, Superintendent Labs, WMD and Dr. R. K. Mishra, OIC, WIP laboratories, WMD, Bhabha Atomic Research Centre, who granted me permission to work for PhD programme and also gave me constant support by encouragement, checking and correcting all the PhD related calculations and paper works.

It gives me immense pleasure to place on record my heartfelt thanks to Dr. D. Banerjee, for his support and encouragement during the course of the work.

I am grateful to Dr. V. Sudarsan, Chemistry Division, for his invaluable support in helping me in understanding the structural characterization of glass samples and critical analysis of the manuscripts. His support has helped me to complete the study.

I also wish to express my sincere gratitude to Doctoral Committee Chairman Dr. A. Dash for his guidance and all members of my Doctoral committee for not only spending their valuable time in reviewing the progress of the work, but also for their invaluable suggestions and encouragement.

It has been a great experience to work as a team with my WIP laboratory team. I acknowledge their invaluable contribution in conducting experiments. I also thank all members of Waste Management Division, for their direct and indirect support during the course of the work. The support received from Shri Darshit Mehta and Shri Aniruddha Dharashivkar cannot be forgotten.

Many of my friends provided invaluable support by extending instrumental facilities available in their laboratories. I wish to express my appreciation of the help rendered by Dr. Ashok Sahu, Dr. Rakesh Shukla, Ms Trupti A. Chavan and Dr. Remya Devi P.S. and Dr. Kallola Swain from Bhabha Atomic Research Centre.

I convey my heartfelt gratitude to my parents and in-laws and my husband Atish, my sister Varsha, my sister-in-law Archana, my brother Vivek, all my family members and relatives who have always inspired my inquisitive mind throughout my childhood, study and career. Their inspiration, encouragement, blessings and support have helped me reach where I am today.

Thorat

(Vidya S. Thorat)

CONTENTS

2 Chapter- 2 : *Experimental and Characterization Techniques* 71

3 Chapter 3: *Development of Nuclear Waste Glasses* 114

Summary of PhD thesis

Name of the Student: Smt Vidya S Thorat
Name of the CI/OCC: Bhabha Atomic Research Centre
Enrolment No.: CHEM01201204018
Thesis Title: Chemical durability assessment of glasses for immobilisation of high level radioactive waste
Discipline: Chemical Sciences

For the containment of High Level Waste (HLW), borosilicate based glasses have been considered as the most accepted matrix worldwide. Depending upon the composition of HLW arising from different reprocessing plants, suitable glass formulations have been developed indigenously and used for immobilization of HLW streams originating from PHWR and thorium containing waste. Sodium borosilicate glass system, containing Al_2O_3 and CaO as additives (GM11 glass) developed for PHWR-HLW and BaO as additive (GM44 glass) was developed for thorium containing high level waste stream. The detailed characterization of the synthesized glasses is done for its homogeneity, thermal stability and chemical durability. Different leaching tests are performed to ascertain chemical durability of nuclear waste glasses. Leach rates are compared with International Standard Glass (ISG) as well as with natural analogue such as basalt. Detailed chemical durability assessment of the waste glasses was done using long term leaching study for the duration of one year at three different temperatures viz 50, 70 and 90°C using actual ground water equilibriated with granite powder and clay to simulate repository conditions. Sodium and boron release rates were maximum, then comes silicon. The elemental release rate trend observed is Na~B > Si > Ba> Ca > Al. For better understanding of the leaching, on mechanism of leaching and kinetics of corrosion products associated with borosilicate glasses, leaching studies were done at high temperature (200°C) and pressures (16bar). The surface alteration studies it indicates presence of crystalline aluminosilicate (zeolite P) phase forms as alteration product in GM11 glass, which is insoluble phase and further retards leach rate leaving the basic glass structure unaffected. Unlike this, for barium borosilicate glass, GM44, leaching leads to formation of silica rich species with change in the residual glass structure. The alteration products, zeolites, do form in laboratory autoclave leaching studies as well as naturally altered basalt glass with hot springs leaching which are stable for millions of years so the waste glass durability also can be predicted to be stable.

List of Tables

List of Figures

Thesis Highlight

Name of the Student	Smt Vidya S Thorat
Name of the CI/OCC	Bhabha Atomic Research Centre
Enrolment No	CHEM012001204018
Thesis Title	Chemical durability assessment of glasses for immobilisation of high level radioactive waste
Discipline	Chemical Sciences

Nuclear glasses are developed for the immobilisation of high level radioactive liquid waste (HLW). Borosilicate glasses are the glass systems being explored across the world for immobilization of HLWs. For plant scale operation point of view, borosilicate glasses are the most preferred option. The selection of specific glass compositions within borosilicate family depends on (a) HLW chemistry and its solubility limit within the melt/glass, (b) chemical durability of the waste glasses and (c) available plant scale technology. The waste glasses are developed, sodium borosilicate glass with aluminium and calcium as modifiers for uranium rich waste solution and another, barium borosilicate glass for thorium containing waste solutions. The glasses are characterised for its homogeneity, thermal stability and chemical durability. Chemical durability was studied using different types of static leaching tests. Waste glasses are supposed to immobilize the hazardous radionuclide for thousands of years and thereby isolate them from the biosphere. However, it is very difficult to carry out any experimental studies to demonstrate this to ascertain integrity of waste product for thousands of years with short term laboratory leaching experiments. The surface alteration studies of glasses after leaching with ground water under hydrothermal leaching studies indicates presence of crystalline aluminosilicate (zeolite P) phase forms as alteration product in the prepared waste glass, GM11 glass. The only source of obtaining relevant database is to examining natural rocks exposed to similar geological conditions. Keeping this in mind, basaltic rock altered by hot spring water has been studied. The basalt samples are collected from natural hot spring region in Vajreshwari, Maharashtra. The temperature of the hot spring is 50-60°C and the hot water is in contact with basalt glass which is natural analogue of waste glasses. The water and the altered natural basalt samples are collected from the site. The basalt glass was also showing surface alterations in the form of precipitate. The precipitates are studies by XRD and are found to be of zeolites. The alteration products observed in high temperature and pressure autoclave leaching are somewhat matching with the Vajreshwari sample which is naturally leached under hot water. It shows that the basalt glass altered at hot springs and the basalt glass altered in laboratory at high temperature is giving similar results. Thus, it is seen that after millions of years of continuous leaching zeolite phases do form over basalt glass. These phases are stable and further retard the leach rate. The zeolite phases were formed in nuclear waste glasses as well under aggressive hydrothermal leach test conditions within short test durations in laboratory. Thus, these test conditions can be extrapolated using suitable model for long term leach measurements.

Chapter 1: *Introduction*

Introduction

1.1 Energy – For the growth of human civilization

Energy is essential for the survival and growth of modern human civilization. A reasonably good correlation exists between the per capita energy consumption and the quality of life, as mentioned by the UN Human Development Index. This correlation is quite strong in the case of developing countries like India where the energy demand is considerably unfulfilled [1]. All the available source of energy, therefore, must be optimally developed and deployed to meet the short as well as long term energy needs of our country. Presently, 2/3rd of the energy demand in India is satisfied by non-renewable sources such as coal, petroleum etc. Continuous usage of these sources for the past centuries have left little inventory for the future. Further, with increasing awareness on environmental pollution has also restricted utilization of many of these sources. Currently lot of research and development work is going on in the fields of renewable energy sources such as solar, wind etc. However, estimates show that even under best possible situation such energy sources cannot supply more than 5% of the demand [2]. Solar and other renewable and non-conventional energy sources must be deployed to the fullest extent possible. However, to meet the large concentrated energy needs for industries and urban centres, the only sustainable energy resource available to us in India and indeed the entire world in a longer time frame, is nuclear energy. Though coal based power plants will continue to be the mainstay of electricity generation, share of nuclear power has to be expanded significantly in India. Hence, to bridge the gap between demands and supply, nuclear energy appears to be the best solution. Towards this, India has taken special drive to utilize all possible fission and fusion energy sources. In case of nuclear fission based technology, enormous energy can be obtained either through bombardment of fissile and/or fertile radionuclides (natural or artificially produced) such as ^{235}U, ^{233}U, ^{239}Pu, ^{238}U, ^{232}Th etc., by slow or fast neutrons, which split them into lighter nuclei. India has already attained some maturity in this technology and currently 6780 MWe nuclear energy is being produced from 22 nuclear reactors [3]. As far as nuclear fusion energy sources are concerned, significant R&D initiatives have been taken by the Department of Atomic Energy and other national research centres. The International Thermonuclear Experimental Reactor (ITER) is a project being developed jointly by international consortium. ITER will be located at Cadarache, in south of France, and aims to develop a plant for demonstrating generation of electricity based on fusion. India is now a partner in ITER project [3]. In case of nuclear fusion reaction, two light nuclei (such as hydrogen) combine to form a heavier nucleus (such as helium). The process releases excess binding energy from the reaction, based upon the binding energies of the atoms involved in the process. The present thesis however focuses on waste management aspect of fission energy and hence matter related to fusion energy will not be discussed hereafter.

Waste generation from nuclear power plants in the form of vitrified waste product is of small volume compared with waste generation from other electricity generation routes such as coal etc. Radioactive waste which can be managed easily and the releases to the environment are insignificant. Thus nuclear technology with an affective environmental management plan and effective safety measures is a much cleaner source of electricity generation as compared to other sources such as coal based thermal power plants etc. With this perspective, India has undertaken nuclear energy programme to share a substantial part of future need of power. Management of nuclear waste is an indispensable part of this programme. A brief account of the nuclear energy programme is given before discussing with the radioactive waste management.

1.2 Indian nuclear energy programme

India has modest reserves of uranium and vast reserves of thorium. To bridge the gap between futuristic energy demand and supply, India has adopted a three stage nuclear energy power program based on closed fuel cycle strategies [1]. “Closed cycle” refers to separation of uranium and plutonium and further recycled while the other radioactive fission products were separated, sorted out according to their half-lives and activity and appropriately disposed of with minimum environmental disturbance. In “Open once through fuel cycle”, the spent fuel is not reprocessed, but after long storage, encapsulated and disposed in geological repositories. The close fuel cycle offers distinct advantage with respect to recovery of fissile and fertile materials for recycling it back in fuel cycle for production of energy. Close fuel cycle also reduces the radiotoxicity burden to be considered during disposal of the nuclear waste in geological repository. A schematic diagram of closed nuclear fuel cycle is presented in Figure 1.1 [4]. Based on the advantages of closed fuel cycle, India has decided to go for it. In the first stage, U based fuels are being irradiated in Pressurized Heavy Water Reactors (PHWR) to generate electricity and produce ^{239}Pu, which can be used as a fuel material for second stage using Fast Breeder Reactor (FBR) technology (Figure 1.2). Within FBR, it is proposed to use

Th-Pu mixed fuels to obtain energy and generate ^{233}U for third stage. To demonstrate the technological maturity obtained in second stage, a 40 MWth Fast Breeder Test Reactor (FBTR) had been constructed by Indira Gandhi Centre for Atomic Research (IGCAR), Kalpakkam.

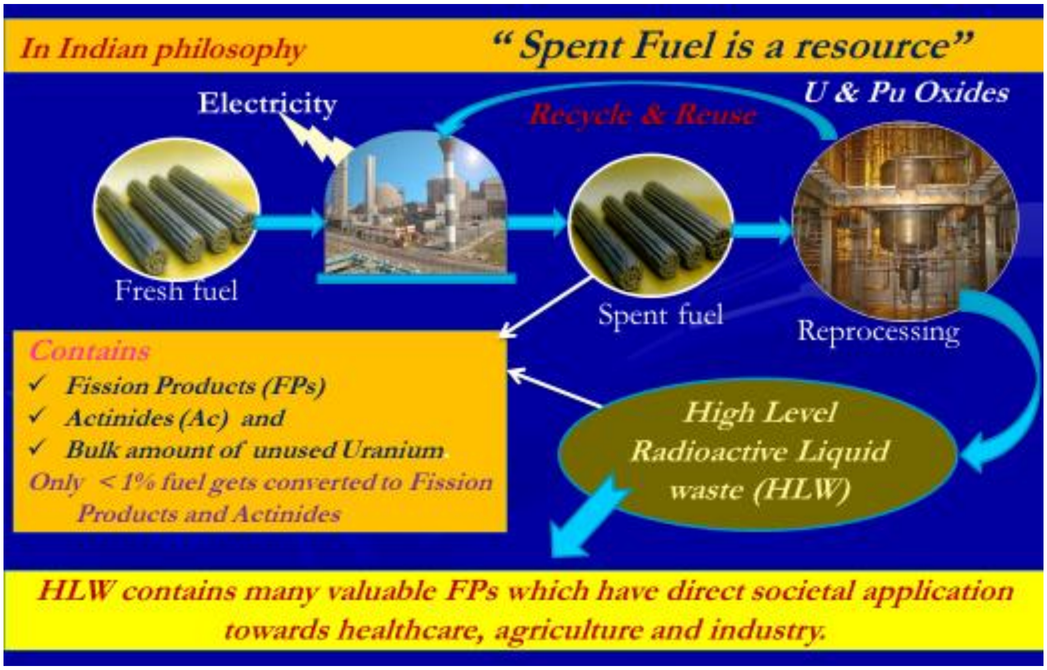

Figure 1.1: A schematic diagram of closed nuclear fuel cycle

FBTR uses indigenously developed mixed uranium - plutonium carbide fuel, at a burn up of 165,000 MWd/t or more. In addition to this, a 500 MWe Prototype Fast Breeder Reactor (PFBR) is also being constructed at Kalpakkam. This together with four more similar units is likely to generate 20 GWe energy. In parallel with the FBR program, R&D work is also being pursued to develop a 300 MWe Advanced Heavy Water Reactor (AHWR) based on $(Th\text{-}U)O_2$ and $(Th\text{-}Pu)O_2$ mixed oxide fuel. Keeping the current international trends in nuclear technology in view, a road map for the third stage of Indian nuclear power program has been proposed, which include construction of Advanced

Heavy Water Reactor (AHWR), High temperature reactor based power packs, Accelerator driven fertile converters and accelerator driven system with a fast reactor sub-critical core together with a mainly thorium fuelled thermal core somewhat similar to that present in AHWR, in succession [5]. The present thesis addresses conditioning of the high level waste likely to be generated from PHWR and AHWR and a brief note on the same along with a general introduction on radioactive waste are described below.

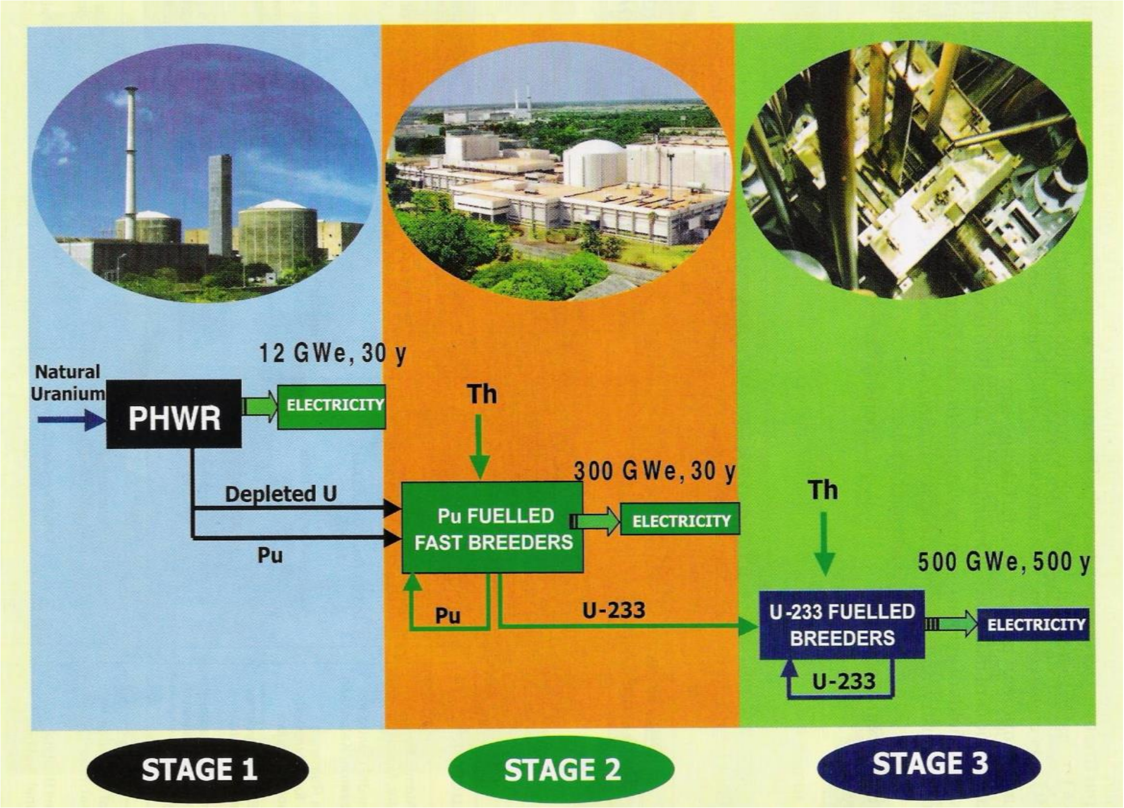

Figure 1.2: A typical sketch of Indian three stage nuclear power programme

1.3 Radioactive waste

In the process of contributing towards the growth and progress of human civilization, all industrial activities inevitably give rise to some unwanted waste product. This is true for nuclear industry as well.

Today, radiation and radioactive materials are widely used in industry, agriculture, medicine and for production of nuclear power. These activities result in generation of residual material, which do not have direct economical use. These materials are termed as radioactive waste and are potentially dangerous due to radioactivity associated with them. Though the radioactivity decays with time, these wastes can remain active for extended periods of time depending on half-lives of the radionuclides present. Management of these wastes essentially aims at isolation of human environment from the radioactivity till it decays to innocuous levels. This is achieved primarily by removing the radionuclides and the fission products from the waste. Recovered material are thereafter put for some useful application or immobilized in an inert solid matrix for storage/disposal. The waste after removing radionuclide and the fission products known as lean waste is either recycled or discharged to environment. Radioactive waste generated at each stage of nuclear fuel cycle needs to be managed safely.

1.4 Classification of radioactive waste

Radioactive wastes are generated in various forms like solid, liquid or gaseous. Classification of waste into different categories is useful in their segregation, selection of appropriate treatment process, storage and disposal. The classification is very important from safety as well as process consideration point of view. Important parameters which are taken into account include physical, chemical, radiological and biological properties as well as criticality aspects and origin of waste. The general categorization of radioactive waste is presented in Table 1.1.

Table 1.1: Categorization of radioactive waste

Category	**Solid**	**Liquid**	**Gaseous**
	Surface Dose (mGy/h)	**Activity level (Bq/m^3)**	**Activity level (Bq/m^3)**
I	<2	$< 3.7\times10^4$	<3.7
II	2-20	3.7×10^4 to 3.7×10^7	3.7 to 3.7×10^4
III	>20	3.7×10^7 to 3.7×10^9	$>3.7\times10^4$
IV	Alpha Bearing	3.7×10^9 to 3.7×10^{14}	-
V	-	$> 3.7\times10^{14}$	-

The concentration of radioactivity also varies depending upon the source of generation. Accordingly, radioactive liquid waste streams are conventionally classified (Table 1.2) as Exempt Waste, Low Level Waste (37-3.7×10^6 Bq/L), Intermediate Level Waste (3.7×10^6 - 3.7×10^{11} Bq/L) and High Level Waste (above 3.7×10^{11} Bq/L). The concentrations of long lived radionuclides and tritium are also taken into account while classifying the liquid wastes.

Table 1.2: Conventional classification of liquid waste

Category	Nature	Activity
Low Level Waste (LLW)	Near Neutral	<3.7 KBq/L
Intermediate Level Waste (ILW)	Alkaline	3.7 KBq/L – 3.7 MBq/L
High Level Waste (HLW)	Acidic	>3.7 MBq/L

1.5 Basic steps in radioactive waste management

Various processes for management of radioactive waste as adopted in India are shown in Figure 1.3. These include waste characterization, treatment, conditioning, storage, disposal, surveillance/monitoring, etc. Options available for treatment, conditioning, storage and disposal of these wastes depending on their physical forms are also indicated.

The descriptions presented herein are intended to be general and apply to the management of radioactive waste from mining and milling, fuel-fabrication, nuclear power generation, medical and industrial application of radioactive materials and environmental restoration. They apply to radioactive waste generated during the operational period as well as during the decommissioning of a facility. The applicability of these steps will vary depending on the type of radioactive waste.

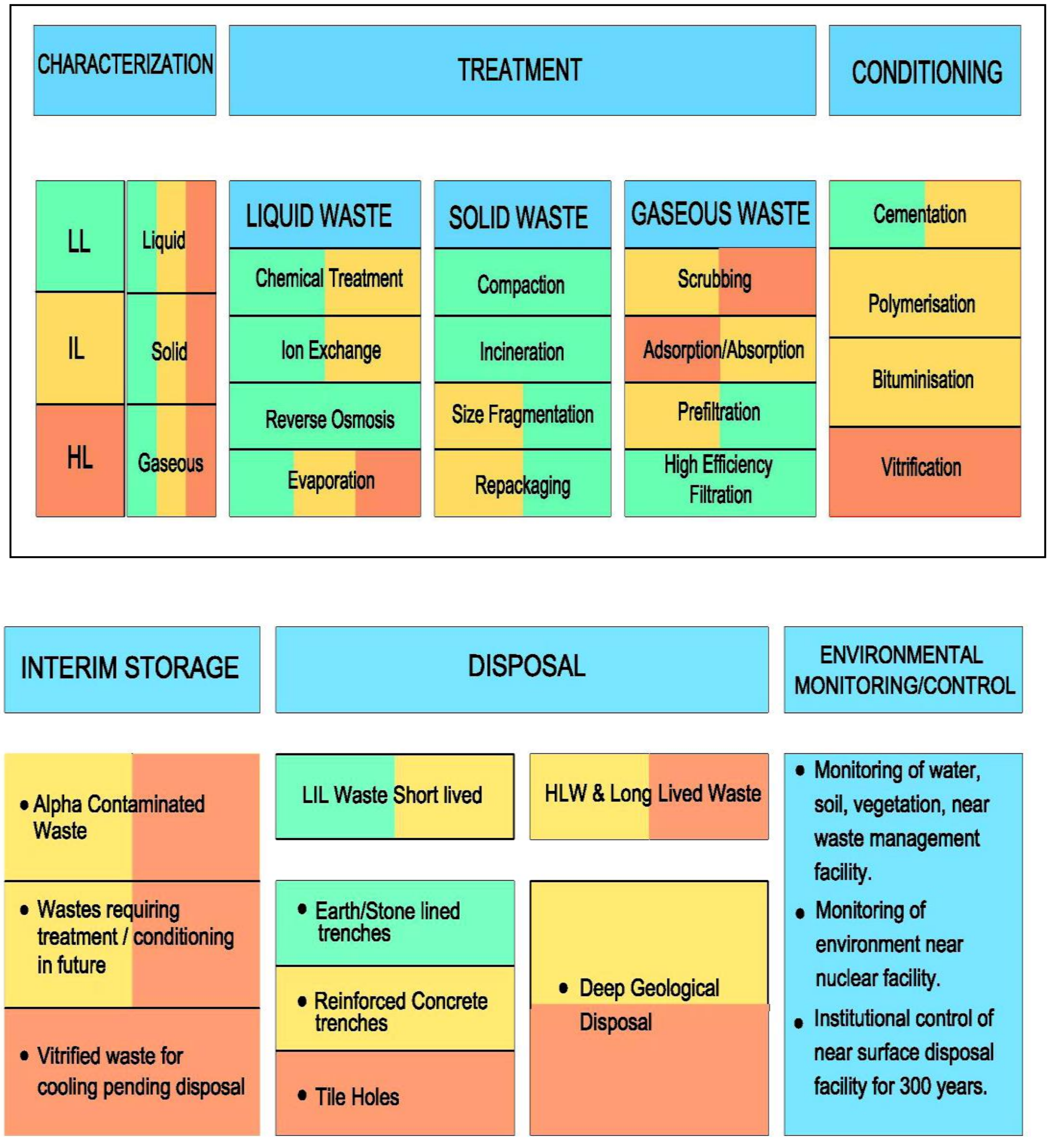

Figure 1.3: A simplified schematic for management of different types of radioactive wastes

1.6 Principles of management of radioactive liquid waste

The basic principles followed in liquid waste management are

- Delay and decay for the waste having short-lived isotopes,
- Dilution and dispersion of very low level activity to the environment well below the nationally accepted levels which are in line with international practices and
- Concentration and containment of radioactivity as much as practicable.

Amongst them concentration and containment is one of the widely adopted processes [6].

1.7 Strategy for management of radioactive liquid waste

Development of strategies for the safe, sustainable and broadly acceptable management of all types of radioactive waste becomes the key component for isolation of radioactive waste from human environment for an extended period of time.

Strategy for management of low and intermediate level waste lies in the development of innovative treatment process having volume reduction factor as one of the important parameter. For achieving the volume reduction, the methodologies are based on separation science. Various active components are separated by using different techniques like chemical co-precipitation, ion-exchange and membrane processes like reverse osmosis, ultra-nano filtration etc. The concentrates obtained from the primary treatment process are conditioned prior to disposal.

A three - step strategy (Figure 1.4) for management of HLW has been adopted in India [3]. This includes: (i) Immobilization of waste oxides in stable and inert solid matrix, (ii) Interim storage of conditioned waste under continuous cooling and surveillance & (iii) Waste disposal in deep geological formations. Immobilization of HLW in borosilicate glass matrix is being practiced using induction heated metallic melter and joule heated ceramic melter in plant scale at Trombay and Tarapur, respectively [7]. An interim storage facility is fully operational for the storage of vitrified high-level waste over packs for thirty to fifty years or more. Nationwide screening of potential regions and evaluation of rock mass characteristics is in progress for a geological repository programme.

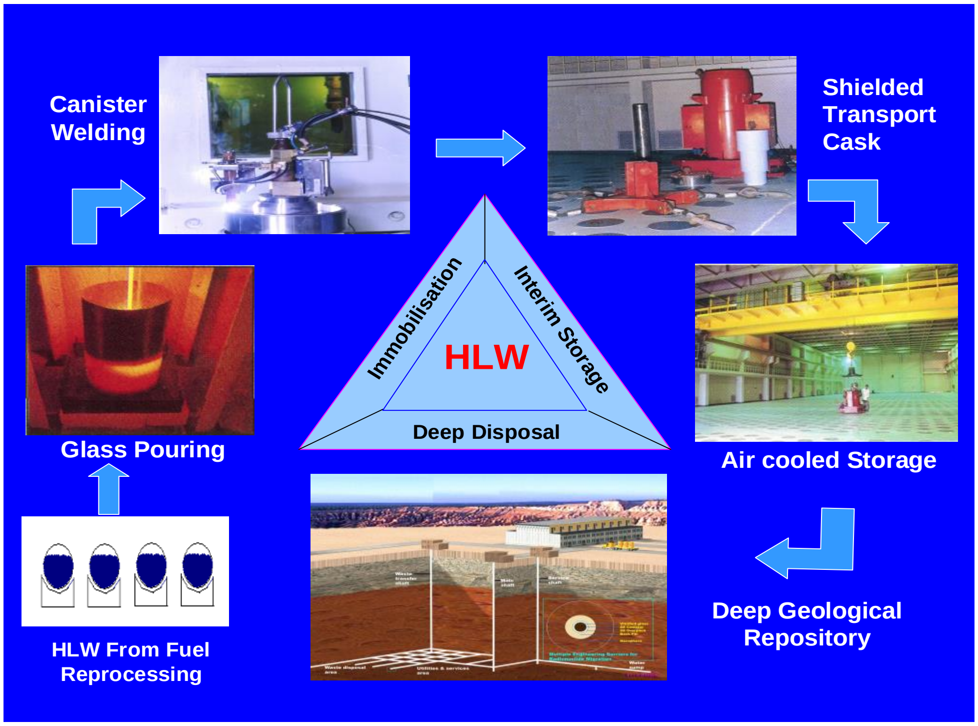

Figure 1.4: A three - step strategy for management of HLW adopted in India

1.8 Management of HLW

The waste after reprocessing, being in liquid form and highly radioactive, requires special treatment to ensure its isolation from human environment for extended period of time. Actinides present in HLW are alpha active and have longer half-life of the order of millions of years and require isolation for longer time span compared to other radioactive fission products and activation products. The strategy adopted all over the world for isolation is to convert the liquid waste into some kind of suitable solid form (immobile form) which is chemically, mechanically and thermally stable over the life time of major long lived isotopes. Solidification provides improved safety during handling and shipping and release of radioisotopes by leaching with ground water is minimized. Leaching is one of the major routes by which radioactivity can enter into human biosphere. Hence solid wasteforms having good chemical durability (poor leaching), high resistance to impact (mechanical strength) and stability over a wide range of temperatures are necessary. Research and development work is therefore directed in search of a suitable matrix. The candidate matrix immobilizing the waste should be able to accommodate all the active and inactive components of the waste and bind them in the structure of the matrix so as to achieve the required isolation. The desirable properties of immobile matrix for fixation of high level waste forms are [8]:

(i) Ability to incorporate a wide range of elements present in HLW.

(ii) Good chemical durability, i.e. low leachability.

(iii) Good thermal conductivity, so that the heat generated due to decay of radioactive isotope is well dissipated.

(iv) Good thermal and radiation stability over extended periods of time.

(v) Good mechanical strength and shock resistance so that transportation to storage or disposal is safe.

(vi) Minimum volume.

(vii) Compatibility with storage canister.

(viii) Compatibility with geological repositories.

(ix) Technical and economic considerations (raw material availability, adaptability of process parameters to easily available engineering materials).

Many candidate matrices have been studied and developed for immobilization of HLW and characterized for aforesaid properties. These are briefly discussed here.

1.9 Candidate matrices for HLW

The candidate matrices studied for immobilization of HLW studied and implemented worldwide are glass based matrices. The lab scale studies are in progress on synroc, sodium zirconium phosphate, ceramic waste forms and glass ceramics.

1.9.1 Glass based matrices

The most extensively studied and used product forms are glass (phosphate and borosilicate) and glass ceramics.

1.9.1.1 Phosphate glass

The phosphate glass system was found attractive in early stages of product development since (a) this matrix can effectively incorporate molybdenum and sulphate, present in the waste. (b) its main additive is in liquid form and (c) formation temperature is comparatively low. However, material of construction is a major limitation in phosphate glass process because of severe corrosive conditions. Also the product in general is inferior from long term durability point of view.

1.9.1.2 Borosilicate glass

Borosilicate glass is now universally accepted as the matrix for immobilization of waste on account of good product durability. The formation temperature is moderate being in the range of 1000 to 1100^{o}C. However, elaborate glass forming additive system is required to feed either in the form of aqueous slurry of mixed oxides or glass frit. Borosilicate glasses will be discussed in subsequent chapters.

1.10 Glass – A candidate waste form for immobilization of HLW

Out of all the listed waste forms, glasses have received major attention in product development as well as in long term product characterization with respect to desired waste form characteristics. It is now the material of choice for incorporating and immobilizing the potentially hazardous radionuclide in high level nuclear waste. The typical material properties, which make it superior as compared to others include (i) Structural flexibility to accommodate wide range of elements, (ii) Simplicity in processing technique, (iii) Highly corrosion resistant, (iv) Good thermal and radiation stability, (v) Provides high volume reduction, (vi) Established long term integrity and (vii) Inexpensive raw materials.

These characteristic properties of the glass make vitrification the focal point of treatment systems for high level radioactive waste around the world. Borosilicate based glass system have been studied in detail and found wide acceptance in the world as one of the suitable matrix having capability to retain radioactivity for long durations. A sound understanding of the processes involved in chemical and other alterations of the borosilicate nuclear waste forms provide the only defensive basis for an extrapolation into the long term. There are volcanic glasses which have been exposed to long term alteration in nature (upto 10^7 years) which have been studied as natural analogs of borosilicate nuclear waste glasses in order to verify predictions obtained from short term test in the laboratory [9]. On the basis of above detailed studies, borosilicate glass constituent presently the only nuclear waste form that has been produced on the plant scale. A total of over five hundred tones of highly radioactive glass have been produced from high level radioactive liquid waste in France and Germany. In India too, borosilicate based glass matrix has been adopted for vitrification of HLW [10].

Chemical durability of nuclear waste glass must be good, means, glass compositions to be deployed for immobilization of HLW must be chemically stable for at least 5×10^3 years in order to satisfy regulatory nuclide release limits [11,12]. High level waste glasses must be able to prevent radionuclide from entering into the human environment. Waste glass composition is the determining variable for properties like process ability and durability [13]. The solution chemistry of glass leachates is direct function of the glass composition [14]. The structural resistant offered by the borosilicate glass matrix is primarily responsible for curbing the radionuclide transport in the aqueous environment [15]. Vitrification is attractive as a waste treatment process mainly because of the properties of the glass. These properties give vitrification its high quality product and flexibility in constituent proportion. To understand the advantages of vitrification as a waste treatment process, an understanding of the properties of the glass is of fundamental importance. A brief summary pertaining to various aspects of the glass structure is presented. Effort has also been made to discuss how this structure relates to durability of vitrified waste product (VWP) containing hazardous waste.

1.11 Glass structure

Glass is an inorganic product of fusion (in the present context) which has been cooled under rigid conditions of temperatures without crystallization. It is rigid, non-crystalline (amorphous) material.

The open random structure of a glass is primarily responsible for achieving high waste loading and high chemical durability. The radionuclides from the nuclear waste are restrained in a glass through primary and/or secondary bonding with the silicate network. This inherent property leads to the incongruent release of different elements from a waste glass [16]. Because of the network structure of glasses, it does not help to express their composition as chemical formulae. The most common way of describing glass is to list relative amount of oxides derived from the raw materials used in the glass formulation even though these oxides do not exist as it is in the glass network. Another advantage of glasses over ceramic waste form is that they do not have any crystallographic limits for incorporation of waste.

According to Zachariasens' view of atomic arrangement [17], the oxides involved in the glass formations can be categorized as follows [18].

a)***Network former*** – Oxides of element that can produce glasses by forming chains and networks in a completely random manner. The elements of these oxides have a co-ordination number of four. The inorganic species increase the network connectivity by covalent bonds with the oxygen atoms in a silicate network. Generally network frames are acidic (e.g. SiO_2, B_2O_3 etc.).

b)***Network modifier*****–** Oxides of elements that can produce glasses by melting with network formers. The elements of these oxides have co-ordination number higher than four in some compounds. The inorganic species interrupt the network continuity by forming ionic bonds with the oxygen or other elements in the glass network. Generally, glass network modifiers are basic (e.g. Na_2O, K_2O, Li_2O, BaO, CaO).

c)***Intermediate*****–** oxides of elements that can produce glasses by fusion with network formers. The element of these oxides has co-ordination number lying in between those of glass formers and glass modifiers. Intermediate can also act like network formers. In some instances, intermediate are referred to as dwellers. Generally, intermediates are amphoteric. (e.g. Al_2O_3, Fe_2O_3 etc).

An oxygen atom involved in interconnecting either two network forming elements or network forming and network dwelling elements is regarded as Bridging Oxygen (BO). Chemical durability of the glass increases with increase in the BO, since they help to maintain the network continuity. Generally, the BO's bond covalently with both formers and dwellers. A Non-Bridging Oxygen (NBO) can be define as an atom interconnecting the network forming and network modifying elements. In general, the

NBO's bond covalently with formers and ionically with the modifiers. However, due to the electrostatic nature of the ionic bond, NBO fails to retain network continuity and hence affect the glass durability adversely [19].

Hazardous constituents of waste can be immobilized in the vitrification process either by main interaction with the glass matrix (as network former) or chemical bonding (network modifier) or encapsulation. Random network structure (Two dimensional) of vitrified waste product is shown in Figure.1.5.

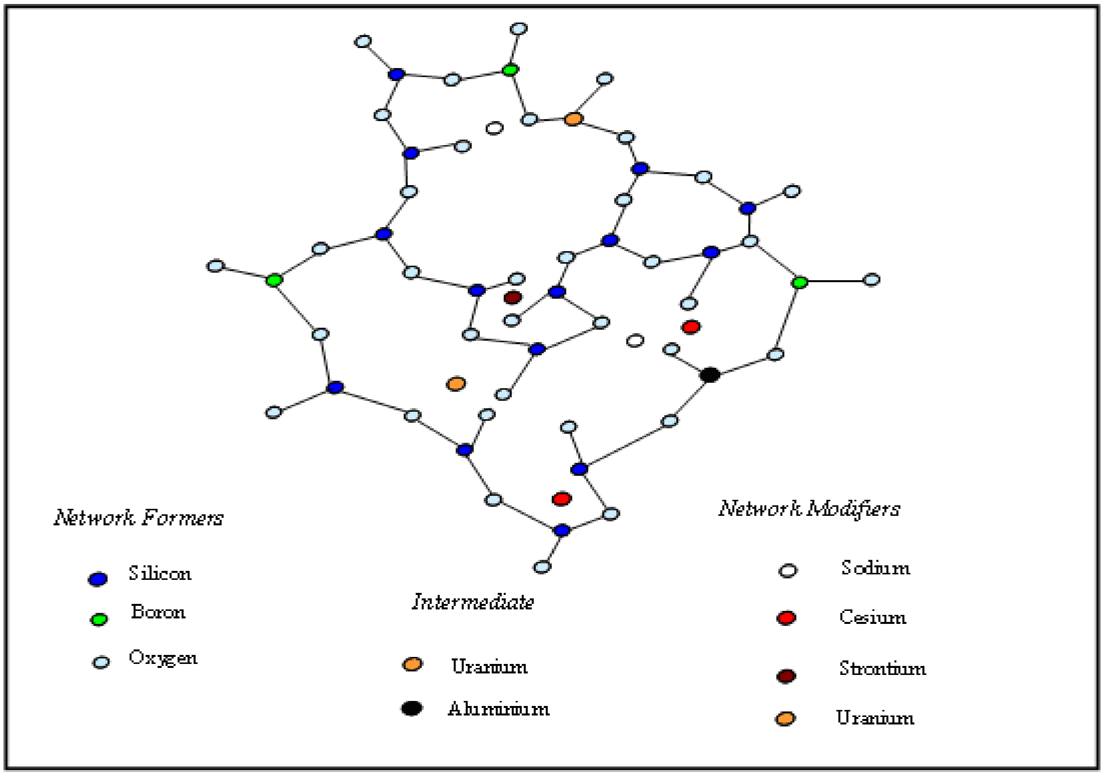

Constituent present in waste streams can themselves serve as primary glass formers and modifiers	**Proportioning of these different waste streams with minimum external additives can result in optimized vitreous waste forms**

Figure 1.5: Random network structure of vitrified waste product

Certain waste constituent can be immobilized by chemical bonding with the glass forming materials, particularly silica present in the wastes to be vitrified. The most notable chemical bonding within vitrified materials occurs, when waste constituent bond covalently with the oxygen atoms in a silica network and become part of the network. Waste constituent like U, Fe, Al etc. that interact this way behaves like network formers since they essentially replace silicon in the glass network structure. Other waste constituent can bond chemically with oxygen or other elements in the glass network. To sum up the above discussion, it is understood that this ionic bonding incorporates the material into the glass but disrupts the network continuity thereby modifying the physical and chemical properties of the vitrified materials. Materials, which interact in this fashion, called network modifiers. Hazardous waste constituent may also be immobilized without direct chemical interaction with the glass network. Since vitrification constitutes a molten phase during some portion of the process, materials that do not interact chemically or have not completely entered solution can be surrounded by a layer of vitrified material and thus gets encapsulated, as the melts cools. This layer of vitrified material protects the capsulated constituents from the chemical attack. This structural characteristic of the glass providing three routes for immobilization of waste constituents make vitrification as the focal point of immobilization of high level radioactive waste around the world.

1.12 Glass matrix development and vitrification in India

Research and Development on HLW vitrification [20,21,22,23] started in 1970s in India. Sodium borosilicate glass was chosen as matrix which was established as good matrix option. The ternary diagram of SiO_2-B_2O_3-Na_2O glass system is broadly divided into three zones. Zone I is no glass forming zone; Zone II is glass forming zone and zone III as immiscibility zone (Figure 1.6). Bulk composition in zone I results in the formation of fused mass due to the presence of crystals whereas melts produced within zone III get rapidly unmixed into silicate and borosilicate fractions. Homogeneous glasses can be obtained from bulk compositions falling within zone II but significant variations in product durability factors such as leach resistance etc. Zone II was thoroughly studied in terms of equivalent leach resistance, pouring temperatures and microstructural homogeneity [24].

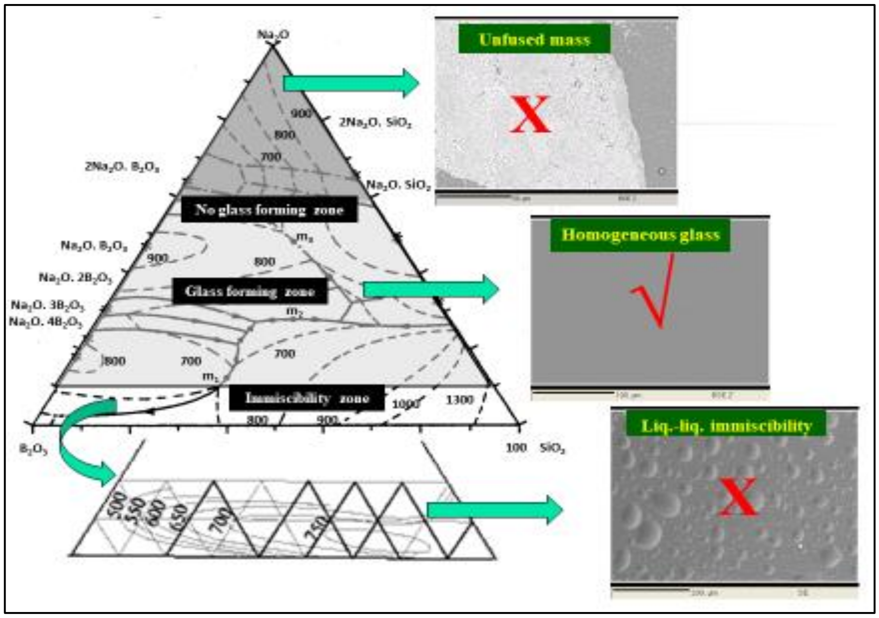

Figure 1.6: Ternary diagram of sodium borosilicate glass system indicating different zones.

Following the IAEA guidelines for acceptable product durability properties and processing constraints, few base glass compositions having homogeneous microstructure, leach resistance of the order of 10^{-4} g/cm^2-day or better and pouring temperature ~950°C were chosen for conditioning of Indian HLW's. Addition of Fe and U in glass was also studied to increase leach resistance. Alkali earth borosilicate glass SiO_2-B_2O_3-PbO system was also studied, the glasses were known to form at low temperatures and possess acceptable leach resistance [25]. Phase separation in glasses. Phase separation aspect is very important in Indian context as good amount of 'sulphate containing legacy HLW' was in store at BARC, Trombay. As it is in knowledge that sulphate bearing minerals are abundant in sedimentary rocks and rare in magmatic rocks. Barite ($BaSO_4$) is known to be the most abundant sulphate bearing mineral and existence of barite ore deposits over geological time scales indicate its leach resistance. To understand the rarity of sulphate bearing minerals in magmatic rocks and the characteristic of barite which has most abundant sulphate bearing phase on earth's crust, insight was sought from 'valance bond theory'. According to the theory, the mean bond valance for SO_4^{2-} group is 1.5 valence units (vu) which means that, any oxygen atom linked to the S^{6+}cation receives ~1.5 vu from it, and can accept ~0.50 vu (max.) from any other coordinating cations so as to polymerize the two units. This limits polymerization of sulphate with silicate tetrahedra (1.0 vu) and suggests that the oxygen atom linked to sulphate tetrahedra can bond only with octahedrally or higher coordinated mono-,di-, or trivalent cations e.g. Ba^{2+}. Given cognizance to these observations, it was decided to add varying amounts of BaO to sodium borosilicate glass compositions and monitor the base glass properties in terms of microstructure, pouring temperature and swelling index [26]. Homogeneous base glasses having pouring temperature lower than 950°C and swelling index less than 2.6 were then loaded with varying amounts of simulated sulfate bearing wastes. The waste glasses so produced were once again subjected to above mentioned assessments. Of these glasses, those capable of incorporating more than 20 wt % simulated waste were then ground and the respective powders were subjected to static leach experiments using distilled water at 90°C. From these glasses, the one showing highest order of leach resistance and high waste loading was then finally selected for plant scale operation. With the introduction of research and development in second and third stage of nuclear energy programme, conditioning of HLW derived from Thorium bearing waste within sodium-barium borosilicate glass matrix were successfully attempted [27].

1.13 Plant scale vitrification process

The experience in vitrification process is essentially gathered from induction furnace operation over last two decades. The induction melter consists of metering of pre-concentrated waste and glass forming additives in the form of slurry into the process vessel located in a multi-zone furnace. A typical sketch of multi-zone induction furnace, which is presently used at Waste Immobilization Plant (WIP), Bhabha Atomic Research Centre (BARC), Trombay is presented in the Figure 1.7. The process vessel is made of high Ni-Cr alloy (Inconel 690) so as to withstand high temperature, oxidizing and corrosive conditions. There is a freeze valve section at the bottom operable by an independent induction coil. With simultaneous concentration and calcination of waste, solid-liquid interface moves upwards.

During operation, susceptor is heated by multizone induction furnace and it radiates heat to process pot to raise its temperature to the desired limit. Thermowell made up of Alloy 690 is attached to process pot to monitor its temperature. Operating temperatures of process pot depends on the pouring temperature of the waste glass and its process flow chart. To the process pot, nitric acid based HLW and glass additive slurry are charged through different channels. The mixture is then subjected to multistage vitrification process [15], which includes feeding (100–105°C), evaporation (105–120°C), calcination (300–700°C), fusion – melt formation (700–850 °C) and soaking (950–1,000°C). After soaking, the homogeneous melt is poured within the stainless steel canister (324 mm outer diameter, 10 mm wall thickness, 770 mm length; each containing ~45 l of HLW loaded glass (~90 kg) incorporating 0.6 million Curies generating ~2 kW of decay heat), cooled in air and a lid is placed on it by welding. Three such canisters are put inside the stainless steel overpack (356 mm outer diameter, 10 mm wall thickness, 2,000 mm length), decontaminated using ultrasonic bath and stored within underground storage. The level of liquid waste is indicated by the temperatures sensed by the thermocouples located at different heights. The calcined mass is fused into glass at about 950^{o}C and is soaked at 950-1000^{o}C for eight hours to achieve homogenization. The molten mass is then drained into stainless steel AISI 304L canisters by operating the freeze valve. The canister filled with vitrified waste product is allowed to cool slowly in an insulated assembly. This is then welded remotely by the Pulse Tungsten Inert Gas method.

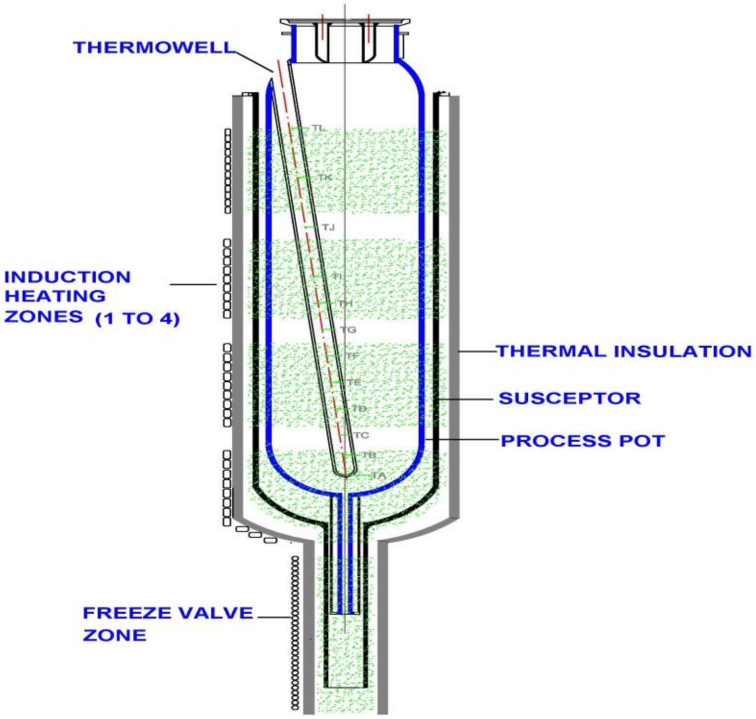

Figure 1.7: A typical sketch of multi-zone induction furnace

The entire vitrification process is carried out in dedicated hot cells protected with radiation shielding windows and each equipped with state-of-the-art remote handling systems e.g. servo-manipulators, in-cell crane, grapping tools, product positioning/removing trolleys, closed-circuit television cameras, remote welding machine, etc. An elaborate off-gas cleaning system consisting of condenser, scrubber, chiller, demister and absolute HEPA filter is used to treat the gas before discharge through a 100 m tall stack to the atmosphere. All the vitrification plants have the central data acquisition and control system to monitor and control the critical process parameters during vitrification operation [28].

Besides hot wall induction furnace, India has recently acquired operational experience in Advanced Vitrification System (AVS) which is essentially a Joule heated ceramic melter furnace (Figure 1.8). Robust continuous vitrification technology, high throughput and higher processing temperature are the main advantages of this process. In the simplest form, electric current across Alloy 690 electrodes immersed in borosilicate melt is used to generate heat by Joule effect (Q ¼ I2R) which maintains the molten condition and sustains evaporation, calcination, fusion and soaking [29]. In the Indian type ceramic melter, the glass contact refractory is made up of high alumina-zirconia-silica fused cast blocks followed by layers of back-up refractory and insulation materials, all encased in a water cooled stainless steel box mounted on a suitable structural support. For vitrification, both HLW and glass formers are directly introduced into the melting chamber and the slurries are heated to as high as 1150°C. The waste-glass melt so produced, is drained to the canister.

In comparison to metallic melters used in WIPs at Tarapur and Trombay, use of ceramic melter has distinct advantage of higher throughput on account of continuous operation and better product durability due to higher achievable processing temperature**.** In view of this, development, establishment and testing of small scale ceramic melter has been successfully completed, and an industrial scale ceramic melter based vitrification facility is operational at Tarapur (Figure 1.8).

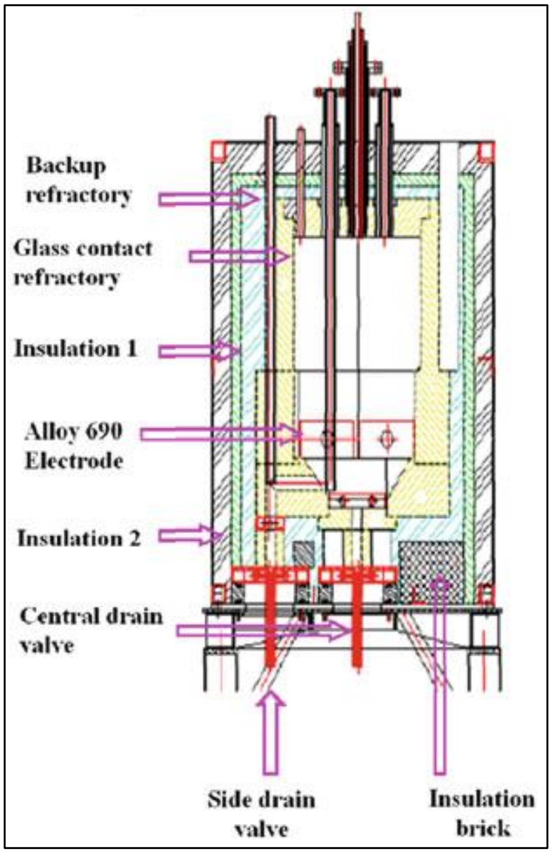

Figure 1.8: Compact ceramic melter installed at Tarapur

One of the major technological hurdles in improving the glass matrix composition is the limitation of furnace operating temperature. To address this problem, Cold Crucible Induction Melter (CCIM) is now being developed at BARC (Figure 1.9) which will offer longer melter life, higher temperature availability, higher waste loading, more tolerance towards noble metal precipitation and higher specific capacity. In this process, glass is directly heated within a segmented crucible (manufactured from contiguous segments forming a cylindrical volume, but separated by a thin layer of electrically insulating material) using high frequency electromagnetic induction. To avoid corrosion of metallic components as observed in metallic melter or ceramic melter, each segment of the cold crucible is fed with circulating water system which produces a solidified protective glass layer on the inner side of the melter.

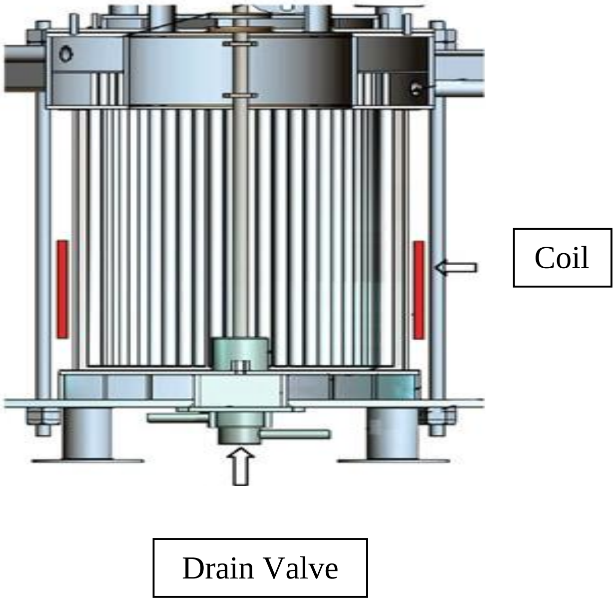

Figure 1.9: Cold crucible

1.14 Emerging strategy for HLW management

Partition and Transmutation (P&T) option for HLW is the recent advancement for HLW management, which can reduce the radiotoxic inventory of spent fuel by a factor 100 to 1000 (Figure 1.10). Partitioning is the selective separation of radiotoxic isotopes from reprocessing streams (minor actinides, long-lived fission products). Partitioning of minor actinides (MAs) or transuranic is the most crucial step in the P&T strategy since it involves the separation of long-lived and highly radiotoxic actinides from the high level waste stream.

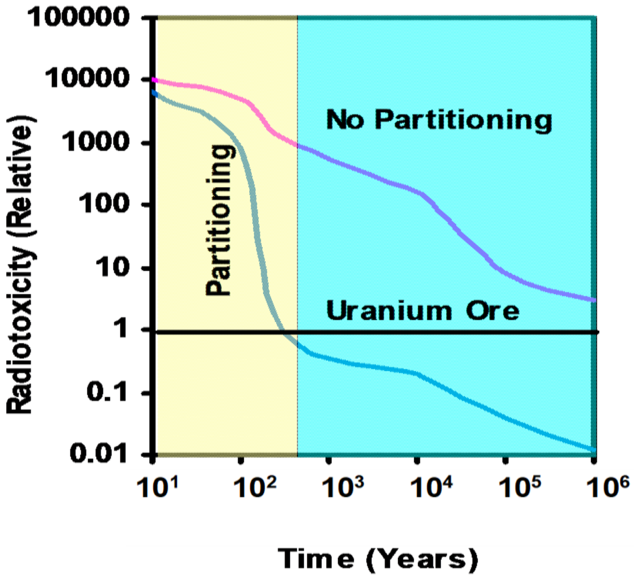

Figure 1.10: Effect of partitioning on radiotoxicity inventory

Transmutation is the general name given to any process in which one chemical element is converted into another. Of specific interest to P&T is neutron-induced transmutation. In this process, the nucleus of an atom absorbs a neutron. The resulting excited nucleus can de-excite through the emission of a gamma photon (radiative capture) and radioactive decay or through fission thereby to other chemical elements. It is the aim of transmutation to convert long-lived radionuclides into shorter-lived or stable nuclides. For transmutation, both thermal and fast neutrons can be used. Thermal neutron reactions generally have higher cross-sections and high reaction rates than fast neutron reactions. However, it may be noted that more number of thermal neutrons are required for transmutation compared to that of fast neutrons. This results in a problem of neutron economy. Currently it is believed that the optimum solution for transmutation lies in the use of fast neutrons reactors including moderated zones. Transmutation of nuclear wastes is interesting from different points of view: the economics (energetic potential of the plutonium), environment (reduction of the hazard associated with the spent fuel) and fuel cycle security (alleviate proliferation risk).

In the direction of transmutation of long lived radionuclides, Department of Atomic Energy, India is designing [30] Accelerator Driven Sub-Critical Reactor System (ADSS). The ADSS will have 3-4 orders higher neutron flux than that available in present reactors (PHWRs, FBRs etc.). This will facilitate into more efficient transmutation/incineration of long lived minor actinides and fission products.

Study on P&T has important bearing for management of HLW and a beginning has been made to achieve the objective in terms of separation and recovery of valuable isotopes such as ^{137}Cs from high level waste and its deployment as blood irradiator for societal benefits,^{90}Sr/^{90}Y has therapeutic applications and ^{106}Ru is also used for eye cancer treatments.

1.15 Properties of glasses

The vitrified waste form must have certain qualities so that its interim storage and ultimate disposal is technologically feasible, safe and economical. The desirable properties of vitrified waste product (VWP) is listed in Table 1.3 as follows:

Table 1.3: Desirable properties of waste form

Sr. No.	Desirable properties
1	Incorporates and immobilizes wide range of radionuclides into chemically durable waste form
2	Established long term integrity
3	Good thermal and radiation stability
4	Provides high volume reduction
5	Highly corrosion resistant
6	Well established manufacturing technology
7	Inexpensive raw materials

A desirable candidate matrix fulfils following criteria.

- ⇒ **Homogeneity**: There should be homogeneous distribution of radionuclides and glass forming chemicals in the vitrified waste product.
- ⇒ **Waste loading**: Product should have ability to contain high proportion of waste to have high volume reduction.
- ⇒ **Thermal conductivity**: Product should have good thermal conductivity so as to facilitate dissipation of heat associated with radioactivity contained in HLW.
- ⇒ **Good chemical durability**: Product should have low leachability in water, a principal mechanism through which radio nuclide can migrate to human environment.
- ⇒ **Viscosity**: Product should have optimum viscosity so that molten vitreous mass can be drained safely into canister.

⇒ **Mechanical strength**: Product should have desirable mechanical strength, so that generation of additional surface area during transport/disposal in accidental conditions can be minimized.

⇒ **Radiation Stability**: Product should have good radiation stability with respect to alpha, beta and gamma radiation.

Among others, chemical durability is the most important parameters of vitrified waste form as it ensures the containment of radionuclide not to go to the biosphere so that it will not come in contact with common public.

1.16 Chemical durability

Chemical durability of nuclear waste glasses is the most important property of nuclear waste glasses and is expressed as leachability or dissolution or corrosion of glasses. Leachability is given in terms of leach rate of nuclear waste glasses. Leach rates are calculated as amount of particular element released or the weight of glass dissolved in leachant per unit of surface area of the glass per unit of time of the experiment in which the glass is in direct contact with the leachant.

Chemical durability has been used to express the resistance offered by glass towards attack by aqueous solution. The term chemical durability of glasses or dissolution of glasses are interchangeable and used to refer glass corrosion. Chemical durability is measured in terms of leaching studies. First the basics of how the leaching mechanism takes place are discussed. When a glass comes in contact with an environment, such as flowing or stagnant ground water, leaching or chemical reaction occurs at the surface.

1.17 Basics of leaching mechanisms

Leaching is a complex phenomenon. As shown in Figure 1.11 below, the elements from glass leach out from glass into the leachant (environment), which is usually water and it is in direct contact with the glass.

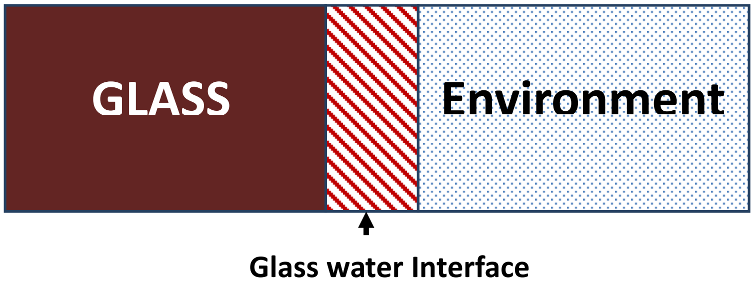

Figure 1.11: Leaching of glass in water

The basic mechanism of leaching is that, water begins to diffuse into the glass matrix (hydration) and an alkali metal ion is exchanged by hydronium ion (inter-diffusion) from water [31,32,33,34,35].

$$\equiv \mathrm{Si\text{-}O\text{-}Na} + \mathrm{H_2O} \rightarrow \equiv \mathrm{Si\text{-}O\text{-}H} + \mathrm{Na} + \mathrm{OH^-} \qquad ....[1]$$

The hydroxyl ion left behind in the water increases the pH of the leachant and also further reacts with the silicate network which continues leaching of the glass further.

$$\equiv \mathrm{Si\text{-}O\text{-}Si} \equiv + \mathrm{OH^-} \rightarrow \equiv \mathrm{Si\text{-}O\text{-}H} + \equiv \mathrm{Si\text{-}O^-} \qquad ....[2]$$

The $\mathrm{Si\text{-}O^-}$ formed further reacts with H_2O molecule producing OH^- ion.

$$\mathrm{Si\text{-}O^-} + \mathrm{H_2O} \rightarrow \mathrm{Si\text{-}O\text{-}H} + \mathrm{OH^-} \qquad ....[3]$$

The OH^- ion produced in equation [3] above is free to react as equation [2].

The reactions occurring at the glass surface leads to the formation of different layers at the glass water interface as shown in the Figure 1.12 below.

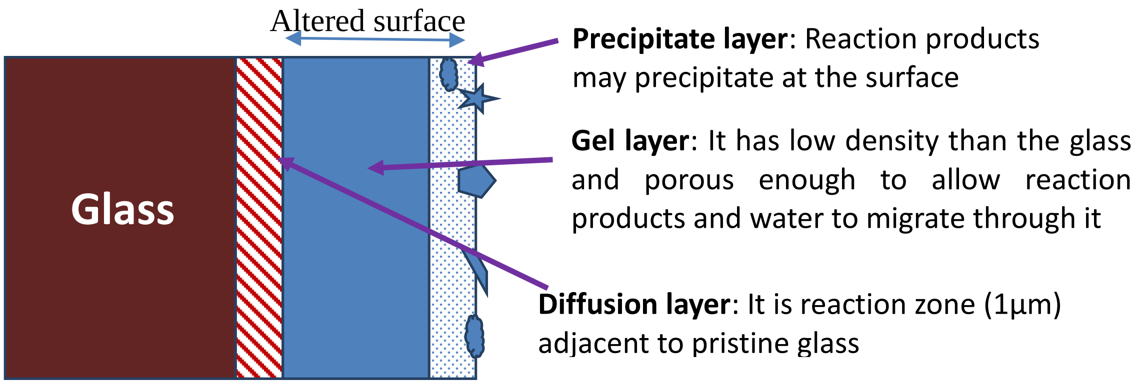

Precipitate layer: Reaction products may precipitate at the surface

Gel layer: It has low density than the glass and porous enough to allow reaction products and water to migrate through it

Diffusion layer: It is reaction zone (1µm) adjacent to pristine glass

Figure 1.12: Formation of layers at glass water interface

The release of Si from glass into contact solution as silicic acid occurs when bonding oxygen bond associated with silicon (Si) are hydrolysed as shown by equation [4] and [5]. [36,37]

$$\equiv\mathrm{Si\text{-}O\text{-}Si(OH)_3 + OH^-} \rightarrow \equiv\mathrm{Si\text{-}O^- + Si(OH)_4} \qquad .....[4]$$

$$\equiv\mathrm{Si\text{-}O\text{-}Si(OH)_3 + H_2O} \rightarrow \equiv\mathrm{Si\text{-}OH + Si(OH)_4} \qquad ....[5]$$

This kinetics is termed as initial/forward dissolution rate (r_o).

As the dissolved silica concentration increases, the dissolution rate decreases, termed as, residual rate (r_r). The decrease in rate is attributed to a decrease of the affinity of the hydrolysis of the silicate network and the formation of an amorphous layers (i.e. gel) that becomes transport limiting in silica saturated conditions. The different leach rate stages with time are as depicted in Figure 1.13.

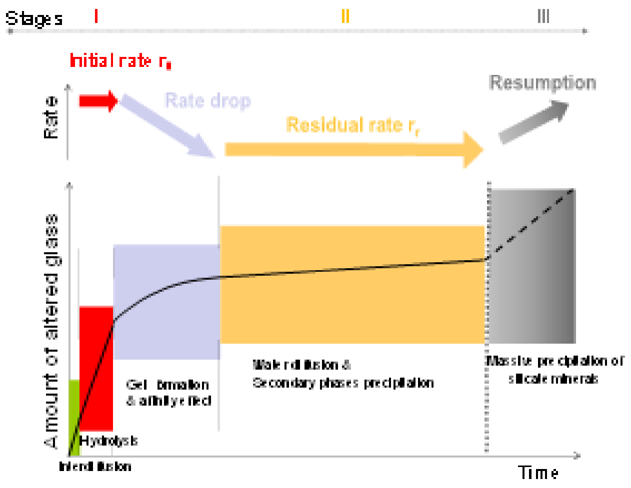

- **Initial rate r_0**:The kinetics of congruent release of Si from glass into contact solution as silicic acid occurs when bonding oxygen bond associated with Si are hydrolysed.
- As the dissolved silica concentration increases, the dissolution rate decreases, **Rate drops**.
- The transition between rate drop and the **residual rate r_r** occurs once the solution is saturated with respect silicon.
- Glass alteration gets accelerated (**Resumption**) when precipitation of silicate minerals occurs.

Figure 1.13: Glass dissolution kinetics[38]

The mechanisms proposed for the formation of the gel layer on the glass surface are either precipitation of silica rich layer or in-situ condensation of Si-O bonds forming porous gel layer or combination of both may occur. In the next section, the factors affecting the leaching mechanism to take place will be discussed.

1.18 Factors affecting leaching

Leaching is affected by various factors. Most of the leaching factors are interdependent and it is difficult to predict effect of one factor alone on leaching of glasses. Leach rate values are always expressed along with the leaching factors involved such as time and temperature. Leaching is interdependent on glass composition, leaching methods and the disposal conditions. The factors affecting leach rate are broadly classified as follows[39].

a) Leaching system (temperature, pressure, time, radiation environment and ratio of surface area to volume of leachant)

b) Leachant (composition, pH, flow or replenishment frequency)

c) Solid being leached (composition, surface conditions)

Leaching system comprises of leaching environment and experimental parameters under which leaching process takes place. Experimental parameters such as temperature, pressure, time and ratio of surface area to volume of leachant affects leaching significantly.

1.18.1 Time

Leaching is function of time. Leach rate of fresh samples decreases with time. At early stages of leaching a negative square root of time is observed and usually associated with a diffusion controlled mechanism of leaching [40]. After initial rapid leaching, the leach rate is then becomes time independent predicting the dissolution or corrosion mechanism [41]

1.18.2 Temperature

Leaching increases with increase in temperature. Temperature affects dissolution behaviour by increasing the rates of surface reaction i.e. ion-exchange and diffusion [42]. Higher temperatures will increase the rate of water diffusion faster that the rate of surface reaction. This will favour the formation of surface hydration layers in high temperature dissolution tests [43].

The relationship of leaching with temperature is described by Arrhenius equation [44]

$$LR = k\ exp^{-Ea/RT} \quad \dots\dots\dots[6]$$

Where, Ea is activation energy.

1.18.3 Pressure

Leaching experiments at elevated pressures are generally done at hydrothermal conditions, where both temperature and pressure are increased together. These conditions are useful to study the alteration products formed during leaching which otherwise takes years of time to get in case of static leaching tests.

1.18.4 Ratio of surface area to volume

The ratio of surface area (SA) of the glass to volume of leachant (V) does affect leachability. As the leachant becomes more dilute, SA/V decreases but the apparent leachability increases. Due to concentration gradient effect leaching kinetics gets accelerated.

1.18.5 Leachant

Leachant affects the leaching process. Generally, demineralised water is taken as leachant for leaching experiments. As it has high concentration gradient so the ion exchange of alkali metals takes place faster in demineralised water than the solutions already having higher salt contents of sodium etc. in the water. The pH of the leachant has strong impact on leaching of glasses. The leach rate increases at higher pH values (>9) and at lower pH values (<4) whereas it is lower at neutral pH solutions.

1.18.6 Solid being leached

The glass composition has impact on the leaching. If two glasses of different alkali content are being leached in distilled water, then the glass with high alkali content will rapidly ion-exchange and raise the pH of the solution to a higher value than the less alkali content glass. And as seen, the leach rate will increase due to higher pH values. Also it is seen that addition of aluminum and zirconium to the glass will increase the leach resistance to glass.

1.19 Methods for evaluation of chemical durability

Leaching studies are done using different leaching methods. An exhaustive list of leaching test processes is given in Table 1.4. Some of the methods have been listed by IAEA. These standard tests determine water durability for vitrified waste product. Tests developed at Materials Characterization Centre (MCC) of Pacific Northwest National Laboratory in US, are now internationally approved standard tests and commonly used worldwide (Table 1.5).

Table 1.4: Leaching tests of glasses

Sr No	Leaching Test	Temperature (°C)	Leachant	Flow Rate	Sample Geometry	Ref
1	PCT	90	Deionized water	Static	Powder	45
2	MCC-1	40, 70, 90	Distilled water and reference ground water	Static	Monolith SA/V = 10 m^{-1}	46
3	MCC-2	110, 150, 190	Distilled water and reference ground water	Static	Monolith SA/V = 10 m^{-1}	38
4	MCC-3	40, 90, 110, 150, 190	Distilled water and reference ground water	Static (agitated)	Crushed 1)149-175µm 2)<45µm	38
5	MCC-4	40,70,90	Distilled water and reference ground water	Static	Monolith SA/V = 10 m^{-1}	38
6	MCC-5 soxhlet	100	Distilled water	~1.5 cm^3/h	Plate, $S=4cm^2$	38
7	MCC-14	25-200	Repository ground waters	Static or periodic sampling	Monoliths and powders	38

8	Grain titration	100	Distilled water	Static	Powder	37
9	Time-dependent	20- ~60	Buffered water	Static	Monolith SA/V = 10 m^{-1}	38
10	Repository simulation	25-90	Granite equilibrated water	Static	Plate SA/V =3cm^2	38
11	Low-flow	25-90	Distilled water	1 cm^3/wk	Plate, SA = 4 cm^2	38
12	HILT (CEC)	90, 110, 150, 190	Distilled water	Static		47
13	Autoclave (HMI)	150-200	Distilled water and brines	Static	Beads or chips	48
14	Autoclave (KfK)	100, 150, 200, 250	Distilled water and brines	Static	Cylinders SA/V =20 or 5cm^2	49
15	Waste / water / rock leach	98	Distilled water or granite water		Glass cube SA/V =6 cm^2 20 g granite powder: 250-710 µm, 60 cm^2 water	50
16	Soxhlet (PNC)	70, 100	Distilled water	60-225 cm^3/h	Bar, SA=2 cm^2	42
17	HIPSOL (HT soxhlet)	100-300	Distilled water	100-900 cm^3/h	Powder or block	51
18	Soxhlet	50-100	Distilled water	1.5 cm^3/min	Plate, SA=3 cm^2	52
19	Modified soxhlet	35-100	Distilled water	Variable	Grains or plate SA = variable	53
20	Hot-cell soxhlet	100	Distilled water	80 cm^3/h	Beads / plates / chips SA = variable	54
21	IAEA	25	Distilled water	Periodic replace-ment	Cylinders with exposed surfaces	55

22	ISO Buffer	23-100	Distilled water, buffers and sea water	Periodic replacement	Monoliths	[47]
23	Powder (P1)	95-200	Distilled water	Periodic replacement	Powder, 100-150 µm	[56]
24	Powder (P2)	40-100	Distilled water	Daily replacement	Powder, 100-150 mesh	[57]
25	Dynamic	35-90	Distilled water	3-1, 200 cm^3/h	Grains or monoliths	[58]

Most important tests are given in Table 1.5 below:

Table 1.5: Common leaching tests

Standard test	Test conditions	Use
ASTM C1220-10/MCC-1 test/ISO 6961	Deionised water, static, monolithic specimen, S/V $10m^{-1}$, open to atmosphere temp 25°C, 40°C,70°C and 90°C	For comparison of waste form
ASTM C1220-10/MCC-2	Deionised water, closed, temp 90°C	Same as above but at higher temperature
ASTM C1285/PCT/MCC-3	Product consistency test, stirred with glass powder, closed, various temperatures	For durable waste forms to accelerate leaching
ASTM C1662/SPFT/MCC-4	Single pass flow through test, deionised water, open to atmosphere.	Used for calculating activation energy and reaction in progress of waste form
ASTM C 1663 VHT	Vapour hydration test, monolithic specimen, high temperatures	Accelerates alteration product formation

1.20 Motivation of the present research

Based on the above discussion, it can be stated that leaching experiments were performed under different conditions as discussed in the different leaching methods. Leaching studies have certain aspects:

a) The ability to predict glass durability and produce glasses to meet specific leaching criteria based on short term tests.

b) The ability to predict the long term dissolution behaviour (of the order of 10,000 year or more).

For the short term, ASTM leaching tests or product consistency tests can be used, but for the long term tests done in laboratory to predict the dissolution of glass for extended period of time. Static experiments are developed using leachant as granitic water. The long term static leaching experiments conducted to evaluate the durability of waste glass as the host matrix for immobilization of high level radioactive liquid waste streams. The disposal of the vitrified waste product is done in deep geological repository, so the case considered here is that of the flooded vault. Ground water flows and its composition is site specific, but the flows are expected to be very small. Given the low water turnover, a static, non-replenished leach test seemed to be the most appropriate choice for the evaluation of candidate waste forms. The temperature at any waste form/water interface would not exceed 100^{o}C, so the experiments were done at three different temperatures viz 50^{o}C, 70^{o}C and 90^{o}C. Two different vitrified waste glasses were tested to study effect of glass composition along with international standard glass which is taken for reference. The roles of silicon, boron and sodium on leaching have been examined.

Chemical durability or leaching in the repository conditions will be in groundwater by which radionuclides could be released from the glass and migrate through the host rock. This condition motivated that the ideal leachant would be granitic rock equilibriated as well as clay equilibriated ground water representative of an area around an actual waste repository. Also, demineralised water was used as leachant, as it provides high concentration gradient as well as gives neutral pH values to start with so that leaching processes can be compared and studied. The leaching time duration was kept for one year.

Accelerated leaching tests were performed by exposing higher surface area of the vitrified waste product sample, at high temperature to enhance the rate of dissolution and using demineralised water as leachant thereby producing large concentration gradient. The objective of putting these stringent conditions is to generate leach rate data within realistic time frame and use them as input in suitable mathematical models for prediction of release of radionuclides as a function of time and composition of glass. So, leaching tests done at accelerated conditions such as high temperature and pressure to study the glass alterations, which are sometimes not possible in temperatures lower than 90ºC and the lower time scales. After completion of the experiment, the complete analysis of the leached solution for all the glass components and a detailed analysis of the leached glass surface were done to get the information about the rate and mechanisms of various elements coming out from glass.

1.21 Scope of the present thesis

The present thesis focuses on the chemical durability assessment of borosilicate glasses used for the immobilization of high level nuclear radioactive waste. For the study, high level radioactive waste streams of two different origin viz., (i) high level radioactive waste generated from reprocessing of PHWR's where uranium is the main matrix element and (ii) thorium containing waste generated from reprocessing of thoria irradiated rods with thorium is the main matrix element, were identified. These high level waste streams are characterized for its radiochemical composition. Suitable borosilicate glass formulations are developed for the selected nuclear waste solutions. The prepared glasses are characterized for its homogeneity, thermal stability and chemical durability. The chemical durability study in terms of leaching was done using different types of static leach tests, including (i) ASTM leach tests (ii) leaching under disposal conditions and (iii) accelerated leach tests. Study of altered phases of the glasses after leaching tests was done using different characterisation techniques such as XRD, SEM, DTA, FTIR and NMR etc. The comparison of the outcome of leaching tests of the glasses was done with International simple glass (ISG). For comparison purpose natural analogue such as basalt glass alteration studies were done which was being leached for many years was collected from hot water springs region from Vajreshwari, Maharashtra.

1.21.1 Stepwise research work followed

The research work is undertaken in following steps, as follows.

1. HLW Waste characterization for two HLW streams originating from PHWR and thorium containing waste
2. Development of glass formulations for immobilization of two selected HLW streams.
3. Detailed characterization of the synthesized glasses (Homogeneity, thermal stability, chemical durability using standard ASTM test etc).
4. Study of long term leaching tests of vitrified waste products in demineralised as well as ground water in near disposal environments.
5. Study of leach rate of (a) International reference glass (b) Natural analogues (basaltic) for comparison purpose.
6. Accelerated leach tests to study alteration products.
7. Analysis of leachant using ICP-AES system.
8. Detailed examination of leach surface to understand structural modification.
9. Understanding the leaching mechanisms.

The results will be discussed in subsequent chapters.

References

---

[1] Kakodkar A, “Shaping the third stage of Indian Nuclear Power Programme” presented at 12th Annual Conference of Indian Nuclear Society (INSAC- 2001), Indore, India.

[2] World Nuclear Association Report, “Nuclear power in India”, Oct. 2008.

[3] Kakodkar A, “Indian nuclear power programme- Materials Challenges”, Proc. Inter. Symp. on Energy Related Materials, Mumbai, India (2007)1.

[4] Ganguly C, “International scenario on conventional and advanced nuclear fuels and fuel structurals, Proc. Inter. Symp. on Energy Related Materials, Nehru Centre, Mumbai, India (2007) 30.

[5] Kakodkar A, Nuclear Energy (2006) 53.

[6]Atomic Energy Regulatory Board (2003), “Safety Code on Establishing Radioactive Waste Management System”, Department of Atomic Energy, India.

[7] Raj K, Prasad KK, Bansal NK, “ Radioactive Waste Management Practices in India”, Nucl. Engg. Design, 236 (2006) 914.

[8] Mohapatra M. and Tomar BS, “Spectroscopic Investigations of Radiation Damage in Glasses Used for immobilisation of Radioactive Waste”, Defect and Diffusion Forum, 2013.

[9] Lutze W and Ewing RC (EDS), “Radioactive waste Forms for the Future”, (North Holland, Amsterdam, (1988) 31.

[10] Kaushik CP, “Indian Program for Vitrification of High Level Radioactive Liquid Waste”, Procedia Materials Science, 2014

[11] Jantzen CM, Advances in ceramic, 20 (1986) 703.

---

[12] Jantzen CM, “Thermodynamic approach to glass corrosion”, Corrosion of Glass Ceramic and Ceramic Superconductor, (1992) 153.

[13] Ellision AJ., “Evaluation of model of waste glass durability”, Argoune National Laboratory, Argoue. IL., 1995.

[14] White, et.al., “Dissolution mechanism of nuclear waste glasses, a critical review, Advance in Ceramics, 20 (1986) 431.

[15] Wicks GG, “Nuclear Waste glasses solubility, surface studies and stability” WSRC-MS-99-000082, Waste Management, Savarnnath River Technology Center, Arken, SC., 1999.

[16] Wicks GG., Nuclear Waste Glasses treatise Material Science and Technology 26 (1985) 57.

[17] Zachariasen WH, J. Am. Chem. Soc. 54 (1932) 3841.

[18] Sun KH, J. Am. Ceram. Soc. 30 (1947) 271.

[19] Vitrification Technologies for treatment of Hazardous and radioactive waste, 1992, EPA/625/R-92/002 Rev.00, prepared for office of Research and Development, Washington, DC.

[20] Dey PK, Bansal NK, Spent fuel reprocessing; A vital link in Indian nuclear power program, Nucl Eng Des 236 (2006) 723–729

[21] Raj K, Prasad KK, Bansal NK, Radioactive waste management practices in India, Nucl Eng Des 236 (2006) 914–930.

[22] Dey PK, Wattal PK, Back-end of fuel cycle. In: Proceedings of international conference on peaceful uses of atomic energy, Nuclear Fuel Cycle, Vigyan Bhavan, 2 (2009) 343–349.

[23] Dey PK, Gupta AK, Achuthan PV, Kaushik CP, Yalmali V, Thorium utilization – back-end challenges. In: Proceedings of international conference on peaceful uses of atomic energy, Nuclear Fuel Cycle, Vigyan Bhavan, 2 (2009) 350–357.

---

[24] Vaswani GA, Jahgirdar PB, Rastogi RC, Sundar Rajan NS, Development of suitable radioactive waste product with low formation temperature and improved leach resistance – a practical approach, Internal report BARC-1028. Bhabha Atomic Research Centre, Mumbai, 1979.

[25] Jahagirdar PB, Wattal PK, Vitrification of sulphate bearing high level wastes in borosilicate matrix. Waste Manage 18 (1998) 265–273.

[26] Kaushik CP, Mishra RK, Sengupta P, Kumar A, Das D, Kale GB, Raj K, Barium borosilicate glass- a potential matrix for immobilization of sulfate bearing high level radioactive liquid waste, J Nucl Mater 358 (2006) 129–138

[27] Mishra RK, Sengupta P, Kaushik CP, Tyagi AK, Kale GB, Raj K, Studies on immobilization of thorium in barium borosilicate glass. J Nucl Mater 360 (2007) 143–150.

[28] Raj K, Prasad KK, Bansal NK, Radioactive waste management practices in India, Nucl Eng Des 236 (2006) 914–930.

[29] Banerjee K, Raj K, Wattal PK (2011) Process technology for vitrification of high-level radioactive liquid waste. In: Proceedings of international conference on peaceful uses of atomic energy, Nuclear Fuel Cycle, Vigyan Bhavan, 2 (2009) 489–495.

[30] Singh P, Rao SVL, Rajni Pandey, Basak T, Shweta Roy, Aslam M, Jain P, Srivastava SCL, Rajesh Kumar, Nema PK, Kailas S and Sahni VC, Pramana, J. Phys., 68 (2007) 331.

[31] "Present understanding of R7T7 glass alteration kinetics and their impact on long-term behaviour modelling", Vernaz E, Gin S., Jegou C, Ribet I, J. Nucl. Mater, 298 (2001) 27-36.

[32] Boksay, Z.,Bouquet, G. and Dobos, S. Diffusion processses in surface layers of glass. Phys. Chem. Glasses 8 (1967) 140-144.

[33] Ojovan, M. I., Pankov, A. & Lee, W. E. The ion exchange phase in corrosion of nuclear waste glasses. J. Nucl. Mater. 358 (2006) 57-68.

---

[34] Gin et al, The controversial role of inter-diffusion in glass alteration, Chem. Geol. 440 (2016) 115-123.

[35] Doremus, RH., Interdiffusion of hydrogen and alkali ions in a glass of surface. J. Non-Cryst. Solids 19 (1975) 137-144.

[36] Hench L, Physical chemistry of glass surfaces. J. Non Cryst. solids 25 (1977) 343-369.

[37] Techer, I, Advocat, T, Lancelot J and Liotard, JM, Dissolution kinetics of basaltic glasses: control by solution chemistry and protective effect of the alteration film. Chem. Geol. 176 (2001) 235-263.

[38] Gin S, Abdelouas A, Criscenti LJ, Ebert WL, Ferrand K, et al., “An International Initiative on Long-Term Behavior of High-Level Nuclear Waste Glass,” Mater. Today, 16 (2013) 243–8.

[39] “An overview of factors affecting the leachability of nuclear waste forms”, Stone JA, Savannah River Laboratory, Nuclear and chemical waste management, 2 (1981) 113-118.

[40] Godbee HW and Joy DS, Assessment of the loss of radioactive isotopes from waste solids to the environment, Part-I: Background and theory, ORNL-TM-4333, Oak Ridge National Laboratory, Oak Ridge, TN (1974)

[41] Mondal JE, A review of leaching test methods and the leachability of various solid media containing radioactive wastes, BNWL-1765, Pacific Northwest laboratory, Richland, WA (1973).

[42] Smets BMJ, Tholen MGW and Lommen TPA, J. Non-Cryst. Solids, 65 (1984) 319.

[43] Petil JC, Della G, Mea, Dran JC, Magonithier MC, Mandona PA, Paccagnella A, Geochim et Cosmochim Acta 54 (1990) 1941.

[44] Stone JA, An overview of factors affecting nuclear and chemical waste management, 2 (1981) 113-118.

[45] American Society for Testing and Materials. Determining Chemical Durability of Nuclear, Hazardous, andMixed Wmte Glasses: The Product Consistency Test. Annual

---

Book of ASTM Standards. ASTM C 1285-97.West Conshohocken, PA: American Society for Testing and Materials., 12.01 (1997) 774-91.

[46] U.S. Department of Energy. Nuclear Waste Material Handbook (Test Methods) Technical Information Center**.**DOE/IIC-11400. Washington, DC: **U.S.** Department of Energy. 1981.

[47] Deutsches Institut for Normung. DIN Leach Test**.** Report 121 1 1. Deutsches Institut for Nomung. 1976.

[48] Van Iseghem, P., et al. Chemical Stability of Simulated HLW Forms in Contact with Clay Media. EUR-8424. CCC.1983.

[49] European Community Static High Temperature Test Summary. CEC Report EUR 9772., 1985.

[50] Altenhein, FK, et al. Scientific Basic International Symposium Proceedqs for the Nuclear Waste Management:.(1981) 363-370.

[51] Kahl, L, Ruiz-Lopez MC, Saidl J, and Dippl T, Preparation and Characterization of an Improved Borosilicate Glass for Solidification of High-Level Radioactive Fission Product Solutions. Part 2: Characterization of the Borosilicate Glass Product. GP 98/12. Kernforschungszentrurn Karlsruhe Report KFK-3251e., 1982.

[52] Igarashi, H. et al., Leaching test of simulated HLW glass in the presence of rock. Atomic Energv Society of Japan, Annual Meeting, 1983.

[53] Senoo, M. et al., High-pressure Soxhlet-Type Leachability Testing Device and Leaching Test of Simulated High-Level Waste Glass at High Temperature. JAERI-M-8571. Japan Atomic Energy Research Institute, 1979.

[54] Nakamura H and Toshiro S, Safety Research of High-Level Waste Management for the Period April 1982 to March 1983**.** Progress Report JAERI-M-83476, Japan Atomic Energy Research Institute, 1983.

---

[55] Hussain, M and Kahl L, Incorporation of precipitation from treatment of medium-level liquid radioactive waste in glass matrix or ceramics together with high-level waste. Symposium Proceedings for the Ceramic in Nuclear Waste Management, 1979.

[56] Commission of the European Communities, Testing and Evaluation of Solidified High-Level Waste Fonns**.** Joint Annual Progress Report EUR 10038, Commission of European Communities (CEC), 1983.

[57] Draft International Standard Report. ISO/DIS-696 1, 1979.

[58] Oversby VM and Ringwood AE, Leaching studies on Synroc at 95 and 200 "C. Radioactive WasteManagement 23 (1982) 223.

Chapter- 2 :

Experimental and Characterization Techniques

Experimental Methods and Characterization Techniques

2.1 Introduction

This chapter deals with the methods of glass preparation and salient features of instruments and techniques deployed for their detailed physico-chemical characterization and property measurement. Instruments like Powder X-ray Diffraction (XRD), Scanning electron microscope (SEM), Magic Angle Spinning Nuclear Magnetic Resonance spectroscopy (MAS NMR), Fourier Transform Infrared spectroscopy (FTIR), Differential Thermal Analysis (DTA), Flame photometry, UV-VIS spectrophotometry, Inductively Couples Plasma – Optical Emission Spectrometry (ICP-OES) and Gamma spectrometry were extensively used for physico-chemical characterization and property measurement.

Nuclear counting systems like Geiger-Muller counter, Scintillation counters were used for estimation of radioactivity contents in the radioactive liquid waste. Instruments like Flame Photometer, UV-Visible spectrophotometer and ICP were used for carrying out detailed chemical analysis of high level radioactive liquid waste. Details of analysis carried out cover presence of alkali metals, alkaline earth metals, transition metals & non-metals, rare earths, actinides and anions like nitrates, sulphates and phosphates. Detailed analysis of waste becomes an important exercise for developing a suitable glass formulation for immobilization of high level radioactive liquid waste (HLW). High temperature furnaces were used for preparation of large number of glasses. Analytical instruments like XRD and SEM/EDS were used for characterization of VWP samples with respect to homogeneity and distribution of different constituents within the matrix. MAS-NMR and FTIR techniques were utilized for structural elucidation of the glass samples. DTA was used for finding out glass transition temperature of glass product samples.

2.2 Waste characterization

2.2.1 Nuclear counting system

The instruments described under this topic are mainly dealing with the detection & measurements of alpha, beta and gamma rays. Radiation detectors are based on the principle that the radiation while passing through the matter deposits its energy through formation of charge carriers either directly or indirectly in the detector volume. Here the detection system is used to get information on the number of disintegrations only, hence it is a gross counting system.

2.2.1.1 Geiger Muller (G-M) counter

When the GM tube has a potential between the cylinder and the metal wire (cathode & anode) in the range of 1000 to 1500 volts, the internal amplification is as high as 108 & the number of ion pairs produced is independent of primary ionization. A plot between applied voltage and pulse size of gas ionization detectors has been depicted in Figure 2.1. It consists of a copper cylinder (cathode) with a mica window at one end. The Cu cylinder is surrounded by a hard glass tube. The Cu cylinder is about 10cm long with a diameter of 2cm. A fine tungsten wire about 0.05mm thick which acts as anode is suspended in the cylinder. The tungsten wire is insulated from the Cu cylinder.

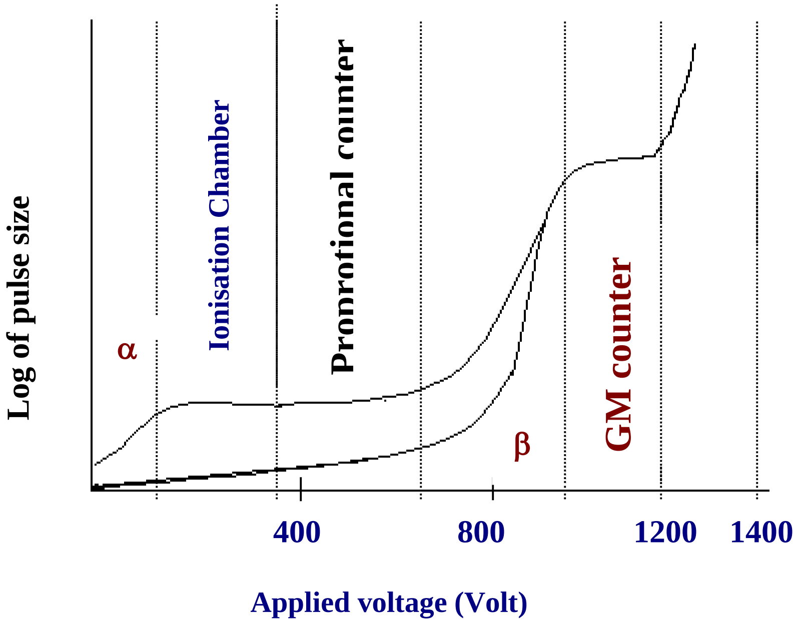

Figure 1.1: A plot between applied voltage and pulse size of gas ionization detectors

The cylinder is filled with a mixture of 90% argon and 10% ethyl alcohol vapours. Argon provides the ion pairs while alcohol serves as the quenching gas. It prevents the formation of secondary ion pairs. The mica window prevents the escape of the gases from the Cu cylinder to the atmosphere. However, it is so thin that it does not prevent the penetration of α or β particles through it, into the cylinder. A radioelement is placed close to the mica window. The nuclear radiation is allowed to enter the cylinder and the measurement starts. In the beginning a voltage of about 100 V is applied & the number of counts per unit time is noted. The voltage is then increased in stages, about 50 V at a time. The rate of counts goes on increasing. When the Geiger Potential is reached, the number of counts per minute becomes essentially constant as shown as shown by the horizontal portion. The range of potential over which this occurs is known as Geiger

Plateau. Beyond this a continuous discharge takes place and counting becomes possible. This voltage is used for measurement of counts per minute, (CPM). The magnitude of this voltage depends upon the geometry of the cathode & the anode.

Under this high voltage, internal amplification is as high as 10^8 times the primary ionization. The current causes a flash of light in a Ne tube and a unit movement over a mechanical counter. The counts per minute are noted for a given source.

2.2.1.2 Scintillation counter

Ionizing radiations produce luminescence in substances like ZnS, diamond & barium platinocyanide. This luminescence when observed under a microscope proves to be consisting of a large number of individual tiny sparks or scintillations. The substances which show this luminescence are known as phosphors. The scintillations can be counted by converting a feeble light of single scintillation into an electric pulse by photomultiplier tube. If the intensity of radiation is not too large, each alpha particle produces a distinct

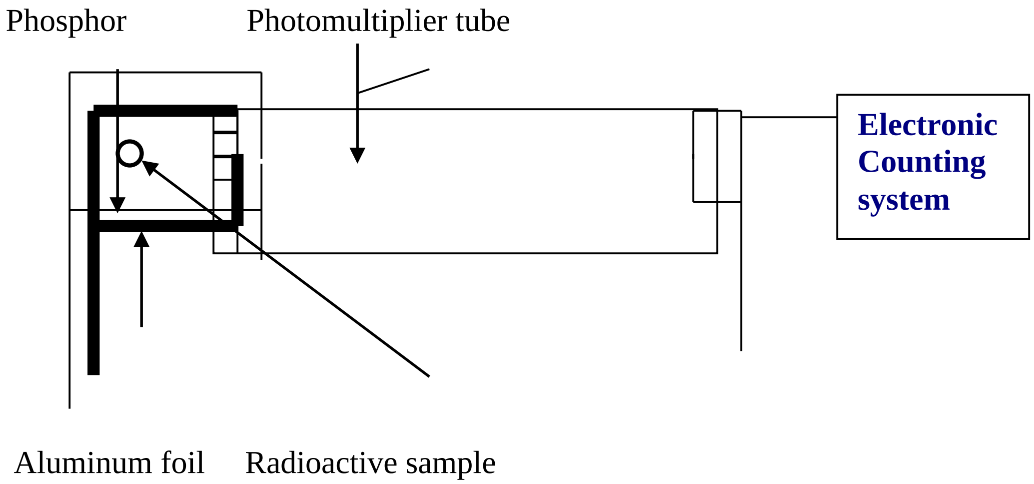

Figure 1.2: A schematic of scintillation counting system

scintillation which can be seen through microscope. Thus alpha particles can be seen through microscope. Thus alpha particles can be counted by counting the number of scintillations. Phosphors are sensitive to all three types of radiations. A modern simple scintillation counter is represented schematically in Figure 2.2.

Construction and working: It consists of three main parts:

I) Phosphor: It may be inorganic or organic compound in which luminescence is produced by nuclear radiation. Organic phosphors are naphthalene, anthracene & transstilbene. They are used in solid state. However, solutions of diphenyloxazole or terphenyl in toluene or xylene can also be used. Inorganic phosphors are NaI activated by thallium, caesium iodide activated by thallium, calcium iodide with a trace of Europium & ZnS activated by Ag. Inert gases like Ar, Kr and Xe can also be used as scintillators in the UV region.

II) Photomultiplier tube: It is essentially a vacuum tube in which a number of electrodes known as dynodes are inserted between the anode and the cathode of the tube. The dynodes produce secondary electrons in multiples of those which are incident on them & a photoelectric current is amplified.

III) Electronic Counting System: The crystal of the phosphor is surrounded by a thin Al foil and kept in contact with the photocathode of PMT. Al foil acts as a reflector. It reflects the light flashes to the photocathode. When the nuclear radiations interact with phosphor a flash of light falls on the photocathode. Electrons are ejected. These are multiplied to produce a large electrical pulse by the PMT.

2.2.1.3 Gamma ray detection system

Detection of gamma rays is based on the principle of charge produced by the interaction of radiation with detector volume. The principle mode of interaction of gamma rays with detector material utilized in detection is photoelectric effect. In this interaction, the whole energy of the gamma rays is transferred to the detector material and ejects energetic electron from one of the bound shell of the atom. High purity HPGe detector has been used in the present study to measure the concentration of ^{137}Cs, ^{144}Ce, ^{106}Ru, ^{125}Sb etc. A brief description of this detector system is given below [1].

2.2.1.4 High purity HPGe detector

High purity germanium detector with impurity levels of around 10^9 atoms/cm^3 are used in gamma ray spectroscopy. Intrinsic property of the germanium crystal is that it generates electron and hole pair under ambient conditions (band gap is 0.7 eV). In order to minimize this, the detector is generally kept under liquid nitrogen temperatures. Further, detector depletion region is made by reverse biasing of the n-p junction. A typical planner configuration of HPGe detector applied in reverse bias is shown in Figure 2.3. The interaction of gamma rays with the detector materials are similar to that of solid materials such as photoelectric effect, compton scattering and pair production. The charge produced due to these interactions is collected and processed with the use of multichannel analyser.

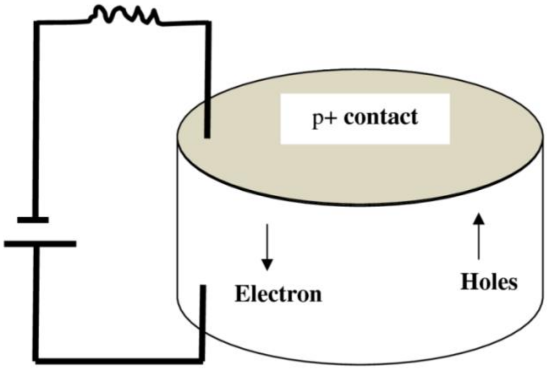

Figure 1.3: Typical planner configuration of HPGe detector applied in reverse bias

It can be noted that the lower atomic number of Ge results in a photoelectric cross section smaller by a factor of about 20 compared with sodium iodide and results in much smaller the intrinsic peak efficiency. Nevertheless, the peaks are still prominent and obvious part of the spectrum is that the line width is so small due to superior energy resolution (around 2 keV at 1332 Kev). The high resolution also helps to identify the other interaction of gamma rays with detector materials, such as compton continuum, pair production, X-ray emission, annihilation and escape peaks etc.

2.2.2 UV visible spectrophotometry

UV-Visible Spectrophotometer was used for carrying out analysis of HLW samples for various constituents like U, Fe, Cl^{-} , SO_4^{2-} and PO_4^{3-}. This instrument works on the principle of Lambert's – Beer's law. It states that equal fractions of the incident light are absorbed by successive layers of equal thickness and equal concentration of absorbing medium. Spectroscopic analysis of a substance is carried out using radiation of a particular wavelength which is absorbed to the maximum extent. This wavelength is called λ_{max} of the substance. Other wavelengths are either not absorbed or absorbed minimally. Thus a substance may show strong absorption at several wavelengths depending on its structure. It is possible to identify a particular group in a molecule by determining its λ_{max} value. In spectrophotometers, monochromators are used to produce monochromatic beams of the required wavelengths. Thus beams are incident on the sample which then absorbs its characteristic wavelengths i.e. different groups in the molecule absorbs their own λ_{max} values.

Visible absorption spectra of specimen were recorded using Shimadzu make spectrophotometer model UV-160. The equipment records absorption or transmission spectra in wavelength range of 200 - 1100 nm using socket type deuterium lamp and 50W long life halogen lamp as source of radiation for ultraviolet and visible region respectively. A photomultiplier tube is used for detection of transmitted radiation. The instrument resolution is 0.1nm with wavelength accuracy of ± 0.5nm. Accuracy of the analysis was in the range of 3-4 % in terms of error whereas relative standard deviation was observed to be less than 1 % indicating desired reproducibility.

2.2.3 Atomic emission spectroscopy

Atomic emission spectroscopy is a method of analysis which uses the intensity of the light signal emitted by excitation source either flame (flame photometry) or plasma (ICP-AES) to determine the amount of element in present in the given sample. The wavelength identifies the element while the intensity quantifies the particular element. The details of flame photometry and ICP-AES are given below.

2.2.3.1 Flame photometry

Flame photometer was used for carrying out analysis of HLW and leachant samples for sodium. In flame photometry, the liquid samples under analysis is sprayed as a fine mist into a non-luminous flame of flame photometer, which becomes coloured according to the characteristic emission of elements (Na: 589 nm, Li: 671nm, K: 768nm). The flame is monitored by a photo detector which views the flame through a selected narrow band optical filter that only passes the wavelengths centered on the characteristic emission of the selected element. The output of the photo detector is fed to an electronic module which provides digital readout of the concentration of the selected element. Before analyzing the unknown fluid sample, the system is standardized with solutions of known concentrations of elements of interest.

In a measurement setup, compressed air from a compressor is supplied to an atomizer. Due to a draught of air at the tip of the atomizer, the sample solution is sucked in and enters in a mixing chamber as a fine atomized jet. Liquid Petroleum Gas (LPG) from a suitable source is also injected in the mixing chamber at a controlled pressure. The mixture of gas and atomized sample is passed on to a burner and is ignited. The emitted light from a flame is collected by optical lenses and passed on to a photo detector through a selected filter. The output of the detector is processed by an electronic unit and the results are appropriately displayed. The instrument is housed inside the fume hood with adequate ventilation system to facilitate handling of active materials as well as exhausting gases generated during analysis.

In the present study, Systronics make Flame Photometer has been used for analysis of sodium from radioactive liquid waste, simulated waste as well as dissolved glass samples, leachant samples etc. A schematic of flame photometer is depicted in Figure 2.4.

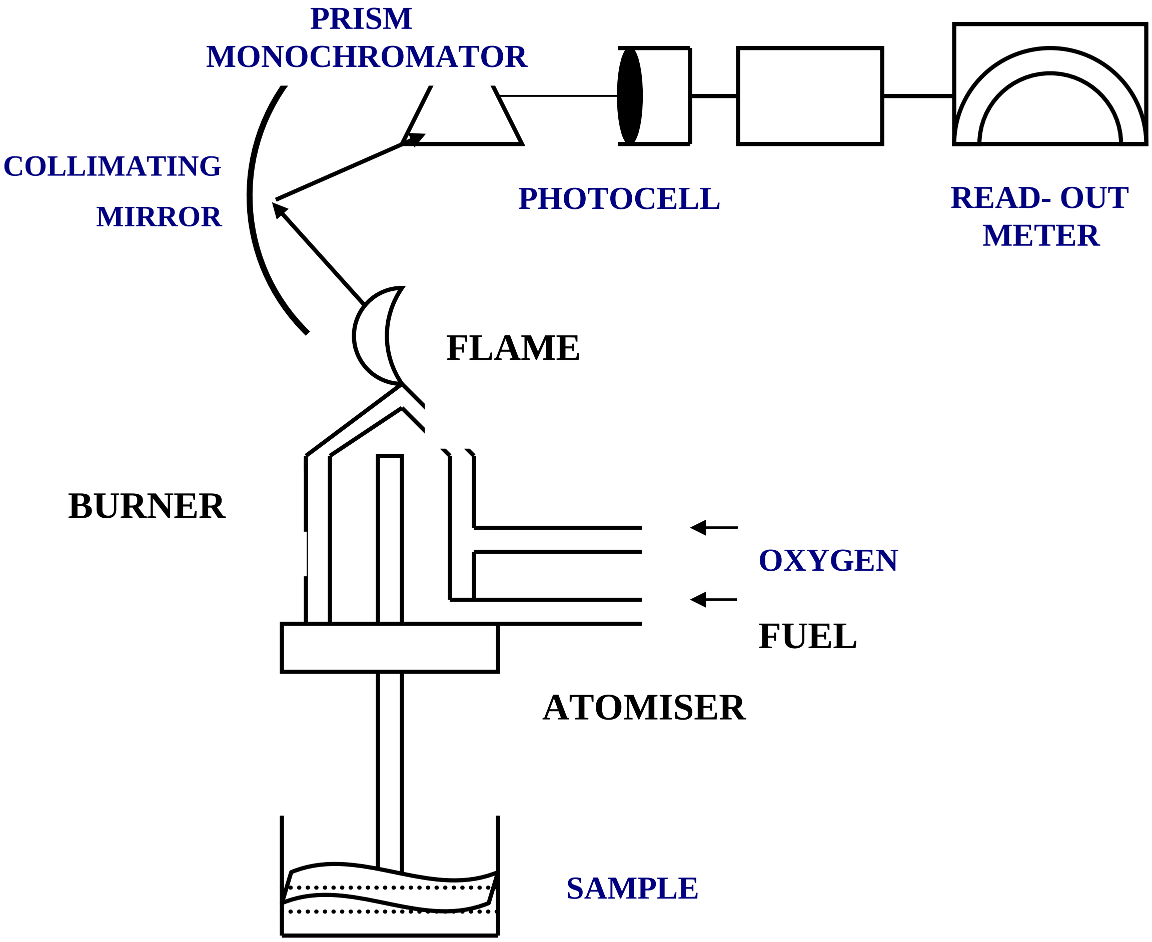

Figure 1.4: Schematic of flame photometer

2.2.3.2 Inductively coupled plasma spectroscopy (ICP-OES)

In present studies, elemental analysis of radioactive liquid wastes and simulated HLW similar to the waste arising out of reprocessing of PHWR fuel by PUREX process was carried out using ICP-AES technique after appropriate dilution. Plasma component of the unit is housed in glove box to facilitate analysis of radioactive samples. Negative pressure of the order of 25-30 mm of water gauge was maintained in the glove box. Glove box is equipped with high efficiency particulate air (HEPA) filter to retain nuclides in the glove box. Outlet of the glove box is connected to exhaustive off gas treatment system.

Among the analytical methods used for compositional analysis, inductively coupled plasma atomic emission spectrometry (ICP-AES) has been selected because of its multi-elemental capability, high sensitivity and linear dynamic range. Main steps encountered during analysis are summarized below.

2.2.3.2.1 Preparation of standards

Standard solutions for analytes were prepared from CertiPUR® ICP standard procured from E-Merck, Darmstadt, Germany. Suprapur® HNO_3 from E-Merck, Darmstadt, Germany and quartz double distilled Milli-Q® water were used throughout the investigation.

Taking appropriate aliquots from their respective stock solutions, composite/individual calibration standards were prepared during the quantitative analysis by ICP-AES. Quartz distilled acid and water were used in all the experiments.

2.2.3.2.2 ICP-AES apparatus

Glove box adopted Jobin–Yvon Ultima high resolution ICP-AES was used throughout the investigation. It has resolution of 0.005 nm and a continuous wave length coverage in the range of 200–800 nm. The instrumental and operating parameters are described in Table-2.1.

Table 1.1: Instrumental operating conditions

Parameters	Description
Focal length	1m
Grating	Holographic
Groove density	4320/2400 lines/mm
Wavelength range	120-800 nm
Resolution	<6pm from120-430nm
Frequency	40.68 MHz
Pump	Dual channel peristaltic pump
Detector	High dynamic PMT detector
Nebulizer	Concentric nebulizer with cyclonic spray
ICP-torch	Demountable, radial viewing
Operating conditions	
Coolant flow	12 L/min
Auxiliary flow	0.2 L/min
Total time of	36 s
Pump speed	20 Rpm
RF power output	1.0 kW
Input power	230 V AC

2.2.3.2.3 Sample analysis using ICP-AES

For calibration, multi-point standardization was carried out after peak search, profiling and auto-attenuation. 10 replicate measurements were carried out for reporting any value. Multi element standard solutions were prepared for the elements to be measured. The blank and standard solutions are run on the ICP system. The signal level for each element is stored as a calibration line in the computer system. The calibration curve for each element is established. The diluted sample of HLW is taken to the glove box of ICP- AES system with proper safety precautions. The sample is analysed using ICP and the concentration equivalent to the signal of each element is calculated and instrument gives the concentration of the sample element directly in mg/L. A minimum of three sequential spectral integrations are done for determining the average concentration for a single element analysis. Each sample was done is triplicate with different aliquots. A dilute acid rinse was given in between samples to ensure analyte signals return to blank concentrations.

The wavelengths of the elements selected together with their detection limits are given in Table 2.2. Detection limit is given by the smallest concentration of an element in a solution that can be determined with 99% certainty. This is the quantity of the element that gives the reading equal to thrice the standard deviation of a series of determinations with solutions of concentrations close to the blank.

Table 1.2: Detection Limits (D.L.) of few analytes in ICP-AES

Element	Analytical line (nm)	D.L. (mg/L)
Th	339.204	0.519
Al	309.271	0.0142
Fe	238.204	0.0043
Ni	231.604	0.0164
Cr	267.716	0.0004
Ce	446.021	0.0169
Na	588.995	0.0089
Sr	215.284	0.0269
U	411.61	0.2881
Mn	257.61	0.0007
Ca	396.847	0.0002
Mo	313.259	0.0366

2.3 Glass preparation

All the glass samples were prepared by conventional melt quench method. Most of the oxides were generated in situ by heating the nitrates, carbonates etc. of the corresponding elements. For effective mixing and reaction among different constituents, the reactants were thoroughly ground and subjected to different heating steps depending on the type of glass, prior to final melting and quenching process. Siliminite, zircon and platinum crucibles were used depending upon the nature of constituents of glasses. Specific details of the method of preparation of various glass samples are given in the relevant chapters.

2.3.1 High temperature furnaces

Laboratory furnaces were used for preparation of glasses. This high temperature furnace is kept inside the fume hood with adequate ventilation system to facilitate handling of active materials as well as exhausting gases generated during glass preparation. The chamber size is 155mm W × 250mm D × 200mm H. The maximum operating temperature is 1400^{o}C. The rating of the furnace is 5KW, 230V, single phase, 50Hz AC. This furnace operates on the principle of resistance heating using silicon carbide as heating elements. There are a total 6 heating elements each having resistance of 5.1 Ω. There are 3 parallel branches each having 2 elements. Heating elements are of type DS and both the ends are accessible at the top so that replacements of the same becomes easy. One number of on-off temperature controller of "Radix" make is employed. Two numbers of chromel-alumel type "Detriv" make thermocouples were used. One transformer with 230V primary and 70, 100, 140, 200V secondary taps is used. A view of furnace used for the study is depicted in Figure 2.5.

Figure 1.5: High temperature furnace

2.4 Glass characterization techniques

The glasses prepared were characterized using different techniques as described below.

2.4.1 Product pour temperature

The temperature at which the molten mass is poured is termed as product pour temperature of the glass. Product pour temperature is one of the important plant processing parameters. The type of furnace and the material of construction used for the furnace advocate the glass pouring temperature. In case of induction heating melters, where alloy 690 (Ni – Cr alloy) is the material of construction of melter, the safe operating temperature is limited up to ~1100 °C, beyond which temperature dependent mechanical deformations becomes significant. In the present case, 1000 °C was selected as the maximum allowable temperature of the glass to improve the usable life of the process pot in view of the enhanced interaction of molten glass and the melter material at higher temperature.

Pour temperatures of the base glass (glass without waste constituents) and waste glass (glass with waste constituents) made in different batches using sodium borosilicate glass formulation. A known volume of the simulated waste was mixed with the required amount of chemical additives of glass formers and network modifiers. For a batch of 100 g of glass of simulated waste was taken. The mass was then dried under infrared lamp, crushed to a fine powder and transferred to a crucible. The powder was heated at 700 °C using resistance based high temperature furnace for 2 hours and further heated at an increment of 50 °C and kept for one hour at each stage, till the mass became pourable. The crucible containing molten vitreous mass was taken out from the furnace and poured on a clean metallic surface. Since we have taken a known volume of simulated waste along with the required amount of glass forming additives, this temperature will be referred as pour temperature of the waste glass. Base glass was also checked for the pour temperature. Method for making base glass is also same, but for the addition of simulated waste. Only glass forming additive will be taken and followed the same procedure as described above.

2.4.2 Density measurement

Density of the glass samples were measured by Archimedes method, with around 1-5 g of glass samples piece using water as immersing liquid. Density measurements for each glass were made in triplicate and the average value is presented.

2.4.3 Homogeneity

Homogeneity of glass product is an important parameter in terms of product durability. As we know glass is an amorphous material, checking the homogeneity of glass in this context include a) checking amorphous nature by X-ray diffraction (XRD) and b) checking homogeneous distribution of glass forming and waste constituents by scanning electron microscope studies. A brief description of the techniques is described below.

2.4.3.1 X-ray Diffraction (XRD)

X-ray diffraction is most widely used technique to confirm the glass phase formation. For glasses, the diffraction pattern is characterized by a very broad and continuous peak. This is because glasses do not have long range periodicity, and there is considerable distribution in the bond angles and bond lengths between the constituent atoms present in the glass. Unlike this, due to the presence of long range periodicity, the crystalline materials are characterized by sharp peaks in their diffraction patterns.

In this study, the glass samples prepared were checked for its amorphous nature by XRD technique. This technique was also used for elucidating the phase purity and identification of phase, separated during glass preparation. Glass samples prepared by standard melt quench method were grounded in agate mortar and sieved through 200 mesh (ASTM) to get uniform particle size. This sieved powder was spread over a perspex sample holder and scanned by XRD. A scanning speed of 1^{o} per minute of 2θ (θ is Bragg angle) was employed and samples were scanned in the 2 θ range of 10^{o} to 70^{o} having an accuracy within 0.02^{o}.

The principle of XRD technique is based on scattering of X-rays by a crystal consisting of well-defined array of atoms, ions and molecules. Since the crystal lattice consists of parallel arrays of atoms equivalent to the parallel lines of the diffraction grating, the inter-planar spacing could be successfully determined from the separations of bright fringes of the diffraction pattern. These interplanar spacings (or distances) are of the same magnitude as the wavelength of X-rays (0.5 to 2 Å) and hence crystal planes act as diffraction gratings. Interaction of X-rays reflected by a set of parallel planes satisfying Bragg′s condition lead to constructive interference only at a particular angle. The Bragg condition for the occurrence of such diffraction can be written as:

$$n\lambda = 2d \sin\theta$$

where,

λ is the wavelength of X-rays,

θ is the glancing angle (called as Bragg′s angle),

d is the inter-planar separations and

n is the order of diffraction

X-rays being electromagnetic radiations, interact with the electron cloud of the atom. Thus, the electrons of the atoms vibrate due to the interaction of the fluctuating electric field of X-ray in the same frequency as that of the X-rays. In turn, these electrons act as a source of radiation, thereby emitting radiation of the same frequency as the incident radiation. Thus, the incident radiation appears to be scattered by the atoms. The scattering of X-rays from the atoms is possible in all the directions. The main steps covering the details of the techniques are described as follows

2.4.3.1.1 Instrumental details

A typical classical powder X-ray diffractometer consists of a source of X-ray and a detector for the detection of diffracted X-rays. Common diffractometer geometries are based on the Bragg-Brentano geometry. A block sketch of the typical powder diffractometer is shown in the Figure 2.6.

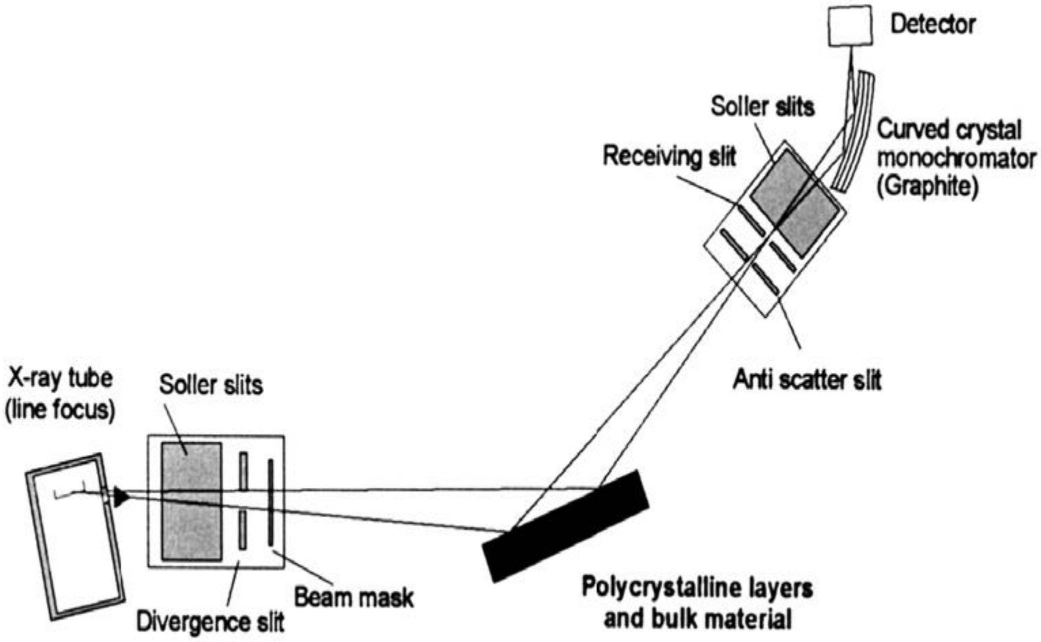

Figure 1.6: A block diagram of a typical X-ray diffractometer

There are several kinds of sources for X-ray that are available, but the most common laboratory diffractometers use sealed tube X-ray source. The X-rays are generally produced from a sealed X-ray tube. The basic construction of the tube is similar to the Coolidge tube. The X-rays are produced by bombarding high-speed electrons on a metal target. A part of the electron energy is used in producing X-ray beam, which is a combination of a continuous radiation with wavelength ranging from a particular shortest value (λ_{swl}) onwards and several intense spikes, which are characteristics of the target elements (called characteristic radiation). The intense continuous radiations or the monochromatic wavelength radiations can be used for the diffraction experiments. The latter is used in the most common diffraction instruments (angle dispersive). The details of the X-ray production and the typical X-ray spectra are explained in several monographs [2,3]. The X-rays are produced in all the direction, however, it is allowed to escape from a particular direction (usually from beryllium window) for experiments. The background and β-radiation are filtered using β-filters. The beam of X-rays is passed through the soller and divergence slits and then allowed to fall on the sample.

The fine grains of sample are generally spread uniformly over a rectangular area of a glass slide. The sample is usually adhered to glass slide either using binders like collodion or grease or wax. The amounts of the sample exposed generally depend on the scattering power of the elements and absorption coefficient of the sample. The crystalline sample usually shows good scattering and sharp diffraction lines.

The X-rays scattered (diffracted) from the sample are collected either by a film or counters. In the diffractometer, the diffracted beams are passed though the soller slits and divergence and receiving slits. Then it is usually allowed to fall on a monochromator before detection. The gas filled tube or scintillation counters are commonly used for the detection of the X-rays. The gas filled tubes can either be a proportional counter or Geiger-Muller counter. The gas filled tube is usually filled with a gas, which gets ionized with the impact of the radiation. The ions are collected by applying a potential difference between the two electrodes. The typical current obtained is proportional to the number of photons reaching the detector.

The diffracted rays are scanned by sweeping the detector from one angle to another. The angle (θ) where the incident beam satisfies the Bragg′s condition for a particular plane, a constructive interference among the diffracted X-rays occurs, giving a sharp rise in the intensity (peak). Thus, the counts or count rates of the X-ray photon are measured at different angles. The output is obtained as plot of the intensity of diffracted X-rays versus angle (2θ).

The peaks (also called as reflections) in the plot correspond to a set of parallel planes with inter-planar spacing d_{hkl}. The *d*-values are calculated from the position of the peaks. Thus, for a particular sample, a set of *d*-values giving constructive interference are observed. The peak positions are related with the unit cell parameters of the lattice. Also, a particular sample gives a characteristic set of *d*-values. Thus, they generally act as fingerprint for the crystalline materials; hence they can be used for identification of the materials. The intensity distribution of the reflections is governed by the nature and kind of distribution of atoms in the unit cell. The absolute intensities of the reflections depend on the source intensity and counting time, in addition to the nature and kind of distribution of atoms in the unit cell.

2.4.3.1.2 Calibration and data collection

The data collection protocols often depend on the specific purpose of the data collections. In general, a short time scan in the 2θ range of 10 to 70° is sufficient for the identification of a well crystalline inorganic material. However, low symmetry samples and samples with not good X-ray scattering power may need a slow scan. Data was collected in the 2θ range of 10 to 70° in a continuous scan mode with a step width of 0.02° and at a scan rate of 1° /min.

Prior to data collections, the goniometer needs to be properly aligned, for correct zero position. After the proper alignment, the instrument has to be calibrated with standard known materials for the accurate peak position. Usually silicon is used for calibration. The silicon peak positions are adjusted by the correct angle and set angle command or by applying the zero settings to the diffractometer.

2.4.3.1.3 Interpretation

After the data collection, the observed *d*-values were fitted to standard patterns (in case of crystalline phases). Fingerprinting of sample materials is normally done by comparing the observed diffraction pattern with JCPDS (Joint Committee on Powder Diffraction Standards, 1974) files available for reported crystalline samples.The use and interpretation of the powder diffraction patterns are explained in several books [2,3,4].

2.4.3.2 Scanning Electron Microscopy and Energy Dispersive X-ray spectroscopy (SEM/EDS)

The SEM-EDS system was used to study the microstructure evolution of the unleached and leached VWP samples. SEM images were recorded for the unleached and leached glass samples using environmental mode with SEM instrument (Philips XL-30). Elemental analysis of a few selected portions of the surface was also carried out using EDS unit attached with the SEM instrument conductive gold coating was applied on the VWP samples using 6" direct current sputtering unit, model 6-SPT, manufactured by M/s. Hind High Vacuum, Bangalore.

In SEM technique [5], the electrons from a finely focused beam are rastered across the surface of the sample. Electrons reflected by the surface of the sample and emitted secondary electrons are detected to give a map of the surface topography of the sample. It is useful for looking at particle size, crystal morphology, magnetic domains, surface defects etc. A wide range of magnification can be used, the best achievable being about 2 nm. The samples may need to be coated with gold or graphite to stop charge building up on the surface.

An electron beam incident on a metal gives rise to the emission of characteristic X-rays from the metal. In electron microscopy, the elements present in the sample also emit characteristic X-rays. These are separated by a high purity semiconductor detector with super ultra-thin window detector and each signal collected, amplified and corrected for absorption and other effects, to give both qualitative and quantitative analysis of the elements present (for elements of atomic number greater than 5) in the irradiated particle, a technique known as energy dispersive analysis of X-rays (EDS).

Sample preparation

(a) Mounting

Glass sample is broken into two or three pieces to make available fresh broken surfaces representative of the bulk sample. Sample pieces are mounted in a stainless steel ring of 20mm diameter using super fast cold setting resin METSET-101. Specimen are allowed to set for 4 hours and cleaned ultrasonically in distilled water.

(b) Grinding and fine polishing

Mounted samples were subjected to rough grinding using series of abrasive papers graded 2,1, 1/0, 2/0, 3/0, 4/0, 5/0, 6/0 emery grades (200 mesh to 800mesh ASTM).Rough polishing was carried out on diamond impregnated grinding wheel containing 1-2 micron size diamond powder fixed in resin matrix. Final polishing was carried out using 0.5µ and 0.25 µ diamond paste lapped on nylon cloth using organic lubricating fluid. Samples were ultrasonically cleaned with isopropyl alcohol between each step to prevent possibility of carry over of coarse abrasive contamination while polishing with finer abrasive material.

(c) Coating

Electron probe investigations require the samples to be conducting. Glass being insulating material requires coating with a conductive film prior to analysis. For this purpose, sample is mounted on aluminum stub by carbon conducting glue, dried with hot hair drier and coated with pure gold using sputter technique. Gold being a very good conductor and having very good secondary electron emission characteristic gives excellent result in image quality. The coating employed is 5-7 nm thick obtained by Balzer’s sputtering machine model SCD-030. Uniform thickness of the conductive film with 5-10 nm thickness has sufficient conductivity. Higher film thickness will obscure the topographical details in the sample and may give rise to its own feature, not representative of the sample.

A focused beam of electrons has been used to locally excite x-rays from a region as small as a few micrometers or less in a specimen. The wavelength distribution of the emitted x-ray is measured by means of one or more crystal diffraction spectrometers. Elemental constituents can then be identified with the aid of Moseley’s law, which uniquely relates the wavelength of each observed spectral line to a specific element through the relationship

$$\mathbf{1/\lambda = k\ (Z\text{-}\sigma)^{1/2}}$$

Where, λ is the wavelength, k is a constant for each spectral line series, Z is the atomic number of the element from which the x-ray originates and σ is a constant associated with atomic screening effects. In addition to qualitative analysis, quantitative analysis is possible. This is done by normalizing the measured X-ray line intensities with pure elemental standard intensities and correcting for atomic number (Z), absorption coefficient (A) and fluorescence (F).

Thoriated tungsten filament is used as a source of electron beam. A potential difference between 5-50 keV is applied between the filament (which acts as a cathode) and the anode, which is grounded. The grid cap of the electron gun is connected to the filament by means of variable bias register. By making it more negative than the filament, the electron guns acts as lens, forming an image of the filament which is then demagnified by two or more magnetic lenses to form final probe. When the electron beam strikes the sample a vast majority of energy is dissipated thermally and electrons and x-rays are produced (Figure 2.7).

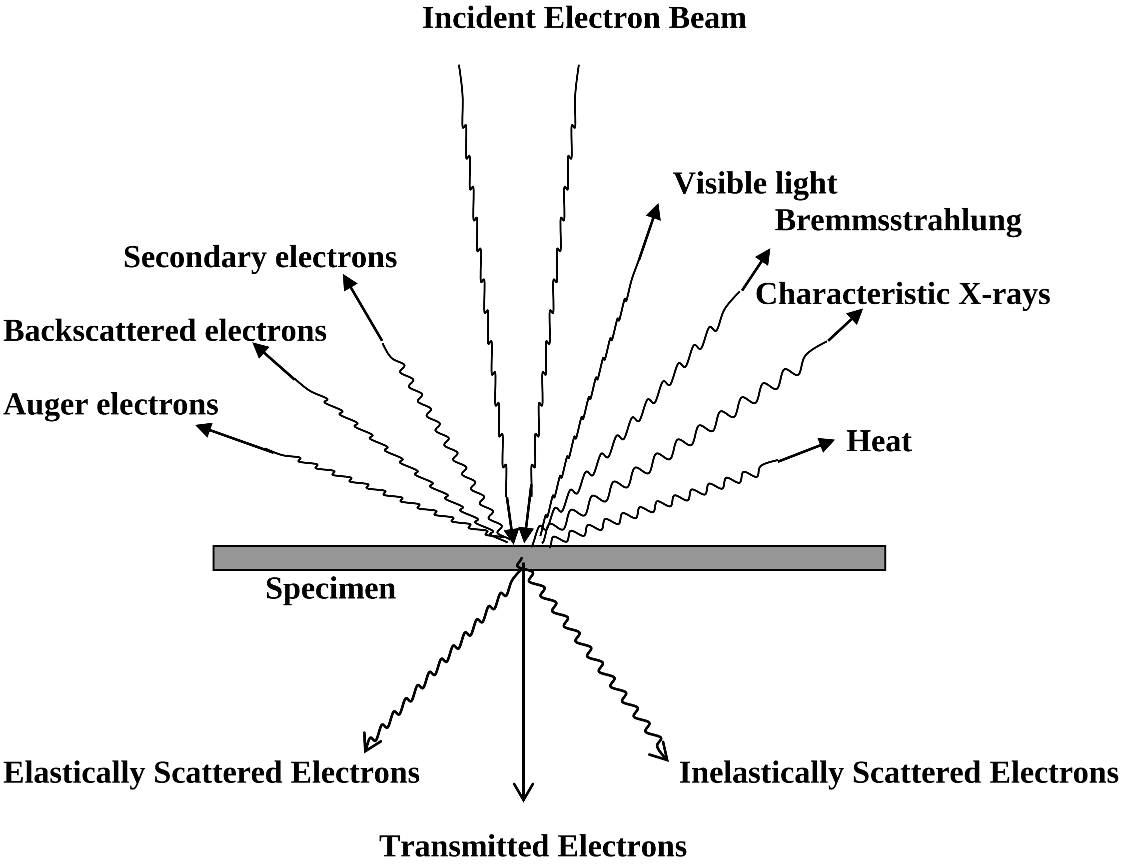

Figure 1.7: Interaction between electron beam and specimen

For electron analysis signals from secondary, back scattered and X-rays are used. Scintillation photomultiplier tube is generally used as detector for secondary electron imaging. Solid state detectors (Robinson type) are commonly used for backscattered electron imaging purpose.

The principle behind the detection of X-ray lines is based upon Bragg's law. The X-ray detector most commonly used is a gas (10% methane + 90% argon) flow proportional counter.

2.4.4 Nuclear magnetic resonance (NMR) technique

During the past fifty years, Nuclear Magnetic Resonance (NMR) techniques have evolved as a major tool for the structure elucidation in Chemistry, Biology, Material science etc. For condensed matters, the information provided by NMR on structure and dynamic is unparalleled by any other spectroscopic techniques. For highly disordered and compositionally complex systems, like oxide glasses, NMR can give valuable information regarding the local environment of the probe nucleus [6], which is not possible with diffraction techniques. Further, the technique is non-destructive and does not require elaborate sample preparation.

2.4.4.1 Fundamentals of NMR

Depending on the number of nucleons and their arrangement in different nuclear energy levels, several nuclei were found to possess finite value of nuclear spin. Quantum mechanically such nuclei are characterized by the nuclear spin quantum number, I. A nucleus with spin quantum number I takes (2I+1) different orientations (components) relative to an arbitrary axis, that are distinguished by quantum numbers m_I and are degenerate in the absence of a magnetic field. The m_I can have values, I, I-1, I-2……-I.

Under an applied magnetic field, these components become non-degenerate and transition between these levels form the basis of Nuclear Magnetic Resonance spectroscopy. The nuclei with non-zero value of I have magnetic moment and spin angular momentum. The z component of the magnetic moment (μ_z) and the spin angular momentum (I) can be expressed as [7,8],

$$\mu_z = \gamma \hbar m_I$$

$$I = [\, I.(I+1)\,]^{1/2} .\hbar$$

where γ is the gyromagnetic ratio of the nucleus, h is Planck's constant and $\hbar = h/2\pi$. Often the magnetic moment of a nucleus is expressed by the relation,

$$\mu = g\, \beta_N [I.(I+1)]^{(1/2)}$$

where 'g' is known as the nuclear 'g' factor and is characteristic of a nuclei, β_N is the nuclear Bohr magneton and is expressed by the relation, $\beta_N = eh/4\pi m_p$ where 'e' is the charge and m_p is the mass of the proton. Table 2.3 shows the values of nuclear spin, gyromagnetic ratio and the natural abundance for some of the nuclei frequently used for carrying out NMR experiments on glasses [8]. The interaction of the z component of the magnetic moment with the applied magnetic field (B_0) is given by the Zeeman Hamiltonian, $H_Z = -\mu_Z B_0$ with eigen values $E_m = -m_I\, \gamma.\hbar.B_0$. Thus the zeeman interaction results in the energy level splitting corresponding to various nuclear spin orientational states. By the application of electromagnetic waves fulfilling the condition $\Delta E = \hbar.\omega$, where ω is the frequency of the electromagnetic waves (also known as the resonance frequency), absorption between these levels can be expressed as $\omega = \gamma B_0$. Classically ω is known as Larmor precessional frequency. Since the γ (gyromagnetic ratio) values are different for different nuclei, NMR spectroscopy is intrinsically an element selective technique.

The resonance frequency of a particular nucleus can be expressed as $\omega = \gamma. B_{net}$, where B_{net} is the net magnetic field felt by the nuclei and can be expressed by the relation $B_{net} = (1-\sigma)Bo$, where σ is the screening constant and is a measure of the electronic environment surrounding the nuclei [7]. Hence, the same nuclei with different chemical environment will feel different net magnetic field around them for a given external magnetic field and thereby come in resonance at different frequencies. This gives rise to the chemical parameter, which is related to the chemical environment, felt by the probe nucleus.

Table 1.3: Values of nuclear spin, gyromagnetic ratio and the natural abundance for some of the nuclei

Nuclei	Natural abundance (%)	γ -values (10^7 rad T^{-1} s^{-1})	Spin
Phosphorus (^{31}P)	100	10.828	1/2
Silicon (^{29}Si)	4.7	-5.314	1/2
Boron (^{11}B)	81.17	8.579	3/2
Boron (^{10}B)	18.83	2.874	3
Fluorine (^{19}F)	100	25,179	1/2
Aluminum (^{27}Al)	100	6.970	5/2
Tellurium (^{125}Te)	7.0	-8.439	1/2
Lead (^{207}Pb)	22.6	5.579	1/2

2.4.4.2 Chemical shift

The chemical shift (δ) of any nucleus is defined as the difference between its resonance frequency and the resonance frequency of the same nuclei in a reference sample and can be expressed as,

$$\delta = \frac{(\omega - \omega_o)}{\omega_o} \times 10^6$$

Where, ω and ω_0 represent resonance frequency of the nuclei in a sample and the reference sample respectively. The chemical shift values are independent of the applied magnetic field and can be used to monitor the structural changes taking place around a particular nucleus.

2.4.4.3 FT NMR technique

Modern NMR machines are based on the principle of Fourier Transformation method, which involves the simultaneous excitation over a range of frequency which covers the entire spectral width and the absorption pattern is deconvoluted from the time domain to the frequency domain by employing Fourier transformation technique. In the following section a brief description of how the NMR signals are collected and fourier transformed in a FT NMR technique is presented.

Let

$$I(V) = \int_0^\infty S(t)e^{2\pi i \nu t} dt$$

Where S(t) is the signal intensity in the time domain and ν is the series of frequencies applied to the sample. A block diagram of a standard FTNMR spectrometer [9] is shown in Figure 2.8.

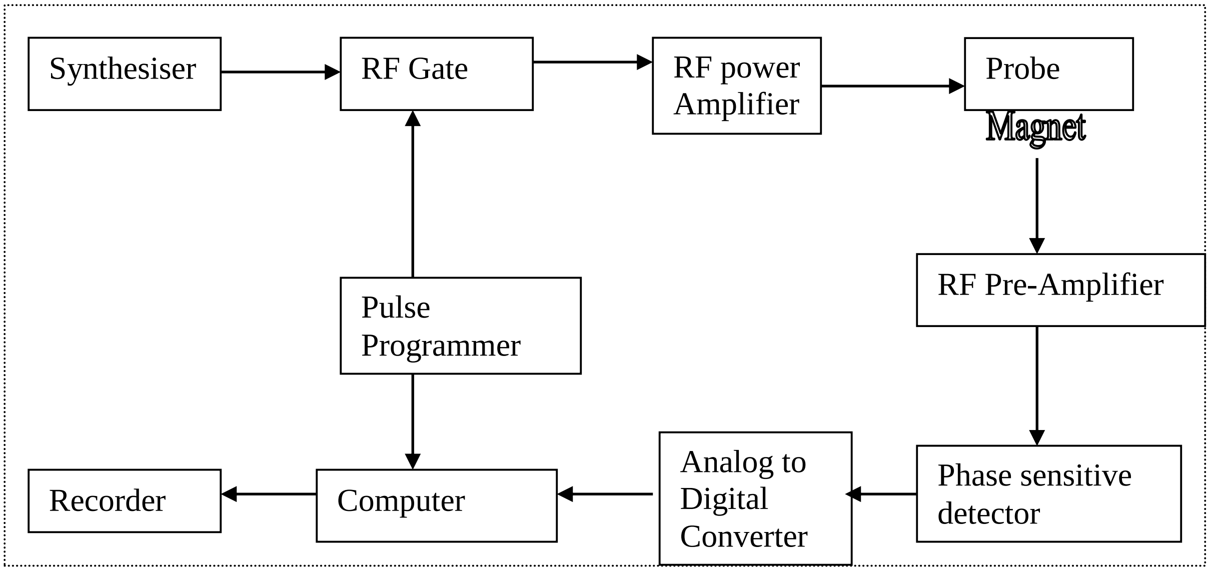

Figure 1.8: A block diagram of a standard FT NMR spectrometer

2.4.4.4 Magic Angle Spinning Nuclear Magnetic Resonance (MAS NMR)

The simplest and most popular experimental method for getting high resolution NMR patterns from solids is the MAS NMR technique, discovered by Andrew et al [10] and Lowe [11]. The technique involves rotating the powder samples at high speeds, at an angle of 54.7° (magic angle) with respect to the applied magnetic field direction. When $\theta = 54.7°$, the term $3\cos^2\theta$ becomes unity. Since the Hamiltonian for different anisotropic interactions have $3\cos^2\theta - 1$ term, these anisotropic interactions get averaged out in time during fast spinning. This is schematically shown in Figure 2.9 and explained below.

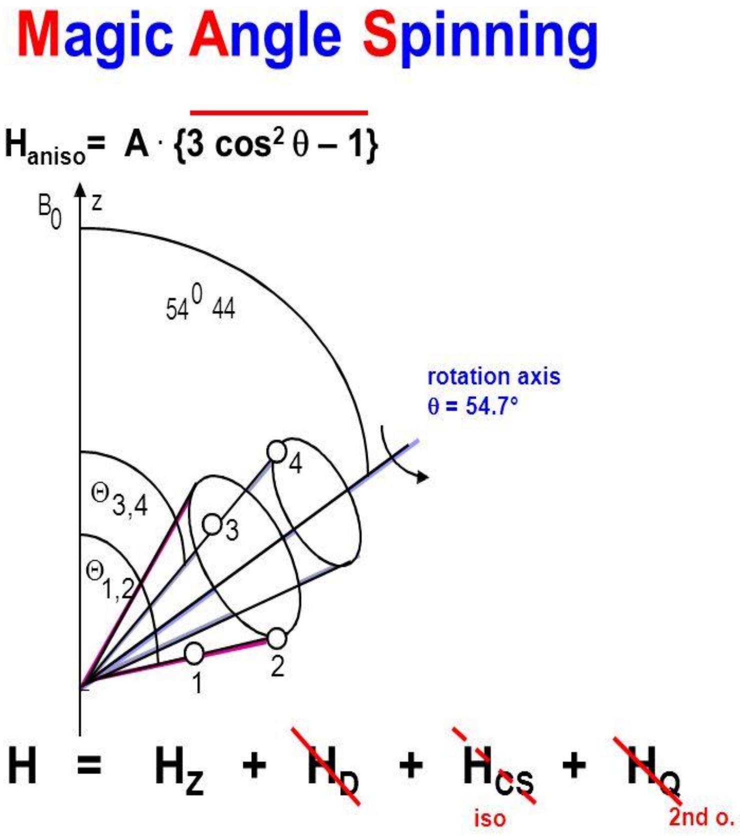

Figure 1.9: Principle of MAS NMR experiment

At sufficiently fast spinning speeds, the NMR interaction tensor orientations with initial angles of θ_1 and θ_2 relative to B_o have orientational averages of 54.7°, resulting in the conversion of $3\cos^2\theta - 1$ term in expressions corresponding to various interactions to a very small value, thereby giving rise to sharp NMR peaks. Thus the MAS NMR technique simplifies the solid state NMR patterns and the individual chemical environments can be correlated with the corresponding chemical shift values obtained from these patterns.

There are many other experimental strategies, which simplify the solid state NMR patterns and improve the quality of information obtained from them, details of which are available in the literature [12].

Although, magic angle spinning is an efficient technique employed for getting high resolution NMR patterns from solid samples, in many cases, due to spinning, sidebands, which are mirror images of the isotropic peak and separated from the isotropic peak by integral multiples of the spinning frequency, appear along with the central isotropic peak particularly for nuclei having wide range of chemical shift values. However, the side bands can be easily identified from the isotropic peak by varying the spinning frequency, which results in a shift of the peak maxima of spinning sidebands without changing the isotropic peak maxima. In some cases, the sidebands have intensity more than the corresponding isotropic peaks. For a nucleus which is having a nuclear spin value $^1\!/_2$, side band pattern is a measure of the chemical shift anisotropy and valuable information regarding the symmetry of the electronic environment around a probe nuclei can be obtained from the intensity distributions of the sidebands. However, in presence of large number of isotropic peaks, the number of sidebands also increases, and there can be overlap between the sidebands and the isotropic peaks, which makes the MAS NMR patterns complicated. In the following section a brief description is given regarding the origin of sidebands for spin 1/2 nuclei.

2.4.4.5 Origin of spinning side bands

A powdered sample can be considered as an assembly of randomly oriented spin packets. Depending on the chemical shift anisotropy of the nuclei, the net magnetic field felt by each spin packet in the sample will be different and hence, the corresponding Larmor frequencies [13]. When such a sample is subjected to fast spinning, around an axis which is at an angle 54.7° (magic angle) with respect to the applied magnetic field, each spin packet feels a range of magnetic fields during one rotational period. However the average field felt by all the spin packets in one rotational period is the same and is independent of their orientation with respect to applied magnetic field. Since each spin packet feels a range of magnetic fields in a time period of one rotation, the magnetization vector which has come to X-Y plane immediately after applying 90° pulse, initially starts spreading (decaying), but after the completion of one rotor period, the spin packet will feel a magnetic field which it was feeling immediately after the 90° pulse. Thus the vectors, which were spreading (decaying) in the X- Y plane, start getting aligned along the detector axis, thereby leading to the observation of a peak. This is known as a rotational echo in NMR terminology. Sidebands are nothing but the rotational echoes, brought about by the sample spinning. As the spinning frequency increases, the time required for one complete rotation and the spreading of the magnetization decreases, thereby reducing the number of rotational echoes.

For quadrupolar nuclei large number of intense sidebands is observed when it is close to the magic angle, which can be attributed to the contribution from both chemical shift and quadrupolar interaction anisotropy. This property of a quadrupolar nucleus can be used to accurately set the magic angle in MAS NMR experiment [14].

2.4.4.6 Setting up the magic angle

Setting up of the magic angle for MAS NMR experiments is normally done by monitoring ^{79}Br resonance of Br present in a powdered KBr sample. Sideband pattern observed from ^{79}Br corresponds to the anisotropies due to both chemical shift and quadrupolar interaction, the latter arises, due to the presence of defects and impurities in the crystal.

About 100 mg of dried KBr powder was packed inside zirconia rotors of 7mm outer diameter and subjected to a spinning speed of 5000 Hz. The 90^{o} pulse duration of 2μs with a delay time of 2 seconds was employed for the ^{79}Br MAS NMR experiments. The basic frequency was 75.16 MHz. When the angle is very close to the magic angle, extensive sideband patterns will be observed due to both chemical shift anisotropy and quadrupolar interaction, which affects both central (+1/2↔-1/2) and satellite transitions (+3/2↔+1/2 and -1/2↔-3/2). A way from the magic angle these sidebands are broadened and lost in the noise level. The experiments were repeated for every 1^{o} change in the angle, till NMR pattern, having maximum intensity of sidebands was obtained.

In the present study all MAS NMR experiments were carried out at room temperature a Bruker Avance DPX 300 machine having a standard bore (SB) MAS probe accessory. The applied magnetic field was 7.04 Tesla. Zirconia rotors of 7mm diameter were used for all MAS NMR experiments. The specific details regarding pulse duration, delay time, spinning speed etc., are given in the relevant chapters.

2.4.5 FTIR technique

FTIR technique was used for carrying out structural characterization of glass samples. FTIR technique is based on Michelson interferometer, which is an optical device consisting of a fixed mirror, movable mirror and a beam splitter. The interferometer shifts the phase of one of the beam with respect to another by moving one of the mirrors and keeping the other mirror at fixed position. When the two beam overlap, depending on whether they are in phase or out of phase, constructive and destructive interference takes place. If the light source is monochromatic, the intensity of the interference pattern will rise and fall periodically and the detector will measure a sinusoidal signal as a function of the optical path difference. When the light source contains many frequencies, like the radiation emitted from a Globar IR source, the intensity measured, I (x), as function of optical path difference, x is known as the interferogram. Fourier transformation of the interferogram results in the frequency spectrum, I (v). The optical path difference x, can be accurately obtained from the interference patterns generated from the interferometer using a laser source, whose frequency is accurately known [15].

In the present study all infra red experiments were carried out using a Bomem MB102 FTIR machine with resolution of 4 cm^{-1} having a range of 200-4000 cm^{-1}. IR radiation was generated from a Globar source (bonded silicon carbide rod). The instrument used CsI single crystal, as the beam splitter and deuterated triglycine sulphate (DTGS) as the detector. A He-Ne laser having a wavelength of 632.9 nm (with a max. power of 25μW) has been used for the calibration purpose. Prior to the IR measurements, the samples were ground thoroughly by mixing with dry KBr powder, made in the form of a thin pellet and introduced into the sample chamber for recording the IR spectra.

2.4.6 Differential thermal analysis (DTA)

In Differential thermal analysis (DTA) technique, the differential temperature (ΔT) of sample, with respect to the temperature of a thermally inert material, known as the reference, is recorded as a function of the sample temperature, as the sample and the reference are heated or cooled simultaneously in the uniform temperature zone of the furnace at a programmed rate. The block diagram of DTA system and a typical DTA curve are shown in Figure 2.10 and 2.11 respectively.

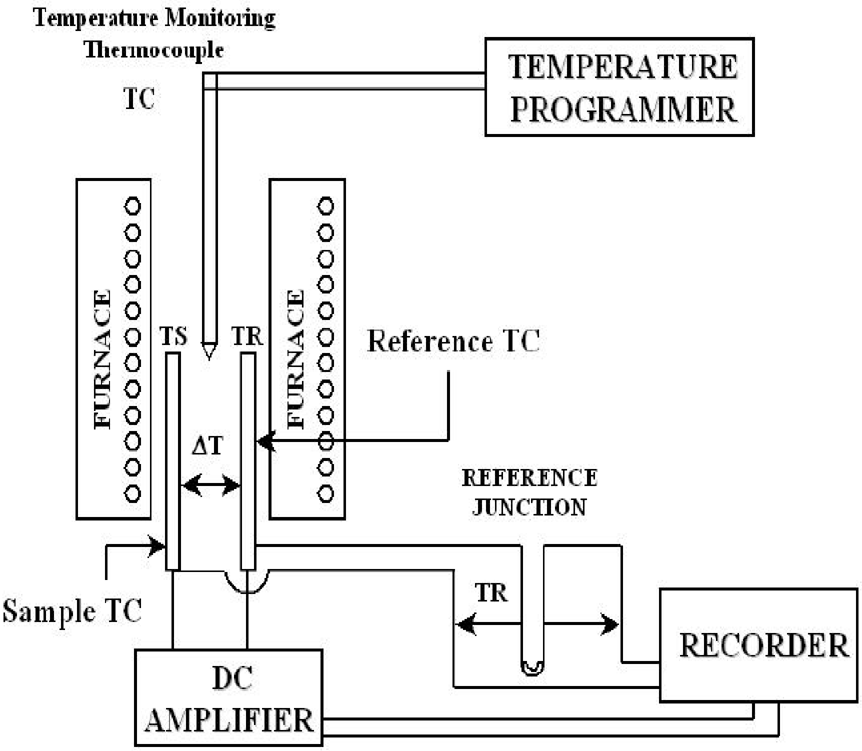

Figure 1.10: Block diagram of DTA system

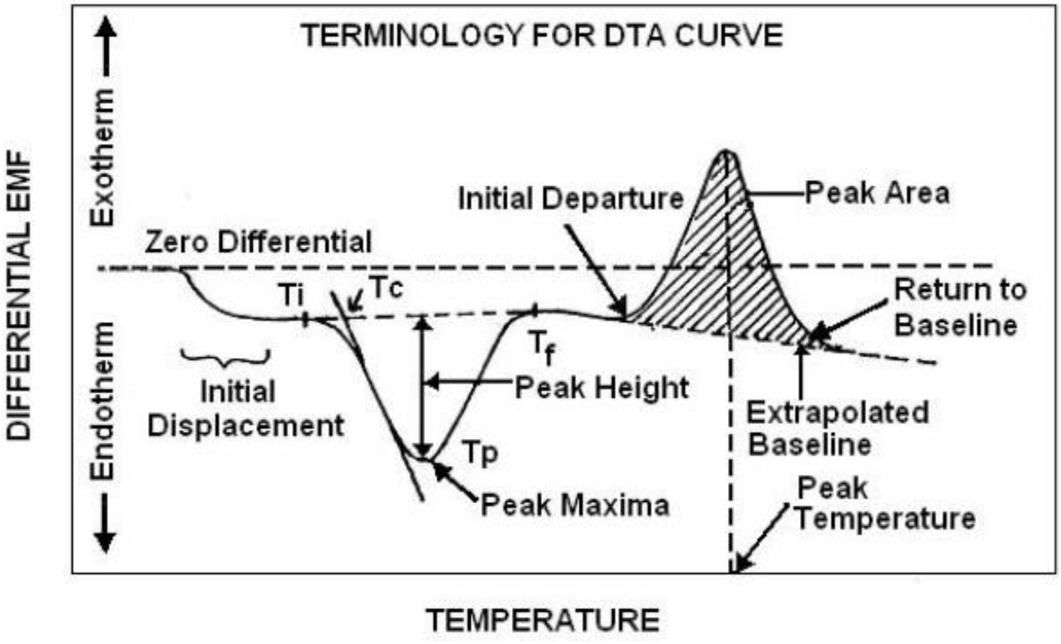

Figure 1.11: A typical DTA curve [16]

The curve is described by the characteristic temperatures. The initiation temperature (T_i), the peak temperature (T_p) and the termination temperature (T_f) are the three temperatures used to characterize the main features of the DTA curve. The initiation temperature represents the temperature where the DTA signal begins to deviate from a steady base line. The extrapolated onset temperature (T_e) corresponding to the point of intersection of the base line with the tangent drawn to the rising part of the DTA curve at the point of maximum slope is often preferred to the initiation temperature. The peak temperature indicates either the end of the reaction or transformation or the temperature at which the rate of transformation is maximum and finally T_f denotes the temperature at which the signal returns to the base line. The temperature changes in the sample can be due to enthalpy changes caused by phase transitions, fusion, decomposition reactions, oxidation or reduction reactions, etc. The nature of the DTA curve and the magnitude of the peak depend on a large number of instrumental factors and also on sample characteristics. The instrumental factors that influence the DTA signal are the geometry and material of the sample holder, nature of the thermocouple and its location, the heating rate and the atmosphere around the sample. The sample characteristics like the particle size, amount of sample used, its heat capacity and thermal conductivity and packing density also play important role in affecting the DTA curve. The extent to which these parameters influence the shape of the DTA curve can be found in several references [17,18,19,20,21,22,23]. Delineation of phase boundary using DTA is done by measuring the evolution or absorption of heat accompanying phase changes when the sample is heated or cooled at constant rate. At the phase changes corresponding to the melting and freezing of pure compound or eutectics, peritectics the plot of temperature vs. time shows a thermal arrest. The DTA instrument requires calibration for both temperature and enthalpy. Several standard materials like pure metals and well characterized compounds have been recommended for this purpose. The melting points of metals like In, Zn, Sn, Sb, Al, Ag and Au and phase transitions in $LiSO_4$, K_2CrO_4, $BaCO_3$ etc can be used for temperature calibration. Enthalpy calibration can be done using the heats of solid-solid transition or fusion of the above materials or organic compounds of high purity.

2.5 Leaching test equipment

The two leaching test are explained viz. ASTM leaching test and autoclave leaching test.

2.5.1 ASTM leaching test

The preliminary screening of the glasses is done using ASTM leaching method (ASTM Designation: C1285-02) [24]. The test method is standard leach test which provides a measure of the chemical durability of homogeneous waste glasses. Test method A which is product consistency test (PCT-A) which was developed specifically to measure the chemical durability of radioactive glass waste forms for screening of different glasses during production. This test method is a seven-day chemical durability test applicable to radioactive and simulated waste forms at 90°C in oven in a leachant of ASTM Type I water. This method is static and conducted in stainless steel vessels with teflon lining. The vitrified waste product in powder form (-100+200 ASTM) is used and the surface area to volume ratio used is 2000 m^{-1}.

Figure 1.12: ASTM stainless steel leaching vessel

Procedure: For each glass tested, the PCT is performed in triplicate. Duplicate blanks are always performed. This test is done in SS vessels with internal lining of Teflon as shown in Figure 2.12**.** In this method, the glasses are crushed to fine powder and sieved through 100-200 mesh and carefully sieved. The sieved glass samples are washed with water and alcohol to remove fines and then dried at 90°C. The dried glass samples are leached in ASTM Type I water at 90°C for seven days. A time of seven days was chosen because experiments showed that this time period gave the sufficient precision while still being short enough for preliminary screening of glasses. Ten milliliters of water are used per gram of glass. After a period of seven days, the test vessels are removed from oven and cooled to ambient temperatures. The final leachate is filtered through a 45-micron filter to ensure that it has been separated from the glass particles. The solution pH is then measured and the filtrates are acidified and analysed by ICP-AES for elements such as Na, B, Si etc.to calculate the normalized release of elements.

2.5.2 Autoclave leaching test

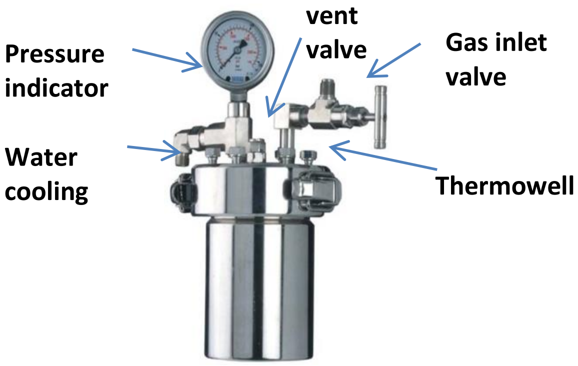

Figure 1.13: Autoclave unit for high temperature and pressure leaching studies

The leaching unit shown in the above Figure 2.13 is autoclave leaching unit. This is laboratory autoclave unit of 250 mL capacity. It can withstand a pressure as high as 100 bars and a temperature as high as 300°C. It is stainless steel vessel with Teflon lining inside. It has pressure indicator to show the running pressure inside the vessel. There is arrangement of thermowell which shows current temperature of the vessel. It has water cooling arrangement to cool the electronic components from high temperatures. There is arrangement of gas inlet valve to facilitate use of any inert gas during the experiment as well as for the use of pressurized air in case of leak test of the equipment. This leaching unit is used for high temperature and pressure leaching studies of glasses. The glass in powder or pellet form can be used. The leachant is then added and the vessel is vapour closed using screw tightening arrangements provided in the vessel. The required temperature and pressure is then applied and the tests are conducted for the required time durations. The leachants are removed and analysed for its elemental release and the glasses characterized for sttructural alterations, if any.

References

---

[1] Noll GF, Radiation detection and measurement, John Wiley and sons Inc.

[2] Cullity BD, Elements of X-ray diffraction., Addison-Wilson Publishing Comp. Inc., USA, 1959.

[3] Klug HP and Alexander LE, X-ray diffraction procedures, Wiley-Interscience Publication, New York, 1974.

[4] Azaroff LV and Buerger MJ, The Powder Method in X-ray Crystallography. McGraw- Hill Book Comp., New York, 1958.

[5] Cahn RW, Haasen P, Kramer EJ, Material Science and Engineering: Characterization of Materials, VCH Publisher Inc., New York, 1991.

[6] Eckert H, Prog. NMR Spectrosc. 24 (1992) 159.

[7] Atkins PW, Physical Chemistry, 4th Edition, ELBS, Oxford,1990.

[8] Gunther H, NMR SpectroscopyBasic principles, concepts and applications in Chemistry, 2nd Edition, John Wiley & Sons, New York, 1995.

[9] Bovey FA, Jelinski L and Mirau PA, Nuclear Magnetic Resonance Spectroscopy, 2nd edition, Academic Press, New York, 1988.

[10] Andrew ER, Bradbury A and Eades RG, Nature 183 (1959) 1802.

---

[11] Lowe IJ, Phys. Rev. Lett., 2 (1959) 1802.

[12] Smith ME, Van ERH, Eck. Prog. NMR Spectrosc, 34 (1999) 159.

[13] Faricq MM and Waugh JS, J. Chem.Phys. 70 (1979) 3300.

[14] Frye JS and Maciel GE, J. Magn. Reson., 48 (1982) 125.

[15] Banwell CN and McCash EM, Fundamentals of Molecular Spectroscopy, 4th Edition, Tata McGraw-Hill publishers Ltd., New Delhi, 2000.

[16] Mishra RK., "Investigations of solubility of different nuclear waste constituents in glasses, their structural and physico-chemical characterisation", PhD thesis, Mumbai university (2008) 48.

[17] Wendlandt WW, Thermal Analysis., Interscience, 1985.

[18] Garn PD, Thermoanalytical Methods of Investigations., Academic Press, New York, 1963.

[19] Blazek A, Thermal Analysis., Reinhold Company, London, 1973.

[20] Daniels T, Thermal Analysis., Kogan Page Ltd, London, 1973.

[21] Judd MD, Pope MI, Differential Thermal Analysis., Heyden, London, 1977.

[22] Differential Thermal Analysis., Eds., Mackenzie RC, Academic Press, London, 1970.

[23] Smothers WJ, Yao Chiang MS, Handbook of Differential Thermal Analysis., Chemical Publishing Company, New York, 1966.

[24] ‘‘Standard Test Methods for Determining Chemical Durability of Nuclear, Hazardous, and Mixed Waste Glasses and Multiphase Glass Ceramics: The Product Consistency Test (PCT),’’ Annual Book of ASTM Standards, Vol. 12.01. ASTM C1285, American society for Testing Materials, International, West Conshohocken, PA, 2008.

Chapter 3: *Development of Nuclear Waste Glasses*

Development of Nuclear Waste Glasses

3.1 Introduction

Development of matrices for conditioning of high Level Waste (HLW) to ensure isolations of radionuclides from human environment for extended period of time is a scientific and technological challenge. Vitrification is attractive as the large number of elements can be incorporated in the open glass structure in durable glasses. The high chemical resistance of glass allows it to remain stable in corrosive environments for thousands and even millions of years [1]. Although glass is able to accommodate variety of elements within its structure, there is a difference in the solubility of different elements into glass matrix. There are different elements from different groups of the periodic table which are present in HLW and have limited solubility in borosilicate glass matrix. For silicate glasses the practical concentrations limits for the metal oxides and other elements are approximated and given in the Table 3.1 below.

Table 1.1: Approximate solubility limits of oxide in silicate glasses

Sr. No.	Range of concentration (wt%)	Elements
1	< 0.1	H, He, N, Ne, Ar, Br, Kr, Ru, Rh, Pd, Ag, I, Xe, Pt, Au, Hg, Ra
2	1-3	C, S, Cl, Se, Tc, Sn, Sb, Te
3	3-5	Mn, Cr, Co, Ni, Mo
4	5-15	Ti, Cu, F, La, Ce, Pt, Nd, Gd, Th, Bi, Zr
5	15-25	Li, B, Na, Mg, K, Ca, Fe, Zn, Rb, Sr, Cs, Ba, U
6	>25	Al, Si, P, Pb

From the Table 3.1 it is seen that molybdenum, chromium, ruthenium, rhodium, palladium etc. are some of the examples having less solubility in the silicate based glasses. Higher concentrations of these elements in the glass can lead to phase separation resulting into heterogeneity in the vitrified waste product (VWP) which is not desirable for the immobilization of HLW. The selection of glass compositions is done in such a way so as to have maximum solubility of HLW components in it and at the same time the VWP shall have durability for few thousands to millions of years.

Sulphate was also one of the troublesome element having limited solubility in borosilicate glass matrix [2] which was major component in the research reactor HLW in BARC, India. Since borosilicate matrix was chosen in India for the immobilization of HLW in glass matrix, it was seen that at higher sulphate concentrations, a separate phase of alkali sulphate known as “gall” is formed. Its presence in the glass was not desirable as this phase was enriched with cesium and had high solubility in water. Attempts have been made to improve the solubility of sulphate using glass formulations based on lead borosilicate system [3]. But, further experiments done on lead borosilicate glasses also shown phase separation due to sulphate [4,5]. From the reported work [6,7], it was seen the preferential formation of alkali metal sulphate in borosilicate glasses. Also, sulphate deposits in nature indicated presence of barite ($BaSO_4$) as one of the chemically durable and thermally stable component. Therefore, it was decided to use barium in the sodium borosilicate glass matrix for successful vitrification of sulphate containing HLW in quaternary $BaO\text{-}Na_2O\text{-}B_2O_3\text{-}SiO_2$ system [8].

After solubility limit comes, volatility of radionuclides which can hamper the immobilization process. The most durable glasses would require very high processing temperatures (>1500°C), which is not suitable for certain volatile elements such as cesium and ruthenium. Due to this, there will be generation of secondary waste as well as this will hamper the immobilization efficiency. As a result, the most common glasses used in vitrification of nuclear waste are borosilicate, aluminosilicate and phosphates which use lower processing temperature (~1000°C) while still forming a durable product. Considering the volatility of cesium, while preparing special cesium glasses [9] with low melting temperatures, glasses such as cesium iron phosphate glasses (Cs_2O-Fe_2O_3-P_2O_5), cesium borosilicate (Cs_2O-B_2O_3-SiO_2) and quaternary system of (Cs_2O-Na_2O-B_2O_3-SiO_2) and Cesium lithium borosilicate (Cs_2O-Li_2O-B_2O_3-SiO_2) with minor additives like Al, Zn were tried. Kaushik et al, [10] also developed special cesium containing glasses using calcium sodium borosilicate (CaO-Na_2O-B_2O_3-SiO_2) system and produced radioactive cesium glass pencils for the use as gamma irradiator.

From the above discussion, it is clear that vitrification of high level waste is a compromise between the desired durability of the final waste form and its processing efficiency [15]. Selection of specific glass compositions within borosilicate family depends on (a) HLW chemistry and its solubility limit within the glass, (b) chemical durability of the waste glasses and (c) available plant scale technology. These aspects will be discussed in details.

3.2 HLW chemistry

Detailed radiochemical analysis of HLW provides qualitative and quantitative information about the elements present in the waste. The composition of HLW depends on various factors such as (a) type of fuel, (b)its history in the reactor and (c) the reprocessing chemistry. HLW chemistry strongly depends on the type of fuel used. The fuel is used in the reactors for power generation by inducing fission reactions. Fission fragments are produced in fission reactions whose masses are approximately half of that of the fissile elements. Figure 3.1 depicts the fission yield curve. Many fission products are formed in the reactor. Most of them have very short half-lives and decay within hours, days or months. Therefore, cooling period is given to the spent fuel to decay short lived isotopes. Neutron capture reactions in reactor, gives rise to actinides. ^{239}Pu is neutron capture product of ^{238}U. Actinides such as Np, Cm and Am gets formed in very small quantities. The high energy fast neutrons can be used for the fission of ^{238}U as well as for minor actinides such as Np, Cm and Am.

In the reprocessing facilities [11], the spent fuel bundles are dismantled and each of the fuel pins are chopped into small pieces and then transferred to dissolver vessel containing concentrated nitric acid solutions. Extraction is done by solvent extraction method called as PUREX (plutonium uranium reduction extraction) process which uses 30% TBP in n-dodecane to recover U and Pu to as high as 99.8 - 99.9%. For the reprocessing of ThO_2 i.e., thoria based spent fuels THOREX (thorium extraction) process which also uses TBP as extractant for the recovery of ^{233}U and thorium. For the dissolution of thoria fuel, HF and aluminum nitrate were added for better dissolution and minimization of free fluoride corrosion activities.

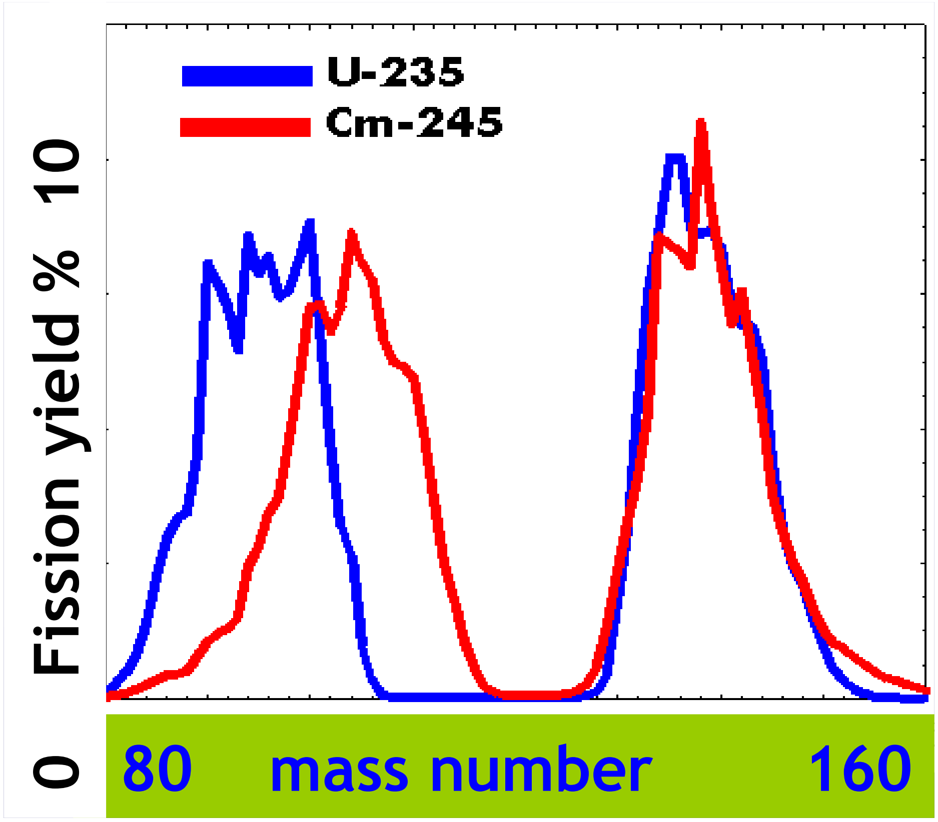

Figure 1.1: Fission yield curve [12]

Major components of HLW are:

- Radioactivity - Gross α, β, γ activity (1 – 1000 Ci/L)
- Corrosion products (Fe, Ni, Cr, Mn)
- Fission products (^{90}Sr, ^{106}Ru, ^{137}Cs, ^{144}Ce, ^{147}Pm etc.)
- Actinides (^{241}Am, ^{244}Cm, unrecovered U and Pu)
- Added Chemicals (e.g. HNO_3:1-5 M, traces of TBP and its degradation products, Na, Al, Ca, etc in the form of nitrates.)

Almost 99% of the radioactivity is present in the entire fuel cycle in the form of HLW. The HLW contains both long and short lived fission products, minor actinides, unrecovered Pu/U/Th, processing chemicals like nitric acid, sodium nitrate, dissolved cladding material like aluminum and zirconium and corrosion products of material of construction of storage tanks and piping [15]. HLW generated from reprocessing of PHWR spent fuel having burn-up of 6000 – 8000 MWd/te contains nitric acid (3-3.5M) along with uranium, aluminum, calcium, iron, sodium etc. The futuristic waste arising from reprocessing of spent fuel from Fast Breeder Reactors and Advanced Heavy Water Reactors will have higher concentration of fission products particularly, belonging to platinum group metals (Ru, Rh & Pd) along with thorium, aluminum and fluoride in addition to other waste constituents. Two typical HLW's are shown in Table 3.2.

Table 1.2: Typical HLW characteristics

Property	**PHWR-HLW**	**Thoria containing-HLW**
Fuel	Uranium	^{233}U-Th, Pu-Th
Burn up	~6500 MWD/te	24000 MWD/te
Volume/te	~0.7 -8 m^3	10 m^3
Total oxide	40-50gm/L	10-12 g/L
Activity (3 years cooling)	30-50 Ci/L	40 – 50 Ci/L
Molarity	3-4M HNO_3	3-4 M HNO_3
Elements of concern	U, Cr, Mo	Th, Al, F

3.3 Radiochemical analysis of HLW

Detailed radiochemical analysis of HLW has been carried out using various experimental techniques. Appropriate dilution of the HLW with respect to its radioactivity and elemental concentration is carried out in the hot cell of sampling system. HLW contains long lived actinides and highly radioactive fission products. The gross β, γ activity of nuclear waste solutions was determined using Geiger Muller (GM) counter to be 10-40

Ci/L and the gross α activity was upto 10 mCi/L done using ZnS(Ag) scintillation detector. Direct analysis of nuclear waste was not feasible for high radiation exposures involved. Therefore, adequate sample dilution is required to bring down the dose rate prior to analysis. HLW dilution minimizes radiation exposures, but concentration of the waste constituents also gets reduced from g/L to mg/L or less. Conventional methods therefore were not applicable for carrying out precise analysis of the radioactive liquid waste. Spectroscopic techniques like Spectrophotometry for U, Fe etc, Inductively Coupled Plasma- Atomic Emission Spectrometry (ICP-AES) for different elements, Gamma spectrometry using HPGe detector for gamma emitting radionuclides such as ^{137}Cs,^{106}Ru, ^{144}Ce and ^{241}Am, Carrier precipitation method for ^{90}Sr and HTTA solvent extraction method for Pu estimation were adopted as they were not time consuming and at the same time precise enough to get the accurate analytical results. Analytical procedures used to estimate the radionuclides like Sr, Pu and uranium are briefly discussed below. Radiochemical analysis of PHWR and thoria containing waste are shown in Table 3.3.

Table 1.3: Radiochemical analysis of PHWR and thoria containing HLW

Property	PHWR-HLW	Thoria containing HLW
Molarity (M)	2 - 3	2 - 3
Gross α (Ci/L)	0.12	0.5
Gross β, γ(Ci/L)	20.21	42.70
^{90}Sr (Ci/L)	4.633	11
^{137}Cs (Ci/L)	4.47	15.58

3.3.1 ^{90}Sr estimation by carrier precipitation method

Radioactive ^{90}Sr is co-precipitated along with inactive Sr (as carrier) as $SrCO_3$using saturated solution of Na_2CO_3. To remove the daughter element i.e.^{90}Y, Fe-nitrate is added as scavenger and is precipitated as ferric hydroxide by using liquor ammonia. The yield of inactive Sr is measured. On the basis of this, the amount of ^{90}Sr is computed.

$$\mathbf{Sr(NO_3)_2}\text{(soln)} + \mathbf{Na_2CO_3}\text{(soln)} \longrightarrow \mathbf{SrCO_3}\downarrow\text{(ppt)} + \mathbf{2\ NaNO_3}\text{(soln)}$$

The precipitated strontium carbonate is dissolved in dil HCl. A known amount is plancheted from the dissolved solution and counted using β-counter and ^{90}Sr is estimated. Counting the same planchet after 64 hours gives substancial increase in the counts, which confirms the growth of ^{90}Y from ^{90}Sr.

3.3.2 Plutonium estimation by HTTA extraction method

Theonyl Trifluoro Acetone (TTA) forms chelate complexes with Plutonium(IV). The metal chelate complex can be extracted with organic solventssuch as Benzene or Xylene. The neutral chelate complexes extracted from the solvent consist of a Pu atom bonded to 4 TTA ions.

$$\mathbf{4\ HT\ (X)\ +\ Pu^{+4}\ (A)\ \rightarrow\ Pu\ T_4\ (X)\ +\ 4H^+}$$
$$\downarrow\downarrow \qquad \downarrow$$

TTA acid enol form Xylene Aq. phase

Pu content in the extract is estimated by counting the α- activity by Scintillation detector, from a portion of the extract plated and fixed on a stainless steel planchet.

3.3.3 Uranium estimation by spectrophotometric method

Uranium (UO_2^{2+}) forms a yellow colored complex with saturated solution of ammonium thiocyanate. However, to increase the stability of the complex and to avoid anionic interference like Cl^-, SO_4^{2-}, reagent is prepared in alcoholic medium. Moreover, the molar absorptive or the extinction coefficient (ε) of this complex is 6000 L/mole/cm at its λ_{max} 360 nm, which provides additional sensitivity to this method. As the reagent itself absorbs incident light of wavelength below 400 nm, working wavelength is selected at 420 nm. Molar extinction coefficient at 420 nm is 1000 lit/mole/cm. Iron as Fe^{3+} interferes in this method. This is eliminated by reducing Fe^{3+} to Fe^{2+} by using suitable reducing agent like $SnCl_2$.

3.3.4 Elemental analysis of HLW using ICP-AES

The elemental concentrations of HLW were determined sequentially by ICP after appropriate dilution. The diluted sample of HLW was taken to the glove box of ICP- AES system. The plasma component of the unit was housed in glove box to facilitate analysis of radioactive samples. Negative pressure of the order of 25-30 mm of water gauge was maintained in the glove box. Glove box is equipped with high efficiency particulate air (HEPA) filter to retain nuclides in the glove box. Outlet of the glove box was connected to exhaustive off gas treatment system. Glove box adopted ICP-AES was used throughout the investigation. Standard solutions for analytes were prepared from CertiPUR® ICP standard procured from E-Merck, Darmstadt, Germany. Suprapur® HNO_3fromE-Merck, Darmstadt, Germany and quartz double distilled Milli-Q® water were used throughout the investigation.

The analytical lines chosen for the experiment of HLW characterization are as shown in Table 3.4. For calibration, multi-point standardization was carried out after peak search, profiling and auto-attenuation. 10 replicate measurements were carried out for reporting any value. Multi element standard solutions were prepared for the elements to be measured. The blank and standard solutions were run on the ICP system. The signal level for each element is stored as a calibration line in the computer system. The calibration curve for each element is established. The diluted sample of HLW was taken to the glove box of ICP- AES system with proper safety precautions. The sample was analysed using ICP and the concentration equivalent to the signal of each element is calculated and instrument gives the concentration of the sample element directly in mg/L.

Table 1.4: Analytical performance of the elements in ICP-AES

Element	Analytical line (nm)	DL (mg/ L)	BEC (mg/ L)	LDR (mg/L)
Th	339.204	0.519 ± 0.007	1.032 ± 0.003	1.1 - 1000
Al	309.271	0.014 ± 0.002	0.268 ± 0.005	0.3 - 1000
Fe	238.204	0.004 ± 0.001	0.034 ± 0.002	0.05 - 500
Ni	231.604	0.016 ± 0.005	0.087 ± 0.002	0.09 - 800
Cr	267.716	0.0004 ± 0.0001	0.046 ± 0.003	0.05 - 1000
Ce	446.021	0.017 ± 0.002	0.473 ± 0.006	0.5 - 500
Na	588.995	0.009 ± 0.001	0.257 ± 0.007	0.3 - 500
Sr	215.284	0.027 ± 0.005	0.217 ± 0.008	0.3 - 500
U	411.610	0.288 ± 0.003	3.63 ± 0.06	3.7 - 800
Mn	257.610	0.0007 ± 0.0001	0.0009 ± 0.0001	0.0009 - 1000
Ca	396.847	0.0002 ± 0.0001	0.0002 ± 0.0001	0.0002 - 1000
Mo	313.259	0.037 ± 0.002	0.036 ± 0.002	0.04 - 500

DL = Detection Limit, BEC=Background equivalent concentration, LDR = Linear Dynamic Range

A minimum of three sequential spectral integrations are done for determining the average concentration for a single element analysis. Each sample was analysed in triplicate with different aliquots. A dilute acid rinse was given in between samples to ensure analyte signals return to blank concentrations. The elemental analysis of few Actual HLW solutions such as Research Reactor (RR), PHWR, thoria containing and Cs rich HLW's are as shown in Table 3.5.

Table 1.5: Analytical results for actual and simulated high level waste solutions from thoria rich solution, PHWR, Cs rich and RR-HLW origin

Element	**Thoria rich-HLW**	**PHWR-HLW**	**Cs-rich-HLW**	**RR- HLW**
	(mg/L)	(mg/L)	(mg/L)	(mg/L)
Th	5000 ± 10	-	-	-
Al	1350 ± 9	-	-	5700 ± 11
Fe	2200 ± 7	350 ± 10	332 ± 6	7500 ± 12
Ni	240 ± 5	50 ± 2	42 ± 2	650 ± 9
Cr	540 ± 8	69 ± 3	85 ± 4	830 ± 8
Ce	1.81 ± 0.09	-	-	92 ± 3
Na	368 ± 8	5255 ± 20	12.5 ± 0.7	-
Sr	26.6 ± 0.8	34 ± 2	-	-
U	-	5000 ± 12	-	1850 ± 15
Mn	-	85 ± 3	-	-
Ca	-	287 ± 9	246 ± 9	1120 ± 17
Mo	-	90 ± 3	153 ± 9	-

3.4 Development of glasses

Sodium Borosilicate (SiO_2-B_2O_3-Na_2O) glass system is used for vitrification of HLW. This selection is based on flexibility of borosilicate glass with regards to waste loading and the ability to incorporate many different kinds of waste elements [72]. Borosilicate glasses have silica (SiO_2) as the major component, then boric oxide (B_2O_3) as second major component, then comes sodium oxide (Na_2O), aluminum oxide (Al_2O_3), Alkaline earth oxides (CaO/BaO), etc. Alkali earth oxide such as Na_2O is used to reduce the pouring temperature of borosilicate glass. Alkaline earth oxides have been used as modifiers to sodium borosilicate system to improve the properties like solubility of nuclear constituents, suppression of cesium volatility, chemical durability etc. SiO_2, B_2O_3 and Al_2O_3 are network formers because they form strong covalent bonds involving SiO_4, AlO_4 and BO_4tetrahedra and BO_3 triangles [13]. Silicon is the main glass forming element in nuclear borosilicate glass and its tetrahedra, SiO_4 which comprises of bridging oxygen (BO) means connecting to another silicon unit and non-bridging atoms of oxygen (NBO) means oxygen connecting to other alkali/alkaline earth elements. Alkali, alkaline earth, transition metals and actinides cannot readily replace Si, Ba and Al, so act as network modifiers and enter the gap in the network structure and produces NBOs. Al is network former at low concentration and occurs as AlO_4 tetrahedra in the glass structure [72]. This structural unit improves the glass stability and hence the chemical durability, but if present in higher quantities, then it increases pouring temperature and phase separation in glasses. Ti is network former and forms TiO_4 tetrahedra like Al and increases the viscosity and stabilizes the glass and also helps in reducing volatility of Cs. Na is network modifier that tends to increase NBOs and decreases pouring temperature of the glass melt. Ca, Mg and Zn improve glass durability by stabilizing the glass structure [72]. Therefore, borosilicate glass is combination of network formers, intermediates and modifiers which is tailor made to obtain specific pouring temperature and desired product characterisation.

3.4.1 Criterion of glass formation

Homogeneity, chemical durability and pouring temperature are among the most important criteria used for the development of glass matrices. The first two can be considered as product durability factors whereas the last one is processing parameter related to plant application. Attempt was made to accommodate maximum waste loading in glass matrix so that the ultimate product volume to be disposed off in the repository can be minimized. In order achieve above objective, factors like solubility of waste components, decay heat associated with the fission products and chemical durability of the final product need to be given due attention. The additives for making the glass were chosen suitably considering above factors and the limitations with respect to processing temperatures. Preparation of nuclear waste glasses is combination of high level waste, glass additives and high temperature as shown in Figure 3.2. For induction heated metallic melters, the safe operating temperature is limited to ~ 1100°C beyond which temperature dependent mechanical deformation becomes significant. Thus, concentration of SiO_2 should not be more than 50 mol%, as pouring temp of glass will go beyond 1000^{o}C. Combination of concentration of glass formers (SiO_2+B_2O_3) should always be more than 60 mol% for better chemical durability of the glass.

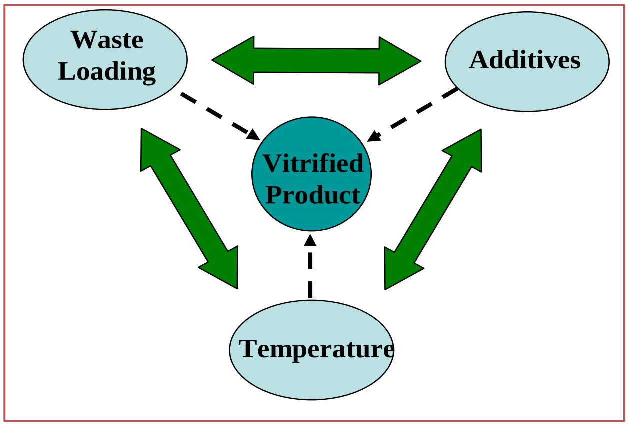

Figure 1.2: Basis of glass formation

In case of base glasses, the HLW is not added while the glass network formers, intermediates and modifiers together form the base glass. The base glass shall have pouring temperature: 950°C to 1050°C. Limitation of maximum operating temperature of 1100°C was kept due to material of construction. Also to avoid formation of any unfused / un-pourable pocket in case of- (a)proportionate waste feeding is not ensured during entire operation and (b) waste feeding stops due to any unforeseen event during plant operation.

3.4.2 Preparation of simulated high level waste

Glasses need to be prepared containing glass forming chemicals and waste constituents. High radioactivity associated with HLW, is the main barrier for its laboratory scale handling. However, for any meaningful study chemical composition of HLW needs to be retained. Simulated waste is a compromise between the two. It does not contain radioactivity but has similar chemical composition as that of HLW. In the present case, certain elements, which are present within HLW in trace amounts, such as transuranic elements (Pu, Am etc), platinum group of elements (Pd, Rh etc), process chemicals (DBP, TBP etc) were not added in simulated waste. For glass preparation, inactive simulated waste of the same chemical composition of HLW has been prepared **b**ased on the ICP-AES results, simulated HL waste solutions were prepared by using inactive AR grade chemicals of all elements in nitrate form. The details of the simulated waste solutions prepared for PHWR and thorium containing waste are given in Table 3.6.

Table 1.6: Simulated waste composition of PHWR and thorium containing waste

Simulated HLW	PHWR-HLW (g/L)	Thorium containing HLW (g/L)
UO_3 powder	6.01	--
$Th(NO_3)_4.5H_2O$	--	11.896
$CsNO_3$	0.2327	0.205
$Sr(NO_3)_2$	0.08116	0.145
$NaNO_3$	19.43	--
NaF	--	0.672
$Al(NO_3)_3.9H_2O$	--	18.756
$Fe(NO_3)_3.9H_2O$	2.532	15.916
$Cr(NO_3)_3.9H_2O$	0.5346	4.1536
$Ni(NO_3)_2.9H_2O$	0.2477	1.188
$Mn(NO_3)_2.6H_2O$	0.4441	--
$Ca(NO_3)_2.4H_2O$	1.6911	--
RuO_2	0.3555	0.0013
MoO_3	0.135	--

Simulated HL solutions prepared before taking up for glass development studies were further cross checked by ICP-AES system. To corroborate ICP-AES results, another multi-elemental analytical technique, energy dispersive X-ray fluorescence spectroscopy (EDXRF) was also used for analysis of simulated high level waste solutions. The analytical results are summarised in Table 3.7 where the simulated high level waste from PHWR and thoria containing waste have been characterized using the optimized ICP-AES method and a comparison was carried out using EDXRF. The ICP and ED-XRF results were also found to be in good agreement with that observed for ICP-AES. The simulated waste solutions were then used for the preparation of simulated waste glasses.

Table 1.7: Characterization of SHLW by ICP-AES and EDXRF

Element	**Thoria rich-HLW**		**PHWR-HLW**	
	ICP-AES (g/L)	**EDXRF (g/L)**	**ICP-AES (g/L)**	**EDXRF (g/L)**
Ca	-	-	0.29±0.01	0.26 ± 0.01
Cr	0.55±0.02	0.44 ± 0.02	0.069±0.03	BDL
Fe	2.41±0.06	2.58 ± 0.06	0.35±0.01	0.3 ± 0.01
Ni	0.24±0.02	0.22 ± 0.02	0.05±0.01	BDL
Mn	-	-	0.084±0.01	0.08 ± 0.01
Al	1.34±0.03	1.31 ± 0.03	-	-
Sr	0.06±0.01	0.06 ± 0.01	0.032±0.01	BDL
Na	0.24±0.01	0.20 ± 0.01	5.20±0.06	5.0 ± 0.06
Mo	-	-	0.088±0.05	BDL
Ce	BDL	BDL	-	-
U	-	-	4.96±0.03	5.40 ± 0.03
Th	4.87±0.05	6.2 ± 0.03	-	-

3.4.3 Preparation of glasses

Waste glasses are prepared by mixing glass additives and simulated waste solutions together and charging the mix in high temperature furnaces till its pouring temperature is reached. For the preparation of glasses in laboratory, required amounts of analytical grade glass forming chemicals like SiO_2, H_3BO_3, $NaNO_3$, TiO_2, $Ba(NO_3)_2$ and simulated waste solutions of a typical glass composition was taken. The composition was thoroughly mixed. The slurry was then dried under IR lamp. The solids are then grinded well and heated at different temperatures up to its pouring point in a platinum crucible. The temperature of the furnace was raised gradually at the interval of 50 °C for 1hr each and then soaked at the pouring temperature for 2 to 3 hrs. The glass was then poured on stainless steel plate (Figure 3.3) and allowed to cool to ambient temperature.

Figure 1.3: Pouring of nuclear waste glass in laboratory

Processes going on at different temperatures during glass preparation inside furnace are as follows: mass charging (100–105°C), evaporation of water (105–120°C), calcination

(300–700°C), fusion – melt formation (700–850°C) and soaking (950–1,000°C). After soaking, the homogeneous melt is poured within the stainless steel plates and allowed to cool to ambient temperatures.

3.4.4 Development of waste glasses

In this section, the glass preparation for the PHWR waste is discussed in detail. Many glass compositions were tried where the pouring temperature of glasses is kept 900-1000°C. The pouring temperatures were noted visually. Also visual observation is done with respect to phase separation if any in the glasses. These experimental observations served as a basis to have preliminary screening to pick up the candidate glass formulation for further detailed product characterisation. Keeping glass formers (SiO_2+B_2O_3) more than 60 mol% for better chemical durability. Alkaline earth oxide, titanium dioxide and Aluminum oxide have been used as modifiers to improve the properties like solubility of nuclear constituents, suppression of cesium volatility, chemical durability etc. Initially base glasses were prepared, base glasses are the glasses without waste constituents in it. As discussed earlier, the pouring temperature for the base glasses was kept in the range of 950^0C to 1050^0C. The different glasses prepared and the visual observations were recorded for the base glass preparation for PHWR waste. The base glass compositions are as shown in Table 3.8**.**

Table 1.8: Base glass compositions of PHWR-HLW glass development

Glass code	Composition (wt %)		Physical observation	Pouring temperature (°C)
	Glass formers ($SiO_2+B_2O_3$)	Glass modifiers ($Na_2O+CaO+TiO_2$)		
GM01	74.11	25.88	Phase separation	1000
GM02	67.19	32.81	Phase separation	1000
GM03	60.55	39.44	Homogeneous	925
GM04	60.96	39.04	Homogeneous	900
GM05	67.85	32.15	Phase separation	1000
GM06	74.38	25.62	Phase separation	1000
GM07	67.37	32.63	Homogeneous	1000
GM08	64.06	35.94	Homogeneous	1000
GM09	64.24	35.76	Homogeneous	900
GM10	67.69	32.32	Homogeneous	950
GM11	70.97	29.03	Homogeneous	1000
GM12	70.82	29.19	Homogeneous	1000
GM13	67.53	32.47	Homogeneous	1000
GM14	71.05	28.95	Homogeneous	975

In the next stage, simulated waste glasses were prepared. The different glass compositions were tried. Ternary phase diagram of SiO_2-B_2O_3-Na_2O was seen in the glass forming region for waste glasses, where CaO, TiO_2 an Al_2O_3 are kept 10 mole% and waste oxides are kept 12 mole%. The composition of the waste glasses is as shown in Table 3.9.

Table 1.9: Different waste glass composition prepared for PHWR glass

Glass code	**SiO_2**	**B_2O_3**	**Na_2O**	**CaO**	**TiO2**	**Al_2O_3**	**Waste oxide**
GM01	48(38.94)	18(16.92)	12(10.04)	6(4.54)	2(2.16)	2(2.75)	12(24.65)
GM02	48(39.18)	12(11.35)	18(15.16)	6(4.57)	2(2.17)	2(2.77)	12(24.8)
GM03	42(34.23)	12(11.33)	24(20.18)	6(4.56)	2(2.17)	2(2.77)	12(24.76)
GM04	36(29.11)	18(16.87)	24(20.03)	6(4.53)	2(2.15)	2(2.74)	12(24.57)
GM05	36(28.94)	24(22.35)	18(14.93)	6(4.5)	2(2.14)	2(2.73)	12(24.42)
GM06	42(33.81)	24(22.38)	12(9.97)	6(4.51)	2(2.14)	2(2.73)	12(24.46)
GM07	45(36.59)	15(14.13)	18(15.10)	6(4.55)	2(2.16)	2(2.76)	12(24.70)
GM08	42(34.12)	15(14.12)	21(17.60)	6(4.55)	2(2.16)	2(2.76)	12(24.68)
GM09	39(31.56)	18(16.88)	21(17.54)	6(4.53)	2(2.15)	2(2.75)	12(24.59)
GM10	39(31.47)	21(19.63)	18(14.99)	6(4.52)	2(2.15)	2(2.74)	12(24.51)
GM11	42(33.91)	21(19.65)	15(12.5)	6(4.52)	2(2.15)	2(2.74)	12(24.53)
GM12	45(36.48)	18(16.90)	15(12.55)	6(4.54)	2(2.16)	2(2.75)	12(24.63)
GM13	42(34.02)	18(16.89)	18(15.04)	6(4.54)	2(2.15)	2(2.75)	12(24.61)
GM14	41.5(34)	21.1(20)	15.4(13)	7.8(6)	1.37(1.5)	1.08(1.5)	11.5(24)

Glasses of all compositions arrived at from the triangular diagram were prepared by melt-quench method as explained in the topic. Out of all compositions, suitable glass matrices were selected after initial screening, based on pouring temperature and visual homogeneity.

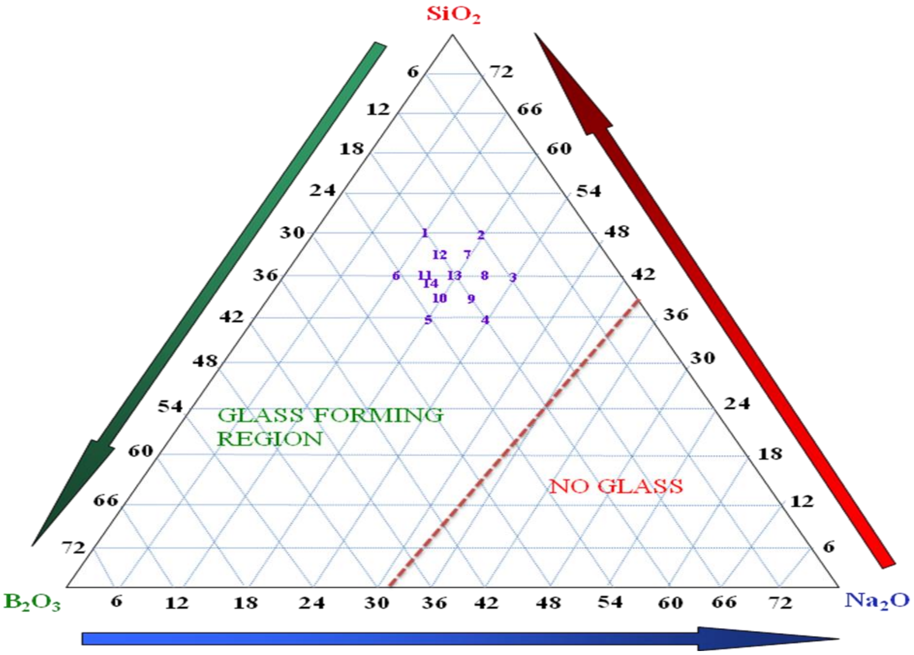

Figure 1.4: Ternary phase diagram of waste glasses where CaO, TiO$_2$ an Al$_2$O$_3$ are kept 10 mole% and waste oxides are kept 12 mole% [14]

The ternary phase diagram is as shown in Figure 3.4. All the selected glasses prepared fall in the glass forming region. The glasses were characterized for X-ray diffraction (XRD) and Scanning Electron Microscope (SEM) to check the structural homogeneity. The glasses were screened for chemical durability test. After that Glass code GM11 glass was chosen immobilization of PHWR waste and taken up for further detailed characterization. On the similar basis, sodium borosilicate glass with barium as modifier (GM44) was chosen for immobilization of thorium containing waste. For thorium containing waste, it was reported that, the solubility of thoria is 2–5% and maximum reported value is 6% in borosilicate glasses The solubility limit of thoria in borosilicate matrices increases with addition of barium as network modifier [15]. It was noted that barium borosilicate glass matrix can contain upto 16 wt% thoria without phase separation. Beyond this limit, thorite and thorianite separates out within the matrix.

Some of the glasses on visual examination gave the evidence of phase separation even after heating temperatures of up to 1000°C. From the homogeneous glasses further refinement of glass composition was achieved by considering the pouring temperature and ratio of glass formers to modifiers. From the region of homogeneous vitreous mass formation, two base glass compositions namely GM11 and GM44 were selected for detailed investigations (Table 3.10). The reason for the selection of these two compositions were the presence of higher concentration (more than 70%) of glass formers such as SiO_2 and B_2O_3, as compared to other compositions, giving better chemical durability. Vitrified waste product (VWP) i.e. base glass additives of the selected two glass compositions namely GM11 and GM44 were prepared with addition of appropriate composition of simulated waste. The waste glass compositions of vitrified waste products GM11 and GM44 are given in Table 3.11. Detailed product evaluation of vitrified waste product has been carried out and discussed in the following topic:

Table 1.10: Base glass composition of GM11 and GM44 glass

Sr No	Waste oxide	GM11mole (%)	GM44mole (%)
1	SiO_2	47.73	48.16
2	B_2O_3	23.87	24.41
3	Na_2O	17.04	21.89
4	CaO	6.82	--
5	TiO_2	2.27	--
6	Al_2O_3	2.27	--
7	BaO	--	5.54

Table 1.11: Waste Glass Compositions of GM11 and GM44

Sr No	Oxide	GM11 mole (%)	GM44 mole (%)
1	SiO_2	39.22	43.95
2	B_2O_3	19.62	22.48
3	Na_2O	27.34	20.02
4	CaO	6.43	--
5	TiO_2	1.87	--
6	Al_2O_3	1.87	2.55
7	BaO	--	5.06
8	ZrO2	--	--
9	Cs_2O	0.07	0.05
10	SrO	0.04	0.07
11	Fe_2O_3	0.37	2.01
12	Cr_2O_3	0.03	0.18
13	NiO	0.10	0.42
14	MnO	0.18	--
15	RuO_2	0.31	--
16	MoO_3	0.11	--
17	UO_2	2.45	--
18	NaF		1.63
19	ThO_2		1.59

3.5 Detailed evaluation of the conditioned product

3.5.1 Product pour temperature

The temperature at which the molten mass is poured is termed as product pour temperature of the glass. Product pour temperature is one of the important plant processing parameters. The type of furnace and the material of construction used for the furnace advocate the glass pouring temperature. In case of induction heating melters, where alloy 690 (Ni – Cr alloy) is the material of construction of melter, the safe operating temperature is limited up to ~1100 °C, beyond which temperature dependent mechanical deformations becomes significant. Pour temperatures of the base glass (glass without waste constituents) and waste glass (glass with waste constituents) made in different batches for GM11 and GM44 glass. A known volume of the simulated waste was mixed with the required amount of chemical additives of glass formers and network modifiers. The mass was then dried under infra-red lamp, crushed to a fine powder and transferred to a fireclay crucible. The powder was heated at 700 °C using resistance based high temperature furnace for 2 hours and further heated at an increment of 50 °C and kept for one hour at each stage, till the mass became freely pourable. The crucible containing molten vitreous mass was taken out from the furnace and poured on a clean metallic surface. Since we have taken a known volume of simulated waste along with the required amount of glass forming additives, this temperature will be referred as pour temperature of the waste glass. Base glass was also checked for the pour temperature. Method for making base glass is also same, but for the addition of simulated waste. Only glass forming additive will be taken and followed the same procedure as described above. The pouring temperature of GM11 and GM44 base and waste glasses are as shown in Table 3.12.

3.5.2 Density

Density of the glass products obtained using Archimedes' principle from different batches was checked and found to be in the range of 2.5-2.7 g/ml. Density of the products in the above said range indicated uniformity in preparation of glasses and consistency in the distribution of the constituents in the vitreous melt. Densities of GM11 and GM44 glasses are as shown in Table 3.12.

3.5.3 Homogeneity

Homogeneity of vitrified waste product is an important parameter in terms of product durability. As it is known that glass is an amorphous material, checking the homogeneity of waste in this context include (a) confirming amorphous nature of glass by X-ray diffraction (XRD) (b) checking homogeneous distribution of glass forming and waste constituents using Scanning Electron Microscope (SEM). Vitrified waste products made from simulated waste were subjected for above characterization. A brief description of the experiments and their observations is described below.

a) Amorphous nature of glass product

Glass matrixes were subjected to XRD examination for ascertaining amorphous nature of the vitreous product. XRD patterns of these samples were taken from 10° to 70° (2 theta) using monochromatic Cu Kα radiation at 40 KV excitation voltage and 30 mA tube current ($K\alpha_1$ =1.5406 Å and $K\alpha_2$ =1.5444 Å). XRD patterns of glasses are presented in Figure 3.5. The XRD indicates that the glasses are amorphous in nature.

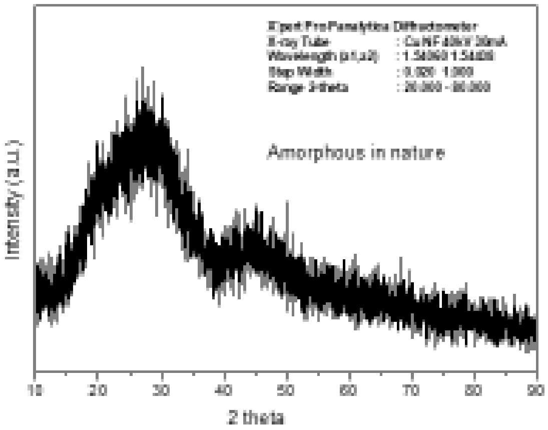

GM11 Base Glass

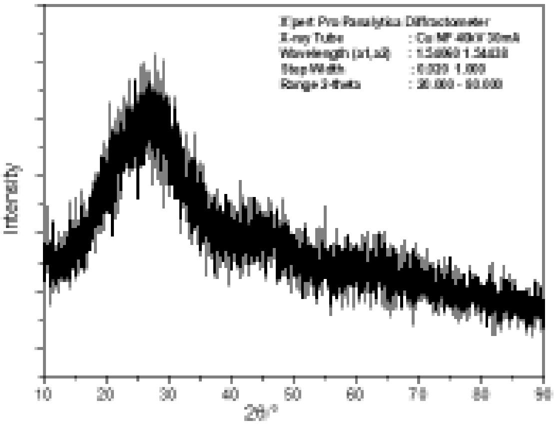

GM11 Waste Glass

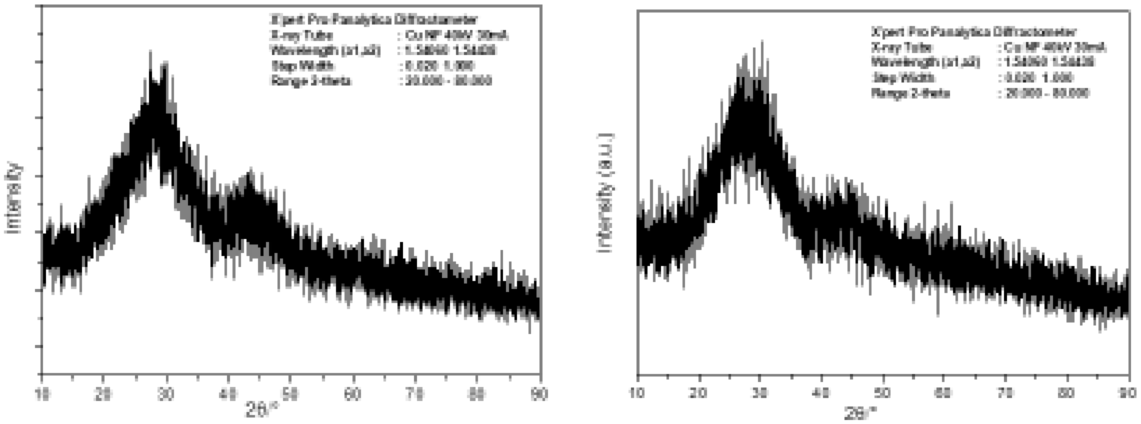

GM44 Base Glass GM44 Waste Glass

Figure 1.5: XRD pattern of glasses

b) Distribution of constituents in the matrix

Scanning Electron Microscope (SEM) images of glass samples were taken using SEM/EDS to check the homogeneity of the product. SEM images of the glass formulation are presented in Figure 3.6 for GM11 and GM44 glass. The SEM images indicate uniform distribution of elements in the glass.

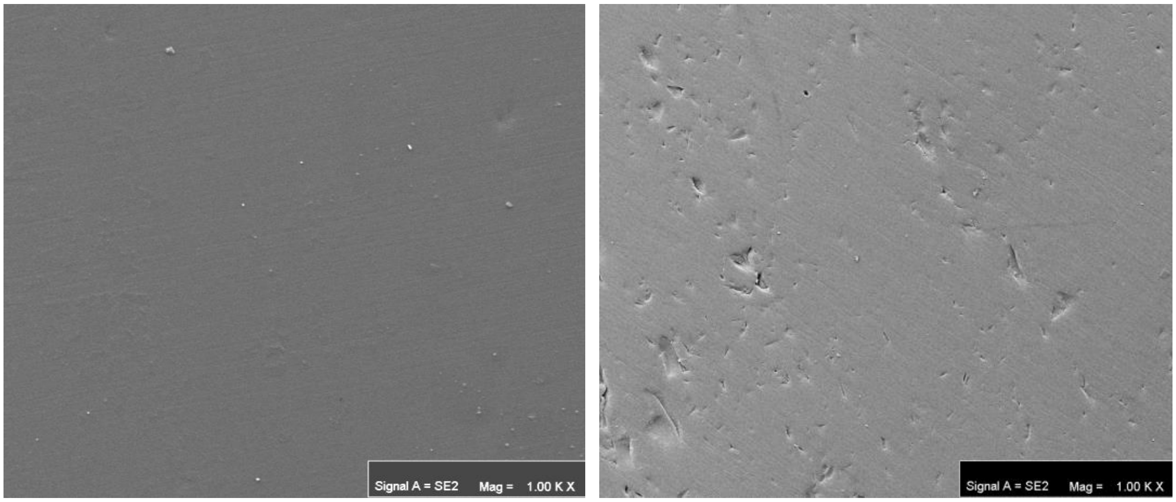

GM11 glass **GM44 glass**

Figure 1.6: SEM image of glasses

3.5.4 Glass transition temperature

Glass transition temperature (Tg) is related to the energy required to break and reform covalent bonds in a somewhat less than perfect 3D lattice of covalent bonds. The Tg is therefore influenced by the chemistry of glass. Addition of B, Na, K, Ca or Ba to a silica glass, which have valency less than 4 and they help to break up the 3D lattice and reduce the Tg. Addition of P and As which have a valency of 5 helps to re-establish the 3D lattice and increases Tg. Estimation of glass transition temperature for a vitrified waste product is important with respect to the limit of radioactivity which can be incorporated so that the decay heat because of different radionuclides does not increase the temperature more than the glass transition temperature. It is important to note that devitrification tendency of the vitrified waste product significantly gets enhanced above transition temperature because of decrease in viscosity of the product. DTA studies of the glass sample also helps in ascertaining complete fusion of the vitreous melt. A DTA curve of a GM11 and GM44 glass are shown in Figure 3.7.

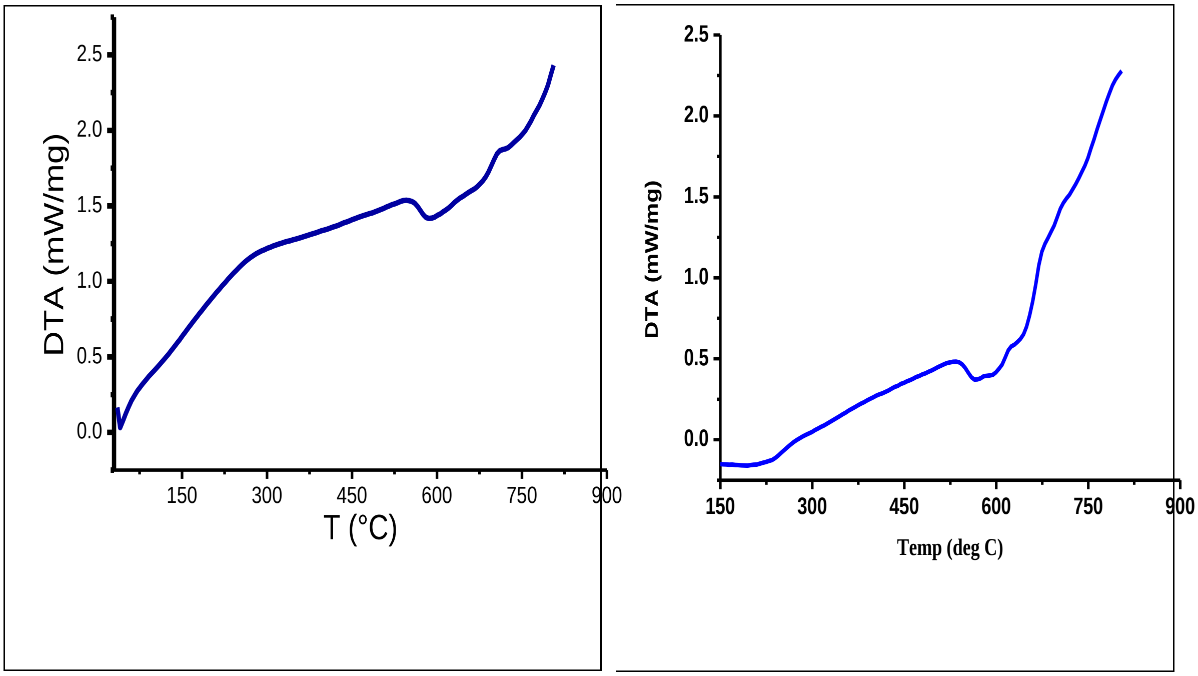

GM11 base glass **GM44 base glass**

Figure 1.7: DTA pattern of glasses

Glass transition temperature of the glass product has been evaluated by DTA, values are shown in Table 3.12.

Table 1.12: Characteristics of GM11 and GM44 glasses

Sr No	Glass Code	XRD/SEM	Density (g/cc)	Pouring temp (°C)	Glass Transition Temp Tg (°C)
1	GM-11 Base Glass	Amorphous /Homogeneous	2.517	1000	578
2	GM-11 Waste Glass	Amorphous /Homogeneous	2.605	1050	541
3	GM-44 Base Glass	Amorphous /Homogeneous	2.7	1000	557
4	GM-44 Waste Glass	Amorphous /Homogeneous	2.715	1025	552
5	International Standard Glass	Amorphous /Homogeneous	2.475	----	603

3.5.5 Chemical durability test

Evaluation of the chemical durability of nuclear waste incorporated glass, the so called vitrified waste product (VWP) is of paramount importance for ascertaining safe containment of radionuclide immobilized in the matrix. Leaching is one of the most important properties of VWP because it is the principal mechanism through which radionuclide can migrate to human environment. The release of radionuclides from the glass is closely related to the dissolution of matrix constituents. The degree of matrix dissolution is a reasonable measure for the release of radioactive species and hence for the chemical durability of the waste form. The preliminary screening and testing of the glasses GM11 and GM44 was done using ASTM leaching test (PCT-A, 7day test method) as per the procedure described in Chapter 2. International Simple Glass (ISG) was also taken for reference. All glasses were crushed, fine powdered, sieved and analysed in triplicate. The leachates are analysed for elements such as Na, B, Si, Ba, Ti, Al etc. The leach rates are calculated.

Calculations: The normalized release rate for element i is given as $NL_i$and expressed in grams of glass waste form dissolved per m^2. The calculation for NL_i is shown in Eq. below.

$$NL_i = \frac{C_i}{f_i \times (\frac{SA}{V})}$$

Where, C_i is concentration of element "i" in the solution, g_i/L

f_i is fraction of element "i" in the unleached waste form (unitless) and

$\frac{SA}{V}$ is the ratio of surface area of the final waste form to the leachate volume, m^2/L.

Table 1.13: Leach Rates of GM11 and GM44 glasses (ASTM 1285-02 PCT-A test)

Sr No	Glass	Leach rate in g /(cm^2.day)				
		Sodium	**boron**	**silica**	**Barium**	**Ca, Ti, Al**
1	GM11 base glass	7.35 x10^{-5}	8.54 x10^{-5}	6.82 x10^{-6}	---	BDL
2	GM11 waste glass	2.13 x 10^{-5}	7.8x 10^{-5}	1.02 x 10^{-5}	---	
3	GM44 base glass	2.32 x10^{-5}	9.58 x10^{-6}	6.67 x10^{-6}	3.87 x10^{-6}	BDL
4	GM44 waste glass	3.63 x 10^{-5}	1.3 x 10^{-4}	7.5 x 10^{-6}	3.87 x 10^{-6}	
5	ISG	3.33 x10^{-5}	1.13 x10^{-5}	1.51 x10^{-6}	---	BDL
6	Basalt glass	2.4 x 10^{-5}	---	1.07 x 10^{-5}	---	

BDL value for Ba= 1.4 x 10^{-6} Ca=3.45 x 10^{-8}, Ti=8.6 x 10^{-6}, Al=7.6 x 10^{-6} g/(cm^2.day)

The details of leach rates are as given in Table 3.13 above**.** The leach rates of sodium and boron were more than other elements. Silicon was the third element coming out from glass. Then it was barium to leach out. The leach rates of Calcium, titanium and aluminum were in BDL level. Detailed chemical durability studies will be discussed in next chapter.

References

---

[1] Ojovan MI and Lee WE, “Immobilisation of Radioactive Wastes in Glass”, Elsevier BV, 2005.

[2] Lutze W, Ewing, RC (Eds), Radioactive Waste Forms For the Future, North-Holland, Amsterdam, (1998) 31.

[3] Jahagirdar PB and Wattal PK, “Development of Melt Compositions for Sulphate bearing High Level Waste, “BARC report, BARC/1997/E/021, (1997).

[4] Thorat VS, Soudamini N, Mishra RK, Kaushik CP and Raj K, “Studies on Barium and Lead borosilicate systems for immobilization of sulphate bearing high level waste,” presented in 14th Conference of Indian Nuclear Society on, “Nuclear Fuel Cycle Technologies: Closing the Fuel Cycle” being held at IGCAR Kalpakkam during December 17-19, 2003.

[5] Verma BB, Morzaria T, Mehta D, Aniruddha D, Ozarde PD and Raj K, “Engineering Scale Processing of Sulphate Bearing HLLW by Vitrfication –an Operating Experience,” presented in 14th Conference of Indian Nuclear Society on, “Nuclear Fuel Cycle Technologies: Closing the Fuel Cycle” being held at IGCAR Kalpakkam during December 17-19, 2003.

[6] Steru H and Weise EE, “High Temperature Properties and Decomposition of Inorganic Salts, Part I, Sulphates,” National Bureau or Standards, U. S. Govt. Printing Office.

---

[7] Kellog HH, "A Critical review of Sulfation Equilibria," Trans. Metal Soc.AIME, 230 (1964) 1622-1634.

[8] Kaushik CP, Mishra RK, Sengupta P, Amar Kumar, Das D, Kale GB, Raj K, " Barium borosilicate glass – a potential matrix for immobilisation o sulphate bearing high-level radioactive liquid waste", J. Nucl. Mater 358 (2006) 129-138.

[9] Shah JG, Wattal PK, "Development of caesium containing glass for gamma irradiator, International Seminar on Science and Technology of Glass Materials, IOP Conf. Ser: Mater. Sci. Eng. 2 (2009).

[10] Kaushik CP, Amar Kumar, Neelima S. Tomar, S. Wadhwa, Darshit Mehta, R.K. Mishra, Jyoti Diwan, Suresh Babu, S.K. Marathe, A.P. Jakhete, Savita Jain, Anand G. and Kailash Agarwal, "Recovery of cesium from high level radioactive waste for societal applications, an important milestone", published in BARC newsletter, BARC, India, 2018.

[11] Dey PK, Bansal NK, Spent fuel reprocessing; A vital link in Indian nuclear power program, Nucl. Eng. Des. 236 (2006)723–729.

[12] Kaushik C.P., "Study on identification and physico-chemical characterization of promising vitreous matrices for immobilization of sulphate bearing high level radioactive liquid waste", PhD thesis, Mumbai university (2007) 50.

[13] M. Ojovan, "Immobilisation of Radioactive Wastes in Glass", An Introduction to

Nuclear Waste Immobilisation, 2005.

[14] Praveena Navneethan, "Development of glass matrix for vitrification of HLW of KARP and analysis of physico-chemical properties of the vitrified waste product", M. Tech thesis (2011) 50.

[15] Mishra RK, Sengupta P, Kaushik CP, Tyagi AK, Raj K, "Studies on immobilisation of thorium in barium borosilicate glasses", J. Nucl. Mater 360 (2007) 143-150.

Chapter 4 : *Chemical Durability Assessment of Glasses*

Chemical Durability Assessment of Glasses

4.1 Introduction

The term chemical durability of glasses or leaching or dissolution of glasses are interchangeable and used to refer glass corrosion. Chemical durability of nuclear waste glasses is studied in terms of leaching tests. The release of radionuclides from the glass is closely related to the dissolution of matrix constituents. The degree of matrix dissolution is a reasonable measure for the release of radioactive species and hence for the chemical durability of waste form. The leaching tests are done in laboratory, generally on short term basis. The data is collected, different graphs are plotted, the leached glasses and the leached solutions are analysed and based on that conclusions are drawn for the chemical durability of the waste glasses. The glasses are usually ranked relative to one another after subjecting them to similar experimental conditions and the nature of the experiment determines the experimental conditions. The experimental conditions include leaching experiment type (static or dynamic), glass composition, aqueous solution chemistry, temperature and time. After completion of the experiment, the complete analysis of the leached solution for all the glass components and a detailed analysis of the leached glass surface provide useful information about the leach rate and mechanisms of various elements coming out from glass.

In this chapter, results on leaching studies of two glasses namely GM11 and GM44 glasses shall be discussed. International Simple Glass (ISG) was also taken for reference purpose. An international simple glass (ISG) [38,1] is based on six oxide components, has been developed by the waste glass community. This development is also aimed to relate testing and modelling approaches that are being developed in several nations with respect to leaching properties of glasses. Gin et al [95] have carried out detailed leaching studies on this simple glass at pH values 9.0 and 11.5. From this study, authors concluded that at pH = 9.0, alteration layers are formed on glass surface due to release of weakly bonded cations like Na^+, Ca^{2+}, and boron species from glass. The ion-exchange process facilitates penetration of water through alteration layers. At higher pH values (pH = 11.5), dissolution of alteration layer occurs in solution. The leaching experiments under static conditions at 90°C and leaching under conditions of high temperatures and pressures (at 200°C and under a pressure of ~17 bars) was carried out for ISG.

This chapter deals with the investigation of long term leaching studies of waste glasses using actual ground water as leachant and leaching studies under accelerated conditions. Accelerated leaching is done under high pressures and temperatures. These aggressive test conditions are suitable for structural alterations which can be seen in short test durations; otherwise it takes time of few years to show. Techniques like X-ray diffraction (XRD), scanning electron microscopy (SEM), solid-state Nuclear Magnetic Resonance (NMR) have been used to monitor leaching-induced structural modifications and phase formations in the leached glass samples. The waste glass NMR and Photoluminescence (PL) spectra are quiet complex, so to study the structural alterations, base glasses are taken up for accelerated leaching study and to study the effect of actual ground water on leaching, waste glasses are taken up for long term leaching studies.

4.2 Long term leaching studies of glasses

Chemical durability of glasses mainly depends on glass composition, leachant composition and temperature. In that static leaching test gives understanding of the chemical durability of Vitrified Waste Product (VWP) for determining the dissolution and release of radionuclides from Vitrified Waste Product (VWP) in a Geological Disposal Facility (GDP) over short and long time scales. The long term leaching studies of nuclear waste glasses were done simulating the disposal conditions. The Figure 4.1 broadly describes the geological repository conditions with multibarrier disposal conditions.

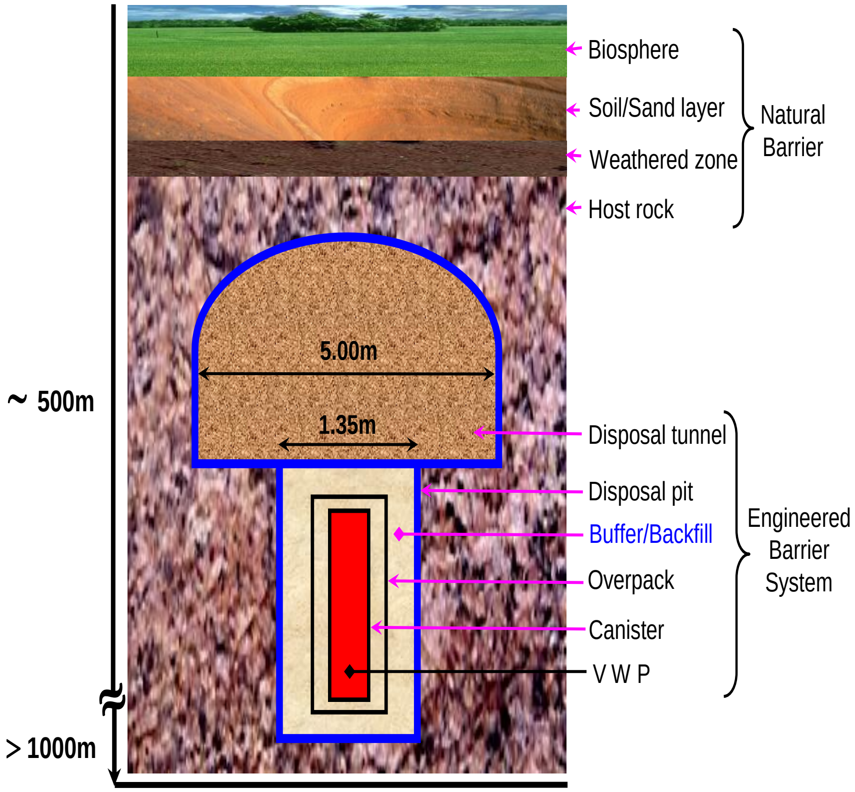

Figure 1.1: Multibarrier disposal concept [2]

Multibarrier disposal consists of two basic units, namely, ‘engineered barrier system (EBS)’ and ‘natural barrier system (NBS)’. The EBS is made up of four components, namely, waste form, canister, overpack and buffer. The ‘waste form’ is the inert matrix generally glass which primarily incorporates the HLW components within its structure. It is then contained within a stainless steel (AISI 304L grade) container called ‘canister’ and two or three such canisters are put inside (one above the other) another stainless steel (AISI 304L grade) container called overpack. Such overpacks are then placed inside underground interim storage facility and finally inside drilled holes dug within suitable host rock such as granite etc. This actually acts as natural barrier (NBS). The gap in between the overpack and surrounding host rock are to be filled up by backfill (broken rock fragments) and buffer (a composite of clay minerals, graphite and sand) materials. It may be noted here that geological repository need to be constructed at a depth of 500–1,000 m from ground so as to minimize or exclude the possible effects of unforeseen surficial geological processes in future, if any. Such deep burial also makes the repository environment extremely harsh due to simultaneous operations of different fields such as thermal-, hydrological-, biological-, chemical-, radiation- and mechanical fields. Computational estimates show that under such environment, stainless steel containers are not likely to last more than few thousand years, which makes proper selection of nuclear waste form material even more challenging [3,4,5,6].

The conditions which control glass dissolution under disposal conditions are:

a) the glass composition
b) the ground water composition
c) the near field materials

d) the nature of the host rock

e) and the temperature

The vitrified waste products are finally disposed in repositories in the granitic rock. Thus an important case can be considered is that of flooded vault, although it is very rare to occur. Ground water flows, but the flow rates are expected to be very small which can be compared with static leach tests. A static, non-replenishment leach test seems to be the most appropriate choice for the evaluation of candidate waste form. Simulated waste glasses, viz GM11WG (Waste glass for PHWR's HL waste) and GM44WG (waste glass for thorium containing waste) are chosen for this study. Leachant used was actual ground water brought from URL's test laboratory site, India. This actual ground water was equilibriated with the granite rock powder and soil brought from same site to simulate disposal conditions.

The test method used was standard leach test (ASTM Designation: C1285-02) which provides a measure of the chemical durability of a homogeneous waste glasses. Test method B which is product consistency test (PCT-B), was developed to measure the chemical durability of radioactive, mixed, or simulated glass waste forms, at various test durations, test temperatures and leachant compositions. This test method is static and can be conducted in stainless steel or TFE-fluorocarbon vessels. This test method is used to characterize the dissolution or leaching behaviour of various simulated waste forms in various leachants under specific conditions of the test based on analysis of the test solution. Data from this test are used to calculate normalized elemental mass loss values from specimens exposed to aqueous solutions at temperatures <100°C. This test was conducted under static conditions in a constant leachant volume and at three different temperatures viz 50°C, 70°C and 90°C. The reactivity of the vitrified waste glass specimens was determined from the amounts of components released and accumulated in the leachant over the test duration of one year.

4.2.1 Experimental

The three glass samples viz GM11 waste glass, GM44 waste glass which are developed in the laboratory and ISG (International Standard Glass) for reference purpose were taken. The glass composition is as shown in Table 4.1

All the glass samples were handled and stored in clean containers. The glass samples were wrapped in clean plastic bag and break it into smaller fragments with a hammer. The smaller glass pieces were transferred to a clean pestle mortar where it was crushed to fine powder. The glass powder was sieved through -100+200 ASTM mesh (0.149-0.074 mm). The fraction of the sieved glass powder was transferred into a clean glass beaker for washing purpose so as to remove adhering fines. The glass powder was washed thrice with DM water by forcibly adding it from squirt bottle in circular motion so that the wash stream agitates all the glass. Then the glass samples were allowed to settle down for one min, then the water was decant off. The glass powders were ultrasonically cleaned twice using DM water for two minutes. The same procedure of washing and ultrasonic cleaning was repeated with absolute alcohol. The beakers containing washed glass powders were put in a 90±10^{o}C oven for drying overnight. The glass powder was then transferred in Teflon bottles. Required amount of demineralised water and actual ground water was added as leachant. The surface area to volume ratio was kept 2 cm^{-1}. The sample bottles with three different glasses and two different leachants were kept in oven at three different temperatures viz 50°C, 70°C and 90°C with temperature variation of ±2°C. The bottles were then removed from oven at different time intervals. The leachates were filtered through a 0.45µm syringe filter and then acidified and analysed for release for elements such as sodium, boron and silicon using ICP-AES.

Table 1.1: Compositions of glasses used in the present study (mole%)

Sr No	Oxide	GM11WG	GM44WG	ISG
1	SiO_2	39.22	43.95	60.13
2	B_2O_3	19.62	22.48	15.96
3	Na_2O	27.34	20.02	12.63
4	CaO	6.43	--	5.73
5	TiO_2	1.87	--	--
6	Al_2O_3	1.87	2.55	3.84
7	BaO	--	5.06	--
8	ZrO_2	--	--	1.71
9	Cs_2O	0.07	0.05	--
10	SrO	0.04	0.07	--
11	Fe_2O_3	0.37	2.01	--
12	Cr_2O_3	0.03	0.18	--
13	NiO	0.10	0.42	--
14	MnO	0.18	--	--
15	RuO_2	0.31	--	--
16	MoO_3	0.11	--	--
17	UO_2	2.45	--	--
18	NaF		1.63	--
19	ThO_2		1.59	--

Here, the leachant used was actual ground water. Around 1L ground water was equilibriated with 50 g of granite rock powder, the water was then filtered. Again, the filtered water was equilibriated with 50 g of soil. The filtered actual ground water was used as leachant simulating repository conditions. The leachant composition is as shown in following Table 4.2.

Table 1.2: Composition of leachants

Sr No	Property	DMW	Ground water equilibrated with granite and soil
1	pH	6 .72	9.57
2	conductivity	1.0µS/cm	1.372mS/cm
3	Total Hardness	<1ppm	175ppm as $CaCO_3$
4	Chloride	<10ppm	300ppm
5	Fluoride	0.0689ppm	3.50ppm
6	Silicon	1ppm	20ppm
7	Total Solids (w/v)	0.001%	0.154%
8	Fe	BDL	0.0351
10	Mg	BDL	5.04
11	Al	BDL	0.141
12	Ca	BDL	66.0
13	Na	BDL	292.8
14	K	BDL	12.33

BDL values are less than 0.01ppm; DMW:Demineralised water

4.2.2 Solution analysis

The leachant solution after completion of the experiment, with different time durations was filtered, acidified and analysed using ICP-OES system. The observations are discussed as follows:

4.2.2.1 Elemental release analysis

Sodium, boron and silicon concentrations obtained from ICP-OES were used to calculate the normalized release of elements (NL_i), the equivalent thickness (ET_i) and the glass dissolution rates (r) and altered glass fraction (AG).

The normalized release rate for element i is given as $NL_i$and expressed in grams of glass waste form dissolved per m^2. The calculation for NL_i is shown in Eq. 7.

$$NL_i = \frac{C_i}{f_i \times (\frac{SA}{V})} \text{............} \quad [1]$$

Where, $C_i$is concentration of element "i" in the solution, g_i /L

f_i is fraction of element "i" in the unleached waste form (unitless) and

$\frac{SA}{V}$ is the ratio of surface area of the final waste form to the leachate volume, m^2/L

Elemental release from glass for a period of one year can be seen from the Figure 4.2 below which indicates the leach rate of GM11waste glass for release of Si, B and Na. It is seen that B and Na are release at higher rate. Silicon is third element coming out from glass. GM44 and ISG glass follows similar trend.

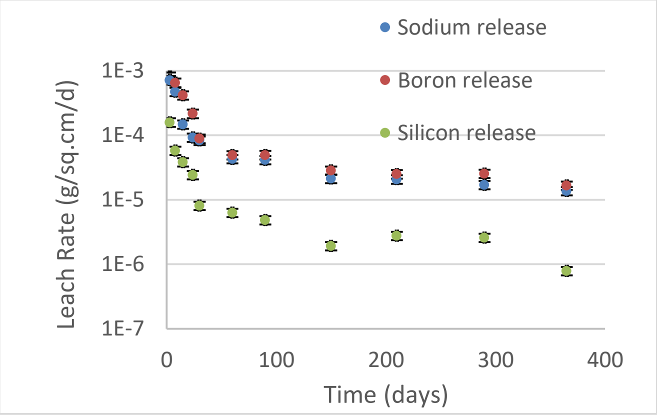

Figure 1.2: GM11 waste glass leach rate using ground water at 90°C

Effect of glass composition, can be seen from the Figure 4.3 below, for three different glasses. It is seen that six oxide glass ISG has minimum leaching than the waste glasses GM44 and GM11 for a period of one year.

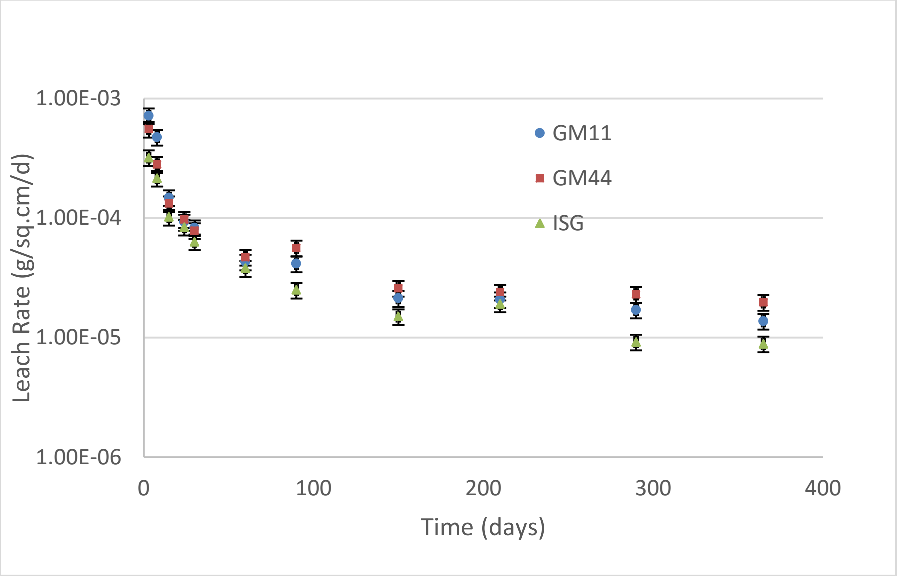

Figure 1.3: GM11, GM44 and ISG glass leaching using ground water at 90°C

Effect of leachant composition can be seen from the Figure 4.4 , the leachant used was demineralised water and another was granite equilibriated actual ground water. GM44 and ISG glasses follow a similar trend.

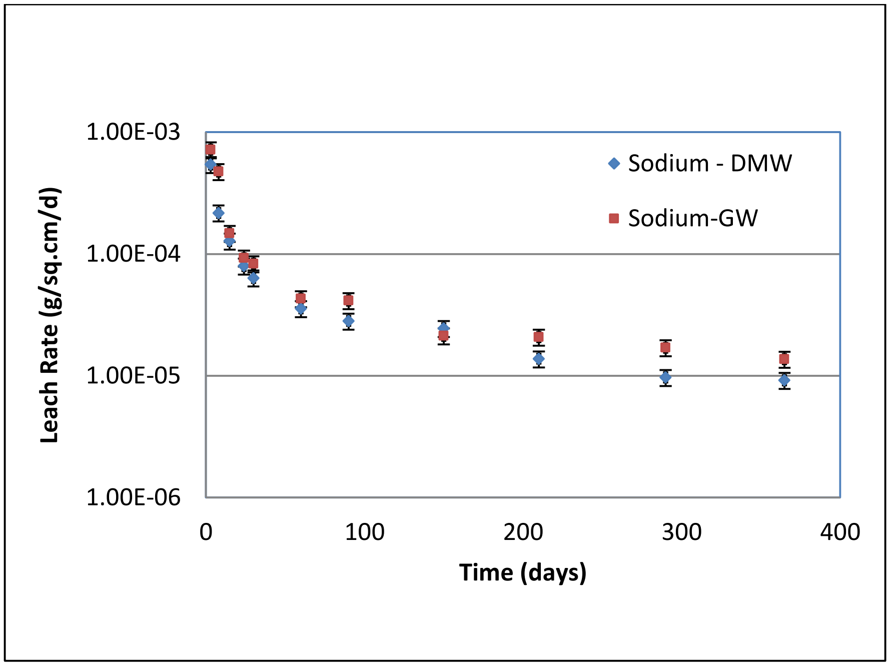

Figure 1.4: GM11 waste glass leach rate at 90°C for sodium release in DMW and GW

Effect of temperature can be seen from the Figure 4.5 . It is seen that as temperature increases leach rate increases.

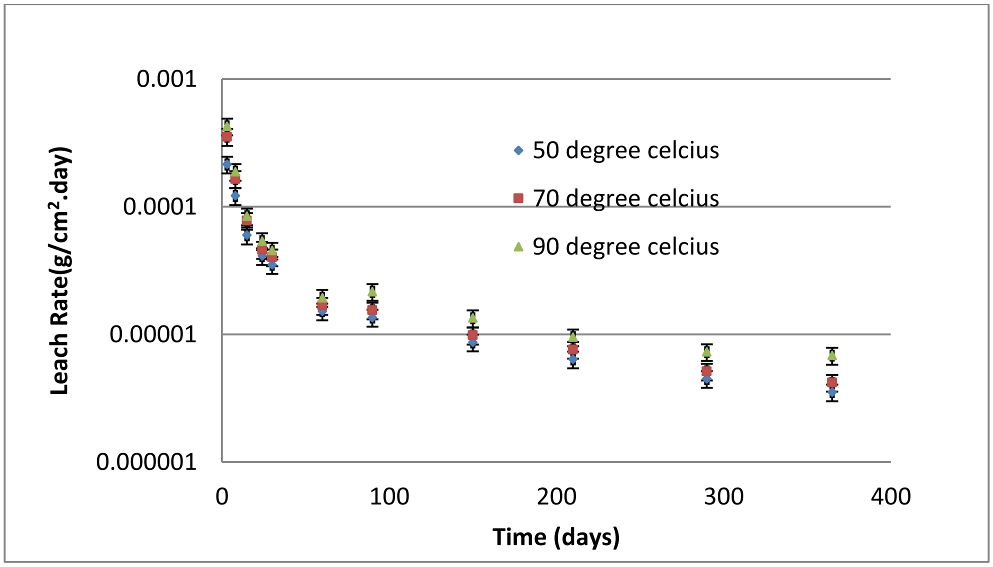

Figure 1.5: Boron release rate for GM11 waste glass at different temperatures

The pH measurements on leachant solutions were done during the experiment; the results are shown in following Figure 4.6. The pH of the solution increases as the reaction proceeds and it starts from reaches to pH 11 which again enhances the leaching of the glasses.

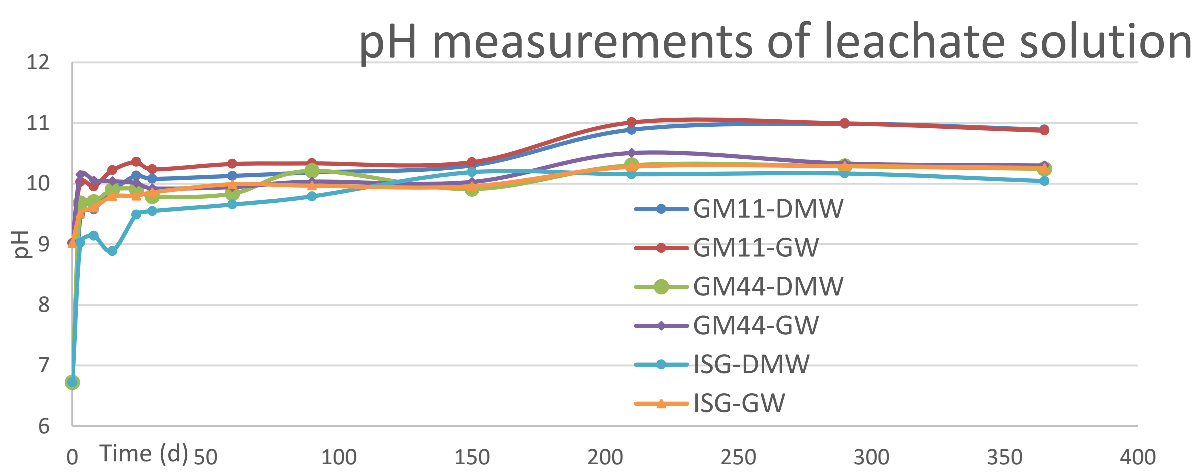

Figure 1.6: pH variation of leachant solutions

4.2.2.2 Equivalent thickness of altered glass

The equivalent thickness of altered glass can be calculated as shown in Eq. 8.

$$ET(i) = \left\{1 - (1 - AG)^{1/3}\right\} R_0 \ldots\ldots \qquad [2]$$

AG is altered glass fraction and calculated as,

$$AG = \frac{m}{m_0 \times f_B} \qquad [3]$$

where, m_i is the concentration of element i leached in g, m_o is the initial mass of the glass powder in g and f_i is fraction of element "i" in the unleached waste form (unitless).

R_0 is average radius of the glass particles and geometrically calculated as

$$R_0 = \frac{3}{\rho \times SA} \qquad [4]$$

Where ρ is density of glass (g.cm^{-3}) and SA is surface area in cm^2.

Boron is good alteration tracer as it does not take part in retention of alteration product formed at the glass surface [7] and also it is network former. Therefore, ET is calculated in terms of boron release.

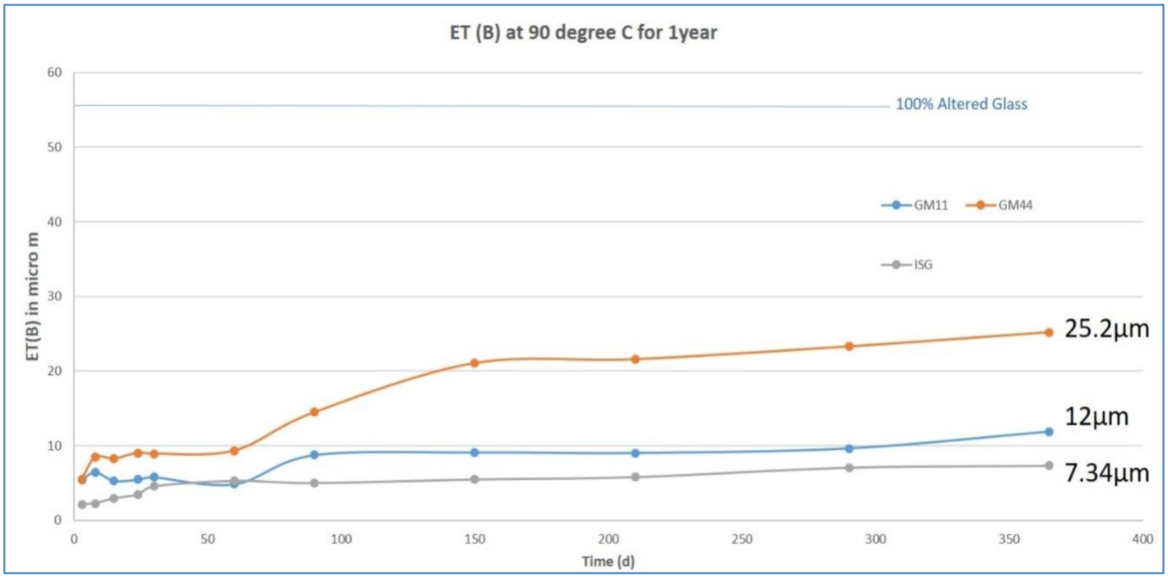

Figure 1.7: Equivalent altered thickness of different glasses

The Figure 4.7 gives the comparison of equivalent thickness of GM11 and GM44 waste glasses in 90°C using the boron solution analysis. The trend followed is GM11> GM44> ISG.

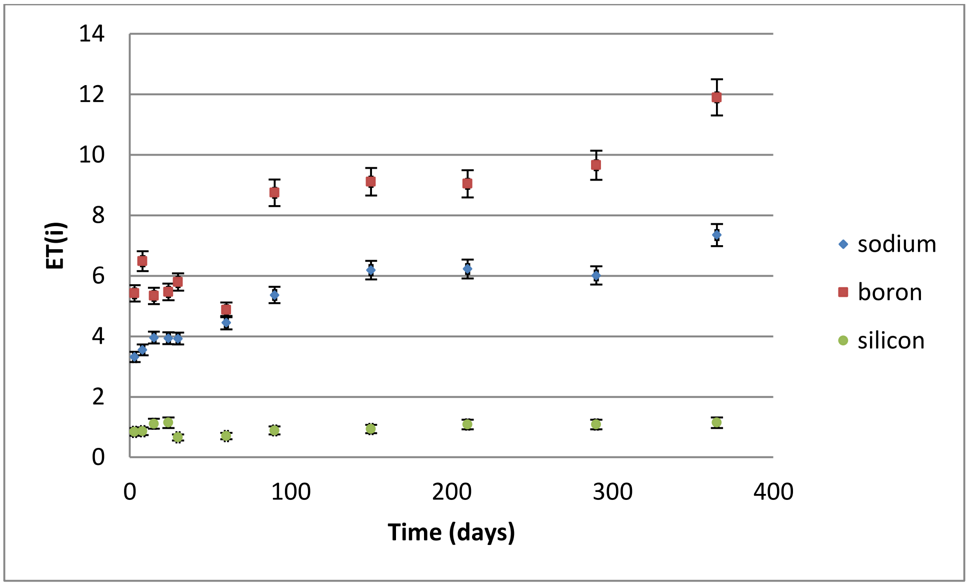

Figure 1.8: Equivalent thickness of different elements of GM11 glass at 90°C

ET for sodium, boron and silicon are compared in above Figure 4.8 for GM11 waste glass. The values for sodium 7.35 µ, boron 11.9 µ and Si 1.14 µ.

4.2.2.3 Alteration rate measurement

The glass alteration rate is calculated from the altered glass thickness as shown in Eq. 11.

$$r = \frac{d(ET_i)}{dt} \ldots\ldots\ldots\ldots\ldots [5]$$

During the initial leaching stage most of the elements are released linearly and congruently at the maximum rate at the given set of conditions controlled by the hydrolysis of the silicate network. The mechanisms during leaching are as shown in the figure below. This maximum dissolution rate (r_o) can be deduced from the slop of the straight line, NL(B)=*f*(t). The residual alteration rate (r_r) also can be calculated from the Eq.11. The results for the glasses are shown in Table 4.3.

Table 1.3: Results of the leaching experiment, r_o is the intial dissolution rate, r_o/r(1yr) is the rate drop, r_r is the residual rate for boron measurements in solution.

Glass	GM11		GM44		ISG	
	DMW	GW	DMW	GW	DMW	GW
r_o(g.m^{-2}.d^{-1})	4.27	5.53	4.5	3.7	1.71	2.06
pH 90°C (1yr)	11.35	11.10	10.33	10.69	10.121	10.216
$r_r(1yr)$(g.m^{-2}.d^{-1})	0.0682	0.0831	0.115	0.0121	0.0435	0.0554
r_o/r (1yr)	62.6	66.55	39.13	39.57	39.31	37.18

Retention factor of element (i) in the alteration products can be easily calculated as follows:

$$RF_i = 1 - \frac{NL_i}{NL_B} \text{.........} \quad [6]$$

Table 1.4: Retention factors, RF_i calculated after 1 year from the solution analysis.

Glass	GM11		GM44		ISG	
	DMW	GW	DMW	GW	DMW	GW
RF_{Si}	0.88	0.87	0.96	0.96	0.83	0.82
RF_{Na}	0.33	0.18	0.42	0.19	0.10	0.01

From the above Table 4.4 it is clear that Si and Na, do participate in the alteration products formed.

4.3 Accelerated leaching tests

For better understanding of leaching, on mechanism and kinetics of corrosion processes associated with borosilicate glasses, leaching studies are done at high temperature and pressure and to avoid the complexity of spectra of waste glasses, only base glasses are chosen for this study.

Accelerated leaching test deals with the investigation of leaching properties and structural changes done in glass samples after leaching if any, under high pressures and temperatures (aggressive test conditions), for sodium borosilicate glass (NBS) i.e. base glass of GM11 waste glass and barium borosilicate glass (BBS) i.e. base glass of GM44 waste glass. The leaching tests are compared with International Standard Glass (ISG). See the detail glass compositions in Table 4.5. The former GM11 (NBS glass) is a candidate for immobilization of nuclear waste from pressurized heavy water reactors and the latter GM44 (BBS glass) for immobilization of thorium containing waste. Till now leaching studies upto 90°C were conducted, it will be of interest to know the leaching behaviour of different types of borosilicate glasses including the ISG under conditions of high temperatures and pressures. Upon subjecting the glass to leaching at 200°C under pressure, both glass dissolution as well as formation of alteration layers of glass gets accelerated, due to the increased reactivity of water molecules with glass. Such type of conditions may not exist in geological repositories. However, with incorporation of waste having high radioactivity, temperature inside the glass may increase significantly, due to decay heat. Also, due to aggressive conditions the alterations can be very fast which may take millions of year to take place which is difficult time frame to measure the in laboratory. The aggressive leaching experiments can be carried out in a laboratory autoclave unit.

Table 1.5: Base glass compositions of glasses under study (mole%)

Name of the compound	GM11	GM44	ISG
SiO_2	47.73	48.16	60.13
B_2O_3	23.87	24.41	15.96
Na_2O	17.04	21.89	12.63
CaO	6.82	--	5.73
Al_2O_3	2.27	--	3.84
TiO_2	2.27		--
BaO	--	5.54	--
ZrO_2	--	--	1.71

4.3.1 Experimental conditions

Leaching experiments were carried out under aggressive test conditions (at 200°C and under a pressure of ~17 bars) in a Teflon-lined autoclave stainless steel pressure vessel as shown in Figure 4.12. For this, initially, the glass samples were crushed to fine power, thoroughly rinsed with water, and sieved through (100 + 200) ASTM mesh to get fine particles having size in the range of 75 to 150 µm. About 2g glass powder was then mixed with 100 mL demineralized water with pH = 6.2, in a Teflon-lined autoclave and heated to 200°C while maintaining a pressure of ~17 bars for different time durations (For each time duration, experiments were started with fresh glass samples). Concentrations of different elements leached out to the solution were determined using an Inductively Coupled Plasma Atomic Emission Spectrometer. Detection limit is 0.05 ppm for each element in presence of other elements.

4.3.2 Solution analysis

The normalized release rate for element i is given as NL_i and expressed in grams of glass waste form dissolved per m^2. The calculation for NL_i is shown in Eq. [1] [8].

$$NL_i = \frac{C_i}{f_i \times \left(\frac{SA}{V}\right) \times t}$$

Where, C_i is concentration of element "i" in the solution, g_i /L

f_i is fraction of element "i" in the unleached waste form (unitless) and

$\frac{SA}{V}$ is the ratio of surface area of the final waste form to the leachate volume, m^2/L. The term "SA" represents surface area of glass powder (cm^2) and V represents leachate volume (L), which is 0.1 L in this study. Duration of leaching is represented by the term "t" with the unit of day.

Normalised leach rate corresponding to different glass constituents from sodium borosilicate glass sample when subjected to leaching in demineralised water (at pH= 7, at 200 °C under a pressure of 17 bar) for different time durations. like 48, 92, and 192 h. The values were calculated from the analysis of leachate solution using ICP-AES. The leach rates are shown in Table 4.6. Initially, the mass loss rate is higher and it decreases with increase in duration of leaching. This may be due to the formation of surface layers (leached layer or passivating layers) which can prevent further loss of glass constituents into solution. Similar observations were also reported by earlier leaching studies on borosilicate glasses [9,10].

Table 1.6: Normalized mass loss rate (normalized release rate).

Time duration	Normalized mass loss rate (g/cm^2.day)			Below Detection Limit
	Na	B	Si	
48h	4.8×10^{-4}	4.3×10^{-4}	7.8×10^{-5}	Ca, Ti, Al
92h	1.9×10^{-4}	4.0×10^{-4}	1.9×10^{-5}	Ca, Ti, Al
192h	1.6×10^{-4}	1.9×10^{-4}	2.6×10^{-5}	Ca, Ti, Al

Normalized release rate based on elements Na, Si, and B present in GM11 glass, GM44 glass, and ISG subjected to leaching for 192 h (at 200°C under a pressure of ~17 bars) are shown in Table 4.7. Uncertainties in the values are found to be less than 3%.

Table 1.7: Normalized mass loss rate for different glasses.

Sample	Surface/vol. ratio (m^{-1})	Normalized mass loss rate (g/cm^2.day)				Elements not detected	pH
		Na	B	Si	Ba		
GM11	426	1.6×10^{-4}	1.9×10^{-4}	2.6×10^{-5}	-	Ca, Ti, Al	9.2
GM44	395	2.6×10^{-4}	1.1×10^{-4}	5.7×10^{-5}	7.21×10^{-7}	-	9.4
ISG	431	2.5×10^{-5}	9.0×10^{-6}	1.0×10^{-5}	-	Ca, Ti, Al, Zr	8.6

For all the three glass samples, mass loss rate for Na and B species are higher than that of Si. For GM11 and GM44 glasses, mass loss rate for Na and B species is found to be an order of magnitude higher than that of ISG. After leaching experiments, pH of the solution has been found to increase as can be seen from Table 4.7. However, extent of increase is lower for ISG compared to other two glasses. One of the reasons for this can be higher SiO_2 and lower Na_2O and B_2O_3 content in ISG compared to other two glasses and presence of ZrO_2 which enhances chemical durability. For silicon, leach rate under aggravated test conditions is found to be comparable for all the three glasses. It is quite possible that during leaching, crystallization can occur from solution due to partial dissolution of glass components in the medium and this crystalline phase can deposit on the surface of glass. Extent of above mentioned types of alterations occurring with glass samples can be determined from concentrations of Na or B species in solution (assuming all Na and B released from the glass are in solution). For example, from the amount of B present in leached solution fraction of altered glass after 192 h of leaching has been calculated[11].

The altered glass fraction was calculated from the earlier equation [9],

$$AG = \frac{m}{m_0 \times f_B} \text{ ....} \qquad [9]$$

Where "m" is the mass of boron in leached solution (100 mL or 0.1 L), "m_0" is the initial mass of glass powder (in grams), and "f_B" is boron mass fraction in the glass (a unit less parameter). The values of altered glass fractions are found to be 0.33 (33%), 0.48 (48%), and 0.015 (1.5%) for GM11 glass, GM44 glass, and ISG, respectively. The values calculated based on Na release is slightly lower (compared to the value calculated based on B release) for GM11 [0.27 (27%)] and GM44 [0.42(42%)] glasses, suggesting that in addition to solution phase, Na must be also existing in a solid phase. From the known value of altered glass fraction (AG) calculated from boron release, altered glass equivalent thickness with respect to the element boron, ET(B), has been obtained based on earlier equations.

4.3.3 Characterization of altered glass

The leached layers of the glass were tested using Techniques like X-Ray Diffraction (XRD), scanning electron microscopy (SEM), solid-state Nuclear Magnetic Resonance (NMR), Differential thermal analyser (DTA), Fourier Transformed Infra-Red Spectroscopy (FTIR), Photoluminescence (PL) spectroscopy have been used to monitor leaching-induced structural modifications and phase formations. The details are discussed in the following sections.

4.3.3.1 Scanning electron microscope

Representative SEM images were recorded corresponding to pristine GM11 and GM44 glasses are shown in the Figure 4.9. From the images it is clear that before leaching, both the glass samples were homogeneous. However, upon leaching, GM11 glass showed crystallization of secondary phase with almost spherical geometry. Leached GM44 glass revealed phases with different morphologies namely flower like, irregular aggregates, small ribbons etc.

4.3.3.2 X-ray Diffraction

XRD patterns were recorded for all the three glass samples before and after leaching and are shown in Figure 4.10. All the three glass samples showed broad peaks characteristic of the amorphous nature, before leaching. XRD of GM11 glass showing sharp peaks at 2ϴ value 12.508°, 17.725°, 28.197° and 33.503° showing presence of crystalline phase of sodium aluminum-silicate ($Na_6Al_6Si_{10}O_{32}$) (Zeolite P) after leaching. However, in the

XRD pattern of GM44 and ISG leached sample, no sharp peaks characteristic of crystalline phase could be seen.

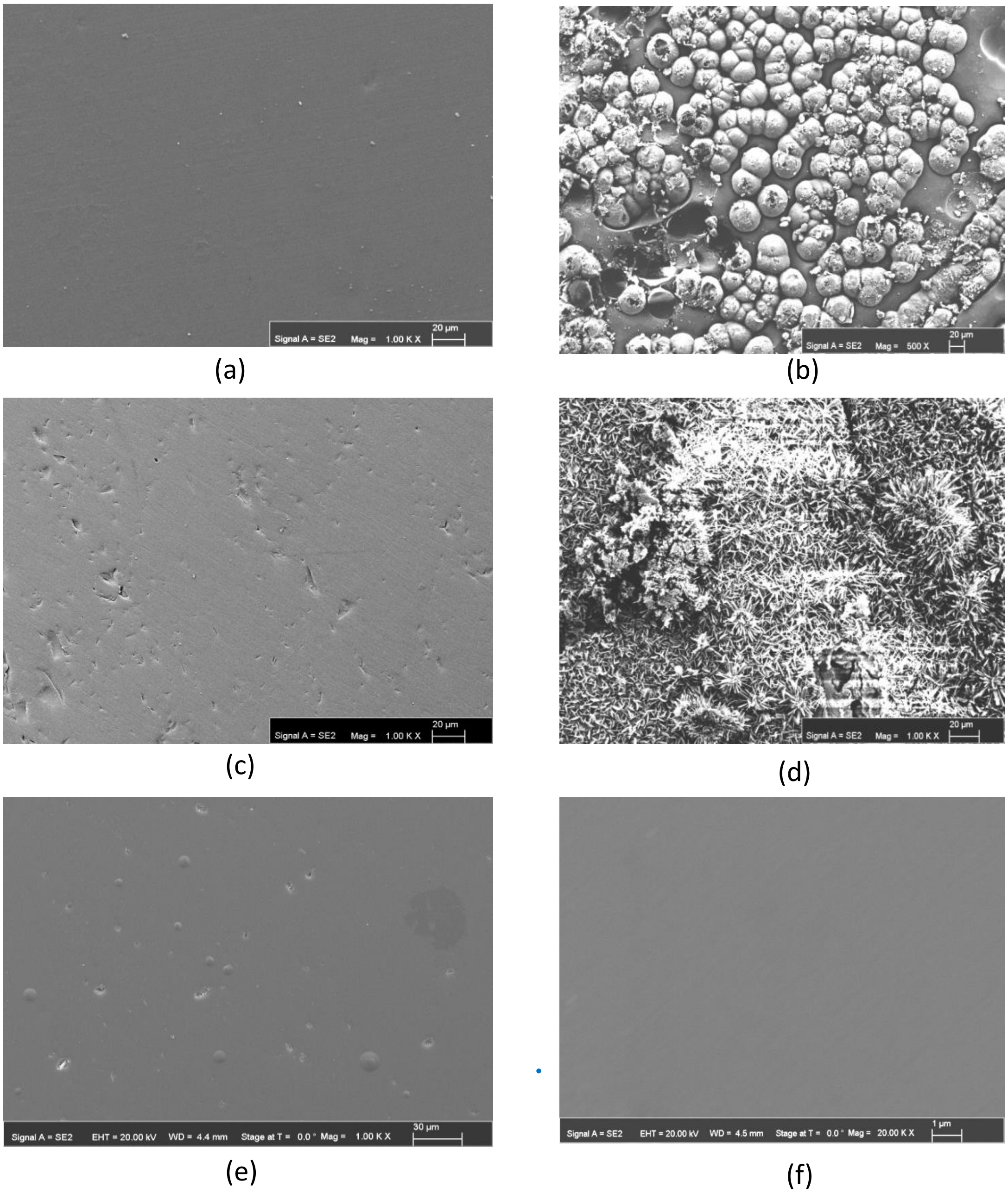

(a) (b)

(c) (d)

(e) (f)

Figure 1.9: SEM images corresponding to (left) before and (right) after leaching of GM11 (a and b), GM44 (c and d) and ISG (e and f) glasses

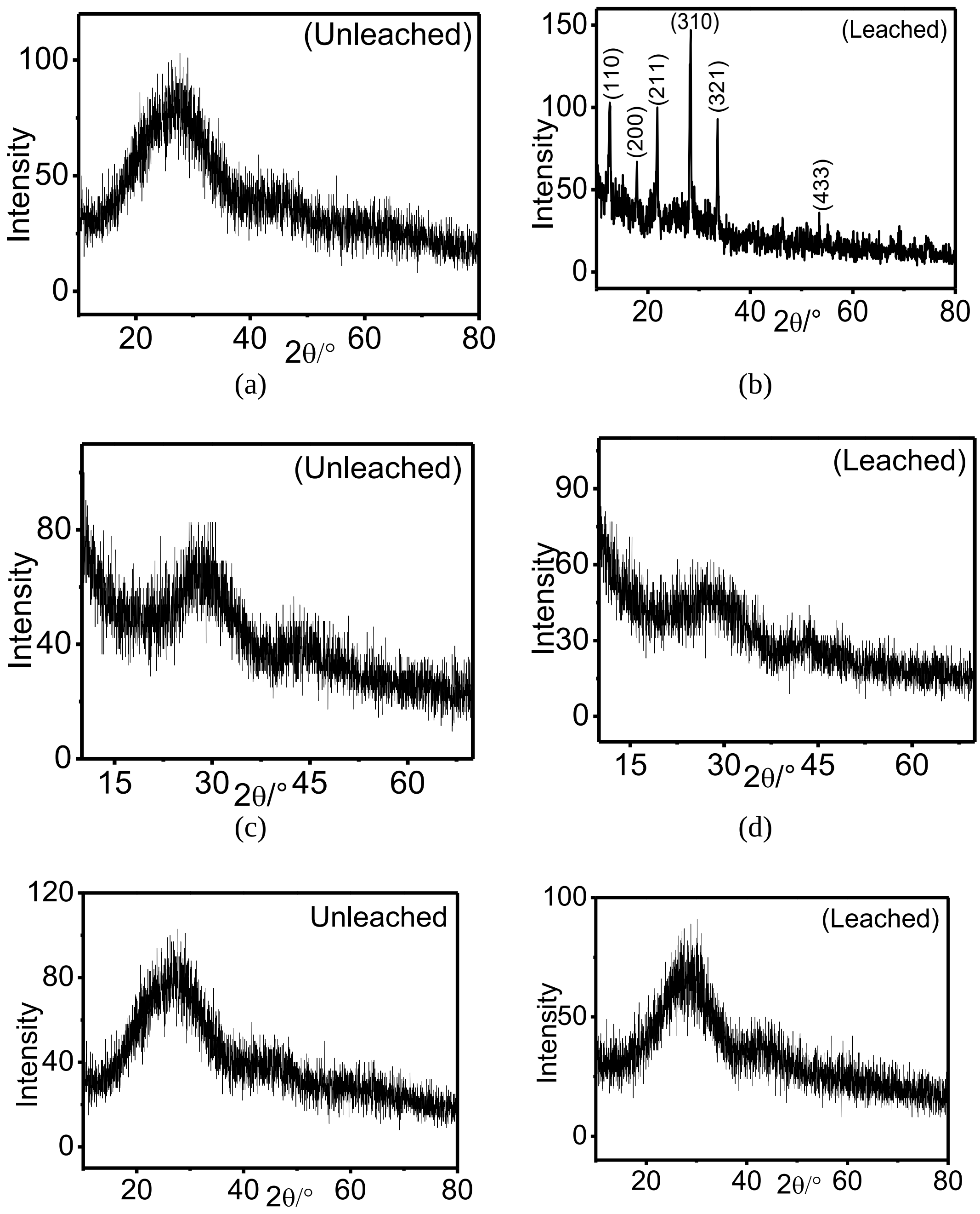

(a) (b) (c) (d) (e) (f)

Figure 1.10: XRD patterns of (left) unleached and (right) leached glass samples of GM11 (a and b), GM44 (c and d) and ISG (e and f).

The reason for the crystalline phase not seen in XRD pattern is due to crystalline phase obtained after the leaching was of a very small fraction and very finely distributed in predominant glassy phase and another reason could be the rough surface generated after leaching, hence sharp peaks corresponding to crystalline phase were not observed in the XRD pattern.

To understand how the structural units constituting the glass change upon leaching, ^{29}Si, ^{27}Al, and ^{11}B MAS NMR studies were carried out on the samples and the results are described below.

4.3.3.3 Nuclear magnetic resonance

^{29}Si, ^{27}Al,^{11}B, and ^{23}Na MAS NMR patterns of these glasses were recorded with a Bruker Avance 400 machine (Rheinstetten, Germany). Powdered samples were packed inside 4 mm zirconia rotors and subjected to a spinning speed of 10 kHz. Typical 90° pulse durations for ^{27}Al, ^{29}Si and ^{11}B nuclei are 3.2, 4.5 and 2.09 μs, respectively with the corresponding delay times of 4, 6 and 2 seconds, respectively. The chemical shift values for ^{27}Al, ^{29}Si and ^{11}B NMR spectra are reported with respect to 0.1M $Al(NO_3)_3$ in water, tetramethylsilane and 0.1M aqueous solution of H_3BO_3 respectively. All ^{11}B NMR patterns were corrected for boron nitride (BN) background arising from Bruker MAS NMR probe. Relative concentration of BO_3 and BO_4 structural units were obtained from fitting ^{11}B MAS NMR patterns after subtracting back ground. The NMR patterns were fitted using WINFIT program supplied by M/S. Bruker Daltonik GmbH, Germany. The details of NMR patterns are discussed in following sections.

4.5.3.3.1 ^{29}Si MAS NMR

Figure 4.11 shows the ^{29}Si MAS NMR patterns of GM11 glass subjected to leaching for different time durations. As prepared glass sample had a broad symmetric peak centered around 93 ppm, arising due to overlapping of mainly Q^3 and Q^2 structural units of silicon with different number of Al as next near neighbors (where Q^n represents silicon structural units with “n” bridging oxygen atoms). Deconvolution of broad peak was not performed as peaks are severely overlapping and significant errors will be associated with peak intensity and area of individual peaks when subjected to deconvolution. As prepared glass sample is subjected to 48 h of leaching and ^{29}Si MAS NMR pattern corresponding to this leached sample is also shown in Figure 4.11. The pattern consists of sharp peaks, with chemical shift values around 98 and 103 ppm, which are superimposed over the broad peak, centered around 93 ppm, indicating the formation of crystalline phase after leaching. With increase in duration of leaching, additional sharp peaks around 93 and 109 ppm started appearing. The relative concentration of crystalline phase increases at the expense of glassy phase with increase in duration of leaching.

This is also clear from relative concentration of glassy and crystalline phases (given in Table 4.8) determined by deconvoluting the NMR spectrum. For all the patterns, line width and peak maximum of both sharp and broad peaks remained same, suggesting that the local environment around Si remain unchanged in both phases with increase in duration of leaching. In other words, in composite sample (containing both glassy and crystalline phases), residual glassy phase has got silicon environment identical with that existing for unleached or pristine glass. The crystalline phase might have formed from the solution containing leached components of glass.

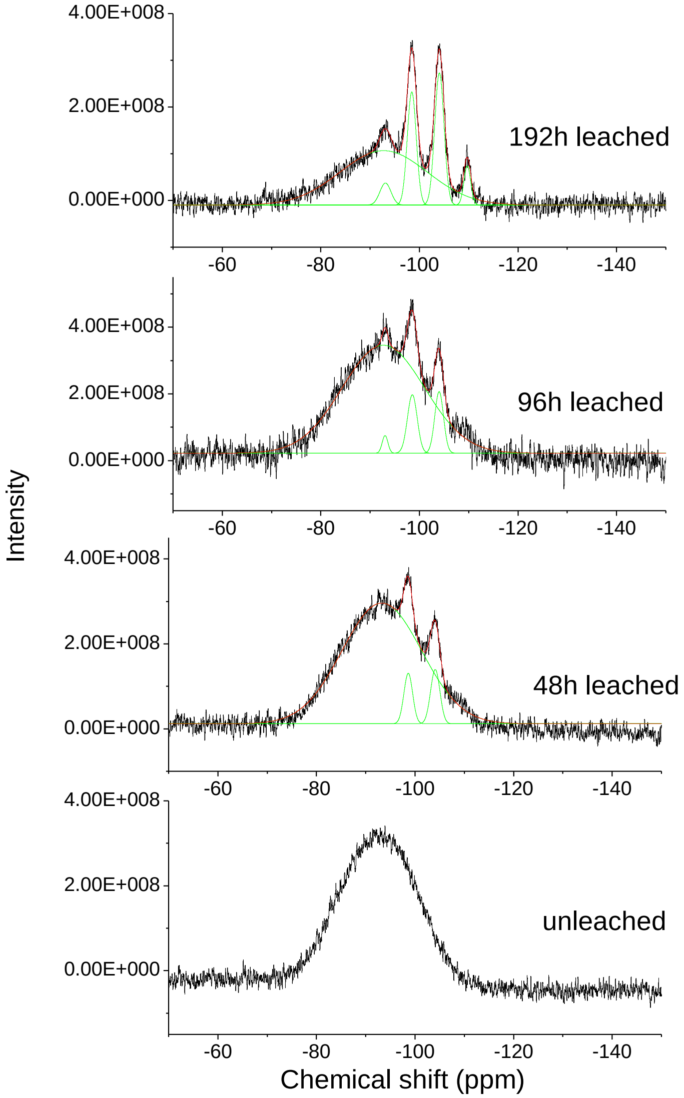

Figure 1.11: ^{29}Si MAS NMR spectrum of GM11 glass subjected to leaching for different time durations. Black color: experimental spectrum, green color: deconvoluted individual Gaussians and red color: overall fit.

Table 1.8: ^{29}Si MAS NMR spectrum of GM11 glass subjected to leaching for different time durations. Black color: experimental spectrum, green color: deconvoluted individual Gaussians and red color: overall fit.

Sample	**Glassy phase (ppm)**	**Crystalline phase (ppm)**				**Glassy : crystalline phase**
Unleached	_92.8(17)	Chemical shift values (line width)				100:0
Leached for 48 h	_93.1(16)	_93.0(2.0)	_98.1(1.7)	_103.0 (1.6)	—	95:05
Leached for 96 h	_93.0(16)	_93.0(1.9)	_98(1.8)	_104.0 (1.9)	—	90:10
Leached for 192 h	_92.7(17)	_93.1(2.1)	_98.2 (1.8)	_104.0 (1.9)	_109 (1.4)	63: 37

Numbers in brackets give line width in ppm (FWHM) of different peaks.

In order to confirm that sharp peaks are not arising due to presence of silicon structural units having OH link-ages, ^{1}H-^{29}Si MAS NMR experiment was carried out for 96 h leached sample (Figure 4.12). Both ^{29}Si MAS and ^{29}Si {^{1}H} CP MAS NMR patterns are identical, confirming that structural units having Si–OH linkages are not present in leached samples. The sharp peaks observed in ^{29}Si MAS NMR patterns are arising from crystalline aluminosilicate phase, namely Zeolite-P with molecular formula $Na_6Al_6Si_{10}O_{32}(H_2O)_{12}$, which is also confirmed by XRD studies discussed earlier. The mineral Zeolite-P is having crankshaft like chain consisting of double four unit rings of (Si, Al)O_4 tetrahedra joined edge to edge by oxygen bridges[12,13] Unit cell of Zeolite-P consists of four different types of Si which are characterized by four sharp peaks around 93, 98, 103, and 109 ppm in the ^{29}Si MAS NMR spectrum. Sharp peaks in the NMR spectrum corresponding to 192 h leached sample in Figure 4.11, match well with that reported Zeolite-P. ^{29}Si MAS NMR and XRD results (discussed above) also confirm that Zeolite-P phase is not getting transformed into Analcime phase, which is a commonly observed phase in leached glass layers of borosilicate glass. It is apparent from the above results that the presence of Al in glass is responsible for formation of aluminosilicate phase. Generally, such aluminosilicate crystals are formed under hydrothermal conditions in an autoclave, an experimental condition which is similar to that employed here.

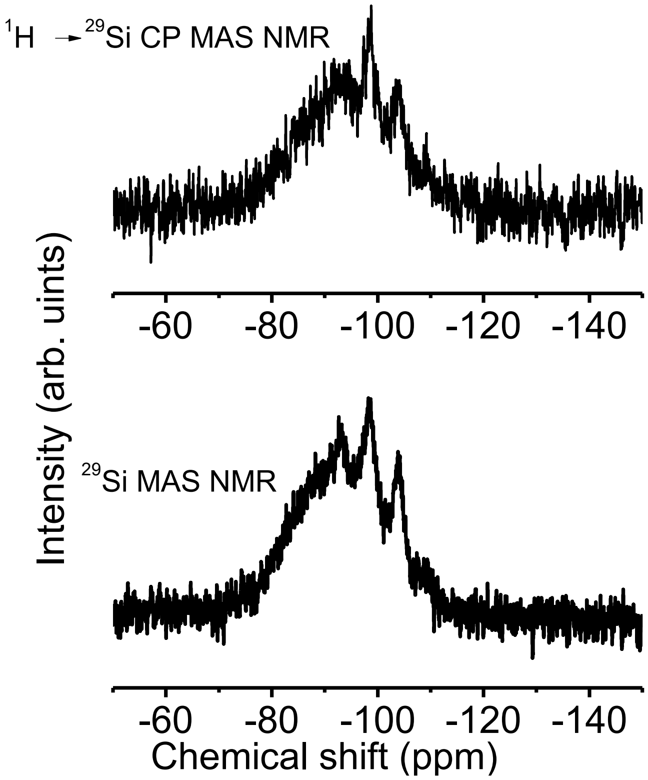

Figure 1.12: 1H→ ^{29}Si CP MAS and ^{29}Si MAS NMR spectrum of sodium borosilicate glass subjected to dynamic leaching for 96 hours.

Figure 4.13 shows ^{29}Si MAS NMR pattern of unleached GM44 glass along with that leached for 192 h. Unleached sample is characterized by a broad asymmetric peak around -90 ppm, arising due to overlapping of peaks corresponding to Q^3, Q^2, and Q^1 structural units of silicon. These peaks are severely overlapping and hence their relative concentration and their chemical shift values could not be determined precisely. For 192 h leached sample, ^{29}Si MAS NMR spectrum is found to change significantly. As well-defined peaks are seen in the spectrum, it was subjected to deconvolution resulting in three peaks with chemical shift values around 111, 105, and 95 ppm, indicating the presence of multiple Si-containing phases in the leached sample. Relatively sharp peaks around 111 and 105 ppm have been attributed to the presence of phases having Q^4 (silica-rich species) and Q^3 structural units of Si, respectively. This must be happening either due to structural reorganization in the glass or due to the formation of multiple silicon containing phases from the components leached out in solution. The broad peak around 95 ppm arises due overlapping of Q^2 and Q^1 structural units present in the residual glass. From these results, it is inferred that, GM44 glass upon leaching, results in the formation of multiple phases along with structurally modified residual glass. These results are further supported by the SEM images which clearly showed ribbon- and flower-like morphologies of materials present in the sample. However, in the XRD pattern of leached sample, no sharp peaks characteristic of crystalline phase could be seen. Lack of Al_2O_3 in the GM44 glass must be the reason for its different structural behaviour upon leaching when compared with NBS glass. It is quite possible that leaching under such high temperature and pressure conditions can also affect boron structural units. In view of this, ^{11}B MAS NMR patterns were recorded and the results are described below.

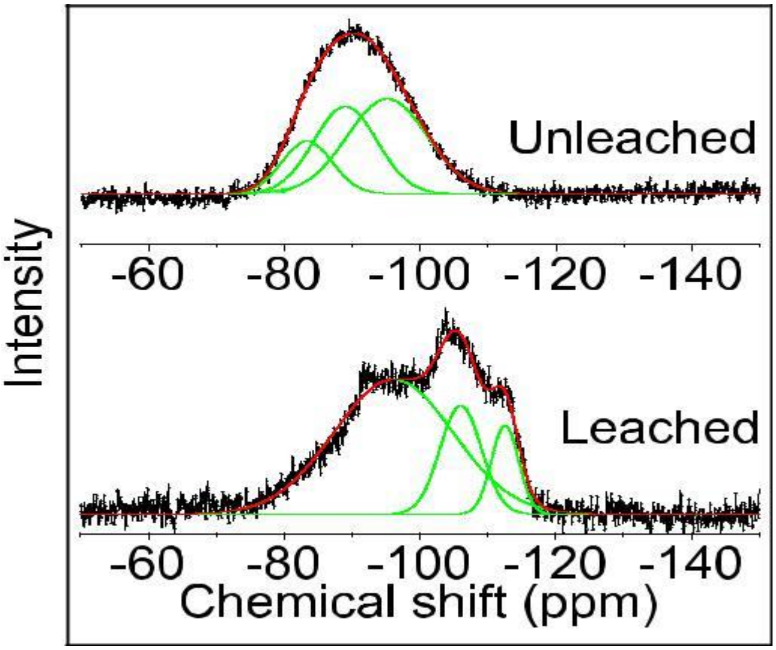

Figure 1.13: ^{29}Si MAS NMR spectrum of unleached and 192 h leached GM44 glass. Black color: experimental spectrum, green color: deconvoluted individual Gaussians and red color: overall fit.

4.5.3.3.2 ^{11}B MAS NMR

Figure 4.14 shows ^{11}B MAS NMR patterns of GM11 glass sample subjected to leaching for different time durations. All the patterns are characterized by a sharp peak around 0 ppm and a broad peak around 14 ppm. The sharp peak has been attributed to boron in tetrahedral configuration and the broad peak to boron in trigonal configuration. Area under broad and sharp peaks has been calculated to determine mole fractions of BO_3 and BO_4 structural units and for unleached sample, values are found to 0.32 and 0.68, respectively, with corresponding quadrapolar coupling constants 2.4 and 0.6 MHz. The values are found to be almost same for glass samples subjected to leaching for different time durations.

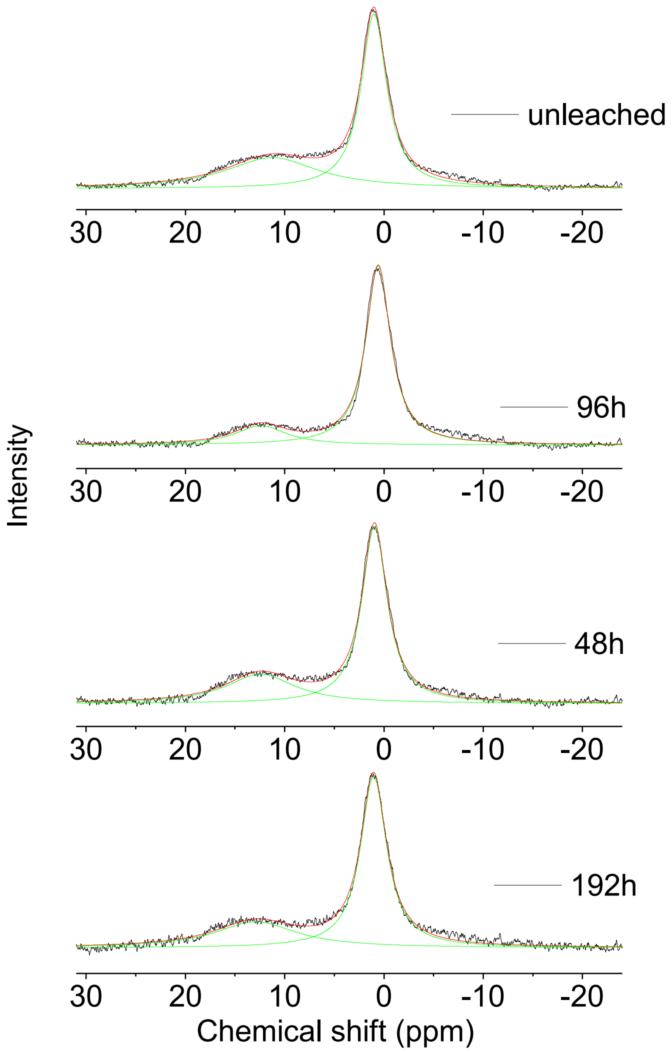

Figure 1.14: ^{11}B MAS NMR spectrum of GM11 glass subjected to leaching for different time durations. Green colour curves represent individual Gaussians and red colour curve represents overall fit.

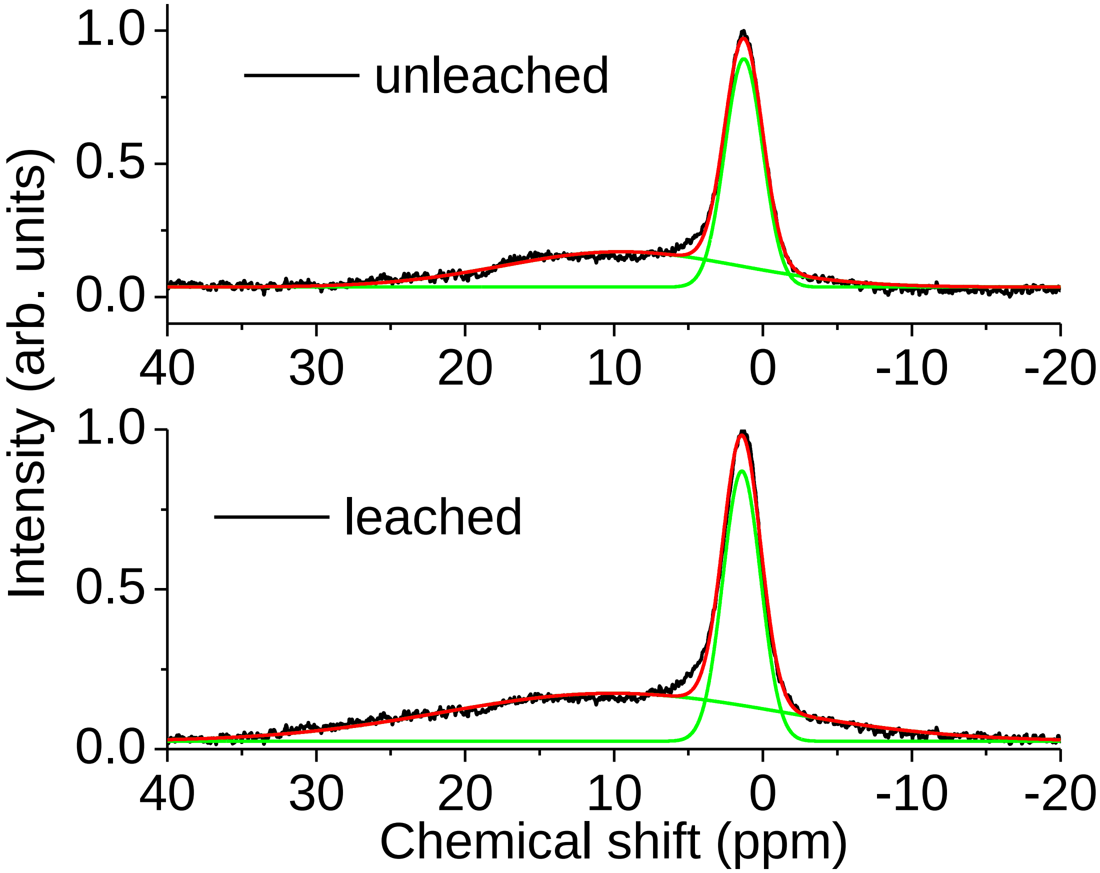

Figure 1.15: ^{11}B MAS NMR spectrum of unleached and 192 h leached GM44 glass.

For unleached GM44 glass also the relative concentration of BO_4 and BO_3 structural units are found to be same as that of GM11 glass (0.67 and 0.33) as can be seen from ^{11}B MAS NMR pattern shown Figure 4.15. Upon leaching for 192 h, relative concentration of BO_4 increases at the expense of BO_3 structural units. The relative concentration of BO_4 and BO_3 structural units are found to be 0.78 and 0.22, respectively. As BO_3 is having trigonal planar geometry, it is susceptible to water attack from both the perpendicular sides of the plane, so this can be the reason that due to leaching BO_3 concentration decreases and BO_4 content increases. The quadrupolar coupling constants are found to be almost same as that observed for NBS glass. All ^{11}B MAS NMR patterns are characteristic of boron structural units in glassy phase. In order understand the changes in local environments around Na and Al (Al is present only in GM11 glass), ^{23}Na and ^{27}Al MASNMR studies were also carried out on the samples and the results are described below.

4.5.3.3.3 ^{23}Na MAS NMR

Figure 4.16 shows ^{23}Na MAS NMR spectra corresponding to unleached, 96 and 192 h leached NBS glass. Unleached sample is characterized by a broad peak around 19 ppm, characteristic of Na ions in an amorphous matrix. However, subjecting the glass for leaching up to 96 h, a sharp peak started appearing around 9 ppm (indicated in the spectrum by drawing an arrow), which became more predominant after leaching the sample to 192 h, based on XRD and ^{29}Si MAS NMR studies discussed above, the sharp peak observed in ^{23}Na MAS NMR patterns (~ 9 ppm) is attributed to Na ions present in crystalline Zeolite-P phase. Further, the peak maximum corresponding to broad peak remains same, as can be seen from the dotted line. In other words, unreacted glass remaining in the leached specimen is having Na environment identical to that in starting glass. ^{23}Na MAS NMR results confirm the presence of both glassy and crystalline phases with GM11 glass. These inferences are further supported by ^{29}Si MAS NMR results discussed earlier.

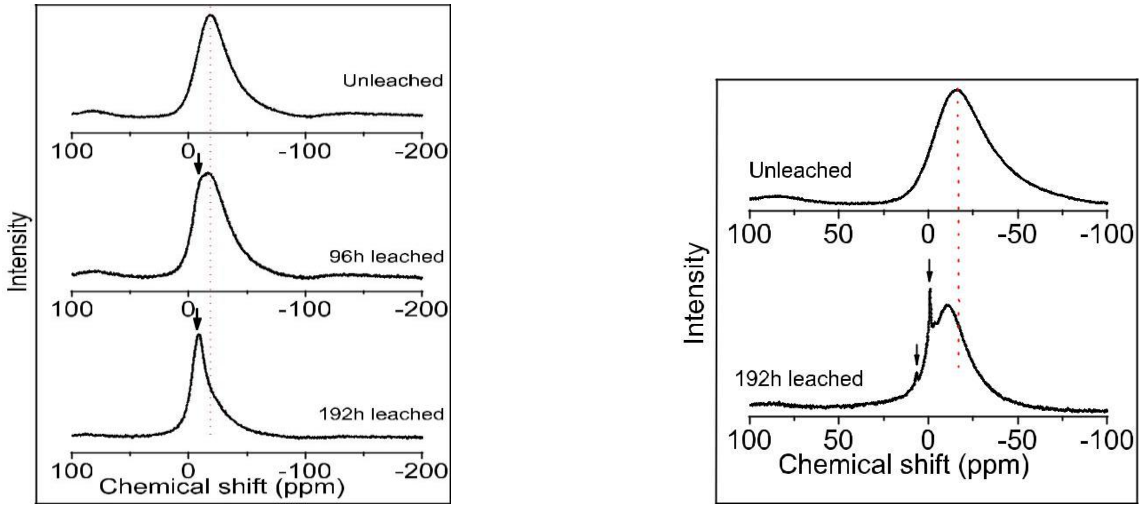

Figure 1.16: ^{23}Na MAS NMR spectrum of GM11 glass subjected to leaching for different time durations and ^{23}Na of GM44 glass

Unleached GM44 glass sample, showed a broad peak around 16 ppm in ^{23}Na MAS NMR spectrum, suggesting wide distribution in bond lengths and bond angles existing around Na^+ ions in the glass sample. However, upon leaching under hydrothermal conditions, sharp peaks around 7 and 1 ppm started appearing (indicated by arrows in the spectrum on Fig. Figure 4 - 1). Further, unlike in GM11 glass, peak maximum corresponding to glassy phase in GM44 glass shifted toward higher chemical shift values after leaching (clear from the dotted line) suggesting that the glass network, and in turn Na^+ environment, changes after leaching. Based on earlier studies [14], it is confirmed that the sharp peaks around 7 and 1 ppm are characteristic of hydrated sodium silicate phases. Possibly due to their low concentration and fine mixing with the amorphous phase, the two phases could not be detected in the corresponding XRD pattern. ^{23}Na MAS NMR studies confirm that natures of crystalline/amorphous phases formed under identical conditions of aggravated testing are different for GM11 and GM44 glasses. This is further confirmed by SEM results discussed earlier, which showed the presence of phases with different morphologies in BBS glass after leaching. Since the phase crystallized from GM11 glass contains Al (as confirmed by XRD and ^{29}Si MAS NMR studies), local environment around Al may also change in the glass with leaching. To confirm this, ^{27}Al MAS NMR patterns were recorded for unleached and leached samples and are described below.

4.5.3.3.4 ^{27}Al MAS NMR

Figure 4.17 shows ^{27}Al MAS NMR patterns of GM11 glass subjected to leaching for different time durations. Unleached sample is characterized by a broad peak around 56 ppm (FWHM = 15 ppm), which is characteristic of Al in tetrahedral configuration existing in the glass network. Glass sample subjected to leaching for 48 h, showed a relatively sharp peak with chemical shift value around 59 ppm (FWHM = 4 ppm) superimposed over a broad peak around 56 ppm (FWHM = 16 ppm). The intensity of sharp peak increased at the expense of broad peak with increase in duration of leaching. The sharp peak (~59 ppm) is arising due to crystalline phase containing Al in tetrahedral configuration. Based on XRD and NMR studies discussed above, the sharp peak has been attributed to Al in crystalline $Na_6Al_6Si_{10}O_{32}12H_2O$ phase formed during leaching.

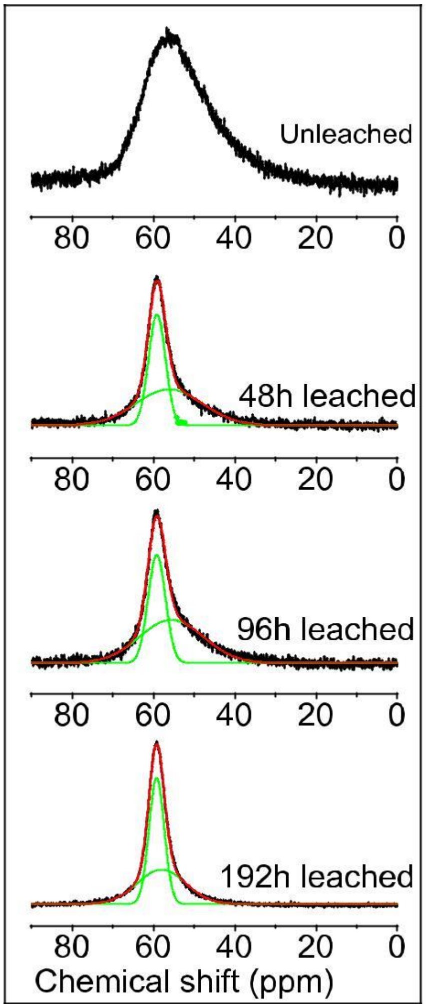

Figure 1.17: ^{27}Al MAS NMR spectrum of GM11 glass subjected to leaching for different time durations. Black color curve represents experimental spectrum, Green color curves represent individual components corresponding to crystalline AlO_4 and amorphous AlO_4 structural units and red color curve represents overall fit.

4.5.3.3.5 NMR studies of ISG glass

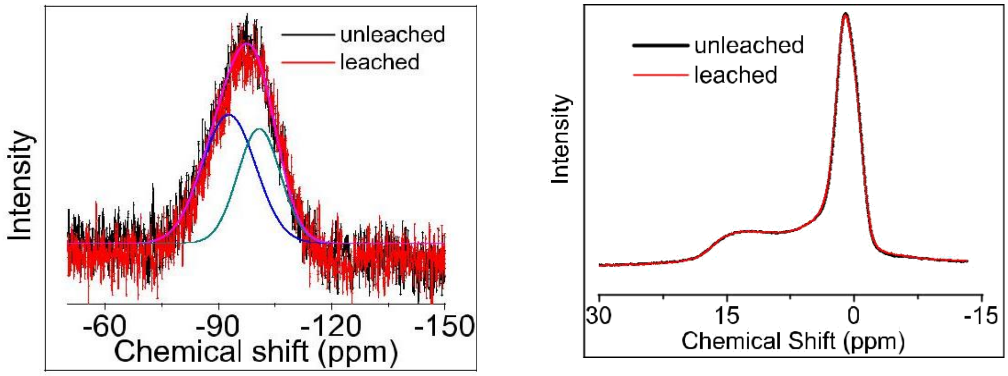

(a) **(b)**

Figure 1.18: (a) Si and (b) B - NMR spectrum of ISG glass

To ascertain whether similar type of crystallization or structural changes are taking place in the case of ISG, ^{29}Si and ^{11}B MAS NMR studies were carried out on ISG sample before and after leaching. In order to see the maximum effect on leaching, NMR studies were carried out for 192 h leached sample. Figure 4.18(a) shows the ^{29}Si MAS NMR spectra for unleached and leached samples. In the case of unleached sample, a broad peak centered round 96 ppm, characteristic of overlapping Q^3 and Q^2 structural units of silicon are observed. Upon leaching, there is no change in ^{29}Si MAS NMR line shape, in terms of peak maximum as well as line width. Similar results are also observed with ^{11}B MAS NMR spectra of leached and unleached samples as can be seen from Figure 4.18(b). Relative concentrations of BO_3 and BO_4 structural units have been calculated and found to be in the ratio 0.39:0.61 for both leached and unleached samples.

4.3.3.4 Differential Thermal Analyser (DTA)

Under aggressive experimental conditions due to the increased reactivity of water molecules significant changes can occur with the glass in short time duration which will be helpful for predicting glass properties (leaching) under normal conditions for long time durations. DTA technique was able to analyse this water reactivity of leached samples.

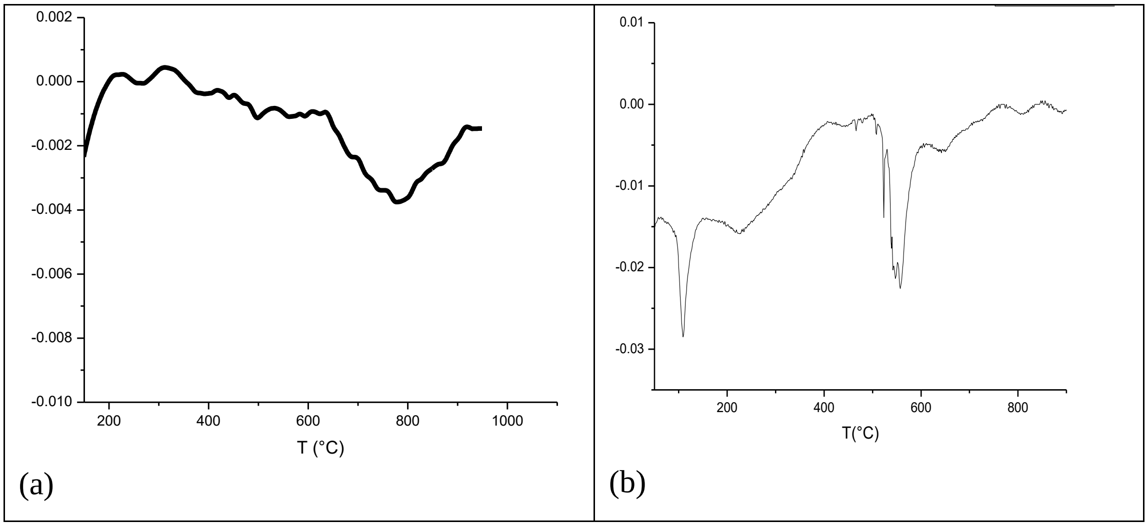

Figure 1.19: DTA patterns of NBS glass pellet before and after leaching

Figure 4.19 shows DTA patterns of GM11 glass pellet before and after leaching. Un-leached sample is characterized by an endothermic peak with an onset around 550°C characteristic of glass transition temperature. Unlike this, the leached NBS glass sample is characterized by three peaks around 100, 220 and 550°C, which have been respectively attributed to the removal of physisorbed water, dehydration of hydroxy boron species (to form boron oxide/borate species) and likely due to melting of some of the borate phase. Unlike GM11 glass of present study, DTA characterization of ISG glass before and after leaching was almost comparable with a glass transition temperature of around 585°C. DTA results also confirm the improved stability of ISG glass against leaching compared to GM11 glass. Drastic changes in DTA pattern of GM11 glass after leaching must be influenced by structural network constituting the glass and this is confirmed by recording FTIR patterns of the glasses. The results are discussed in the following section.

4.3.3.5 Fourier Transform Infra red (FTIR) studies

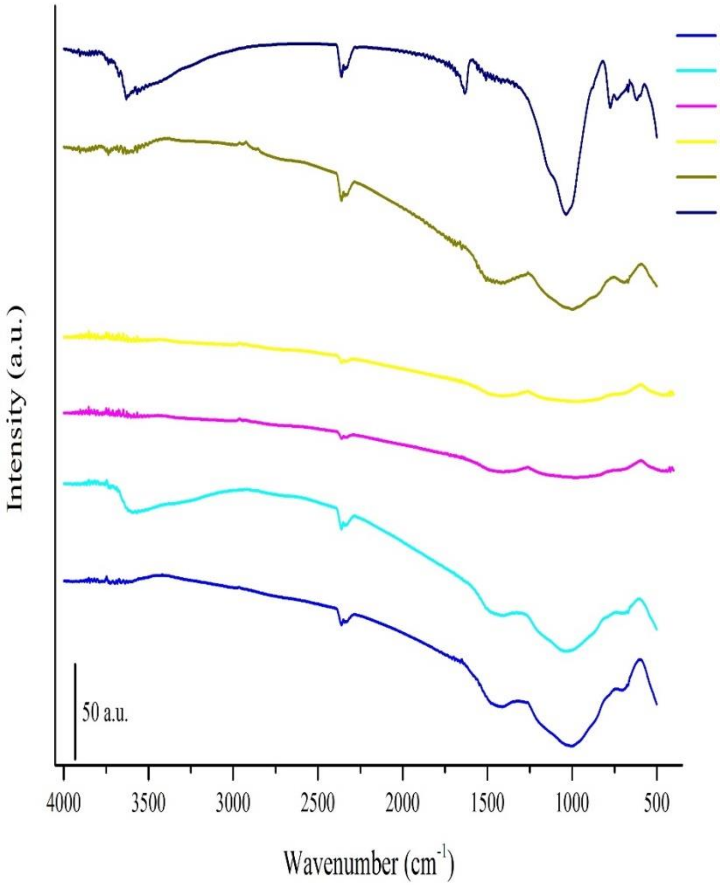

Figure 1.20: FTIR spectrum of GM11, GM44 and ISG glasses before and after leaching

Figure 4.20 shows FTIR spectrum of GM11, GM44 and ISG glasses before and after leaching. All the glass samples are characterized by mainly an intense peak around

1034cm^{-1} along with less intense peak around 1456 and 696 cm^{-1}. For GM11 glass subjected to leaching, line width of the peak at 1034 cm^{-1}decrease significantly, although the peak maximum is nearly same compared to the other glass samples. From earlier studies [15] intense peak around 1034cm^{-1} is attributed to the asymmetric stretching vibrations of Si-O-Si/Si-O-B linkages. Symmetric stretching vibrations corresponding to this mode appears around 696 cm^{-1}. The peak appearing around 1456 cm^{-1} is due to the B-O stretching vibrations of BO3 structural units in the glass. For GM11 glass, there is a significant reduction in the line width corresponding to vibrations of Si-O-Si/Si-O-B linkages up on leaching as can be seen from Figure 4.20. Significant reduction in the line width indicates reduction in strain (disorder) occurring with the glass network. This is possible when the extended borosilicate glass network undergoes. For ISG the line width remained nearly same before and after leaching confirming that the glass network remains unaltered up on leaching. The results confirm that there is considerable reduction in the extent for networking in GM11glass upon leaching. It will be of interesting to know whether such structural changes do have an effect on the photoluminescence properties of the glass samples and the same is used in the following section.

4.3.3.6 Photoluminescence (PL)

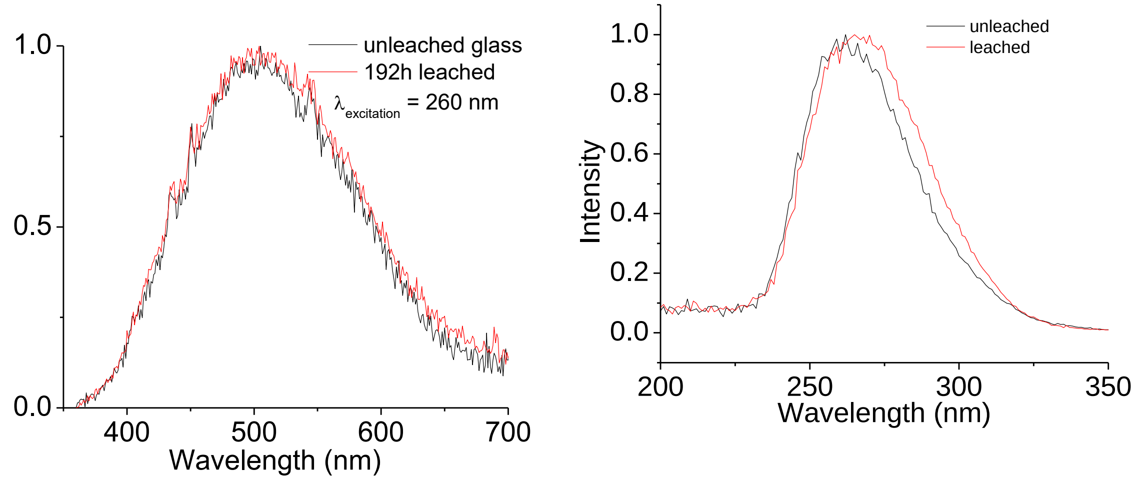

(a) (b)

Figure 1.21: Emission spectrum (a) and excitation spectrum corresponding to 506nm emission (b) from unleached and 192 hours leached GM11 glass.

Figure 4.21 shows emission spectra from GM11 glass before and after leaching under hydrothermal conditions for 192h at 200°C. The emission spectra are identical for leached and un-leached glass samples and are characterized by a broad peak centered around 500 nm with tailing towards higher wavelength region. Corresponding excitation spectrum showed wavelength maximum around 260 nm. Line shapes are similar for both emission and excitation spectra. The high value of Stoke shift indicates that the excited state undergoes strong interaction with local environments in the glass. Further, the excitation spectrum of leached sample is slightly red-shifted with respect to that of unleached sample, which further confirms the interaction in the excited state. Based on the reported luminescence studies of alkali silicate glasses [16], the peak around 500 nm is attributed to recombination of electron and holes associated with localized centers also known as the L-centers present in the glass. The fact that emission spectra is not affected even after leaching, confirms that L-centre does not get modified even under aggravated leach conditions. L-centres arises due to the presence of structural groupings of type Si–O$^-$Na$^+$ and such linkages form localized states in sodium silicate glasses (example of a colour center). The ground state of the L-center corresponds to the ionic bonding between O$^-$and Na$^+$ ions (bonding state) and the excited state is formed by transfer of one electron from the non-bridging oxygen atom to Na$^+$ ion resulting in covalent bonding between Na^0 and O atoms (anti-bonding state). The L-center luminescence in sodium silicate glasses arises due to the transition between anti-bonding and bonding states and is observed in the visible region.

It can be seen in Figure 4.22 that decay is found to be multi exponential, suggesting the variation in the local environment around L-centres present in the samples. Average value of lifetime is found to be 242μs for unleached and 220μs for leached samples. Lifetime values are also characteristic of L-centre emission.

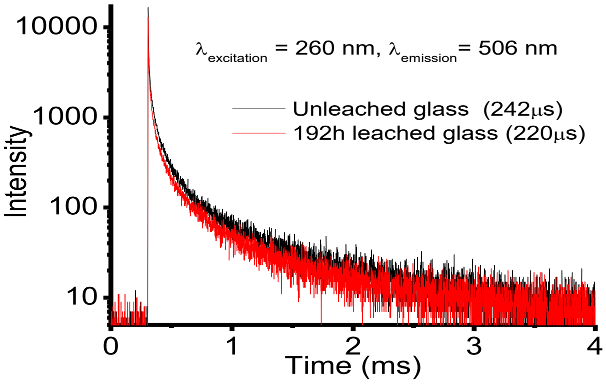

Figure 1.22: Decay curves corresponding to 500 nm emissions from unleached and leached GM11 glass samples.

Figure 4.23 shows emission spectra from ISG before and after leaching. It is observed that the signal to noise ratio of the emission spectra is very poor when compared with that of GM11 glass.

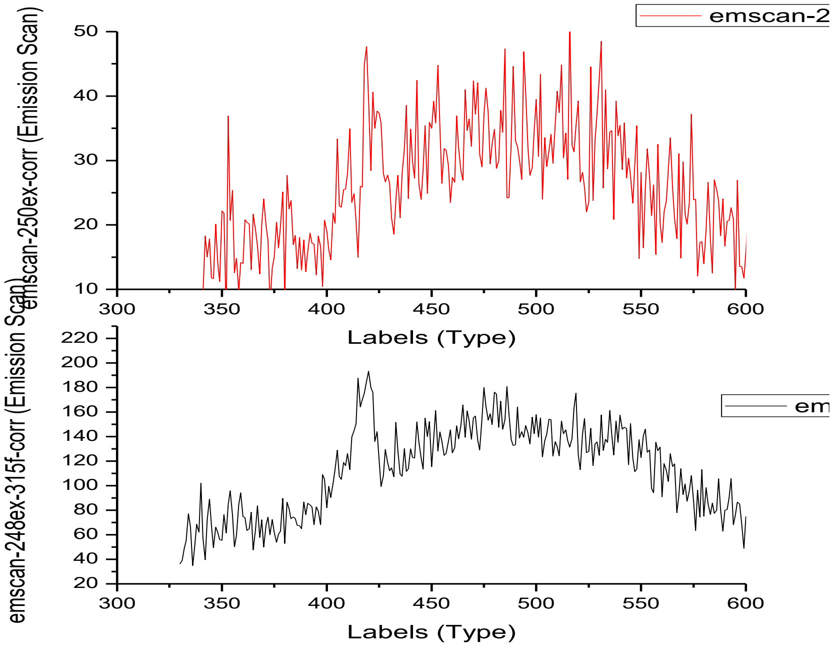

Figure 1.23: Emission spectrum from leached (top) and unleached (bottom) ISG glass samples

4.4 Conclusions

Based on leaching studies under aggressive test conditions and structural studies with XRD, SEM and solid-state NMR techniques, it is concluded that for GM11 glass, formation of aluminosilicate phase, $Na_6Al_6Si_{10}O_{32}12H_2O$, occurs upon leaching leaving the unreacted with the same structure as that of the pristine glass. Unlike this, for GM44 glass, leaching under identical conditions leads to formation of silica-rich species with change in the residual glass structure. From ^{11}B MAS NMR and normalized release rate corresponding to B, it is confirmed that simultaneous dissolution of BO_3 and BO_4 structural units occurs from GM11 glass. For GM44 glass, BO_3 structural units undergo preferential dissolution compared to BO_4 structural units. The International Simple Glass also undergoes alteration under the aggressive test conditions. However, fraction of altered phase is relatively small compared to unaltered glass. Based on XRD, SEM and NMR studies in case of ISG, it is confirmed that the ISG is more resistant to leaching compared to GM11 and GM44 glass compositions that were studied. However, from leach rate table, it is clear that ISG sample also releases different glass constituents in solution. Due to relatively low concentration of altered layers and its fine mixing with unleached glass fraction, changes could not be detected by XRD, SEM, and NMR techniques.

From ^{11}B MAS NMR patterns of GM11 and GM44 glasses as well as from the dissolution rate values, it is inferred that, boron structural units dissolve congruently (stoichiometrically) from GM11 glass (simultaneous dissolution of BO_3 and BO_4 structural units from the glass), whereas BO_3 structural units undergo preferential dissolution in the case of GM44 glass).

From PL studies, the results suggest that localized centers like Si-O$^-$..Na$^+$ are present to a lesser extent in ISG compared to GM11 glass. For the GM11 glass, mole ratio of Na_2O to SiO_2 is 0.356 whereas the value for ISG is 0.209. Higher value of Na_2O/SiO_2 ratio, leads to large number of Si-O$^-$.. Na$^+$ linkages in the glass samples which leads to increased intensity of L-centre emission from the former glass compared to latter. It is interesting to see that emission maximum is nearly same for both the glasses suggesting that the local environment for the L-centre is nearly same in both the glass compositions. As the emission spectra are too noisy for the ISG samples, decay curves could not be recorded from the glass samples.

References

---

[1] Gin S, Jollivet P, Fournier M, Berthon C, Wang Z, et al., “The Fate of Silicon During Glass Corrosion Under Alkaline Conditions: A Mechanistic and Kinetic Study with the International Simple Glass,” Geochim. Cosmochim. Acta, 151 (2015) 68–85.

[2] Pente A.S., “Characterisation of swelling clay minerals for evaluation of their suitability as buffer/backfill material for nuclear waste repository”, PhD thesis (2010) 49.

[3] Organization for Economic Co-operation and Development, Confidence in the long term safety of deep geological repositories. NEA/OECD, Paris, 1999.

[4] Rempe NT, Deep geological repositories. The Geological Society of America, USA, 2008.

[5] International Atomic Energy Agency, Monitoring of geological repositories for high level waste, IAEA-TECDOC-1208 (2001) 25.

[6] Ewing RC, Natural glasses: analogues for radioactive waste forms. In: McCarthy GJ (ed) Scientific basis for nuclear waste management, Plenum, New York, 1 (1979) 57–68.

[7] Scheetz BE, Freeborn WP, Smith DK, Anderson C, M.Zolensky M, White WB, Mater. Res. Proc, 44 (1985)129.

[8] ASTM-C-1285-02. Standard Test Methods for Determining Chemical Durability of Nuclear, Hazardous, and Mixed Waste Glasses and Multiphase Glass Ceramics: The Product Consistency Test (PCT), ASTM International, West Conshohocken, Pennsylvania, 2002.

---

[9]. Iseghem PV, Aertsens M, Gin S, Deneele D, Grambow B, et al., “Glamor - or How We Achieved a Common Understanding on the Decrease of Glass Dissolution Kinetics,” Ceram. Trans., 207 (2009) 115–26.

[10] Vienna JD, Ryan JV, Gin S, and Inagaki Y, “Current Understanding and Remaining Challenges in Modeling Long-Term Degradation of Borosilicate Nuclear Waste Glasses,” Int. J. Appl. Glass Sci., 4 (2013) 283–94.

[11] Rajmohan N, Frugier P, and Gin S “Composition Effects on Synthetic Glass Alteration Mechanisms: Part 1. Experiments,” Chem. Geol., 279 (2010) 106–19.

[12] Khodabandeh S and Davis ME, “Synthesis of a Heulandities Type Zeolite by hydrothermal conversion of zeolite PI”, Chem.Commun, (1996) 1205-6.

[13] Cook HL, “Some aspects of zeolite synthesis”;PhD thesis,University of Edinburgh, 1979.

[14] Koller H, Engelhardt G, kentgens APM and Sauer J, “^{23}Na NMR Spectroscopy of Solids: Interpretation of Quadrupole Interaction Parameters and Chemical Shifts”, J.Phys.Chem., 98 (1994) 1544-51.

[15] Banerjee D, Sudarsan V, Joseph A and Das D, J.Am. ceram. Soc, 933252 (2010)

[16] Iseghem PV, Aertsens M, Gin S, Deneel E D, Grambow B, Strachan D et al, Cream Trans 207 (2009) 115.

Chapter 5 : *Chemical Durability of Leached Natural Analogue*

Chemical Durability of Leached Natural Analogue

5.1 What are natural analogues

Natural analogues for nuclear waste disposal are the geological systems in which processes similar to those expected to be there for the isolation of vitrified waste product (VWP) have been operative for long periods of time. Study of such systems may permit validation of chemical and physical processes demonstrated over short term laboratory experiments. The high level waste is vitrified in glass matrix by the robust way in hot cells where the product formed by the fusion of glass forming materials with high level liquid waste is poured in stainless steel canisters. The vitrified waste products prepared must be homogeneous and stable in time scale of few hundreds of years. The laboratory test methods of leaching are short term methods and so it is difficult to extrapolate the data accurately over large timescales such as 10^4 to 10^5 years. Natural analogues, as the name implies, are naturally occurring glasses of great age that can be analysed to gain understanding of the long term behaviour of synthetic waste forms. Such analogues can provide information which may be able to confirm whether or not the thermodynamic and kinetic models used to extrapolate the short term behaviour of nuclear waste forms are valid within the given timescales involved. The studies are performed on natural analogues as their corrosion takes place in natural environment and that can serve as analogue for the corrosion of VWP which are going to dispose in natural environments. The composition of natural glasses which are studied are shown in following Table 5.1.

Table 1.1: Compositions of natural analogues (wt%)

Composition	**Tektites**	**Rhyolite**	**Volcanic-1**	**Obsidian**	**Basalt**
SiO_2	71.2	73.1	60.5	73.18	50.4
Na_2O	1.5	3.5	2.0	1.43	3.0
K_2O	1.9	4.5	0.4	5.04	1.2
MgO	2.9	1.0	2.6	0.25	10.2
CaO	3.1	2.6	7.5	1.39	8.8
SrO/BaO	-	-	-	0.04	-
TiO_2	0.8	0.2	1.2	0.86	2.2
Cr_2O_3	-	-	-	-	-
MnO	0.1	0.4	0.2	0.09	-
Fe_2O_3/FeO	5.2	2.2	11.5	5.12	11.9
Al_2O_3	12.5	11.9	13.0	12.42	12.2
P_2O_5	-	-	0.2	0.09	-
Others	-	-	0.05ZrO_2 0.03 B_2O_3	-	0.04B_2O_3

5.2 Previous work

Basalt glasses are of volcanic origin, outer surface of volcanic flows when basaltic magmas come in contact with air or water. Basalt glasses are studied extensively as their silica content (50%) is close to nuclear waste glasses [1,2,3] and hence can be used as analogues for borosilicate glasses Man-made archeological glasses were also studied as natural analogues [4] due to their origin of few thousand years and weathering in open nature. Tektites and rhyolites are analogues for high silica containing waste forms (70%) and low alkali containing glasses. Tektites and obsidian also have similar corrosion behaviour such as network hydrolysis, ion exchange and diffusion processes. These processes occur in natural environment of weathering action of water. Tektites are formed by meteoritic impact due to high temperature, soil and rocks formed millions of years back. Barkatt et al [5] conducted dissolution experiments on tektites found that hydrated surface layer gets formed on the surface (0.1µm) along with alteration product magnesium rich, magnesium silicate hydrate gets formed.

Basalt and waste glasses have been found to form similar alteration products when reacted under similar conditions. Laboratory leaching tests on natural and synthetic basaltic glasses on SON68 at temperature 200°C yield similar alteration mechanisms and give similar kinetic results [6]. Initial dissolution rates have same activation energy of 72 KJ/mole and thus similar dissolution mechanism. Measurement of thickness of the altered layer was found to be same. The studies of naturally altered basaltic glass thus gives deeper understanding of the alterations formed and the mechanisms involved. Therefore it can be used to extent the analogy for longer time scales [7]. The studies are done on alteration products produced on natural analogues as these analogues have origin of few millions of years. Hydrothermal alteration studies were done at Lonar lake [8] which is crater formed in basaltic region in India (the 65-million-year-old Deccan trap), the alteration products were found to be saponite, with minor celadonite, and carbonate.

When current kinetic parameters measured in the laboratory are extrapolated to natural system, they predict rates of reactions up to several orders of magnitude faster than those observed in nature [9]. Several reasons for this discrepancy have been proposed.

(1) The glass does not remain in contact with water or are cut off from water flow.

(2) The glass surfaces are poisoned by adsorbed species (e.g. phosphate adsorbed on calcite surfaces drastically reduces its dissolution rate).

(3) Surface layer's form on the mineral surfaces, armor the minerals from further reaction.

5.3 Basalt glass lab experiments

Leaching experiments are done on the basalt glasses. The ASTM product consistency test at 90°C and autoclave test at 200°C procedure as described in chapter 3 is one on basalt glass and the results are as shown in Table 5.2 below.

Table 1.2: Leaching tests done on basalt glass

Sr No	**Leaching conditions**	**SA/V(m^{-1})**	**Na**	**Si**	**Others**
1	ASTM PCT-A test Leachant = DM water Temperature = 90°C Sample type = powder (-100+200 ASTM) Time = 7 days	2000	2.4×10^{-5}	1.07×10^{-5}	BDL
2	Autoclave leaching Leachant = DM water Temperature = 200°C Pressure= 16bar Sample type = powder (-100+200 ASTM) Time = 8 days	440	2.77×10^{-5}	8.67×10^{-6}	BDL

BDL: Below Detection Limit

The altered basalt samples after autoclave high temperature and pressure leaching studies are examined using XRD. The results are as shown in Figure 5.1 below.

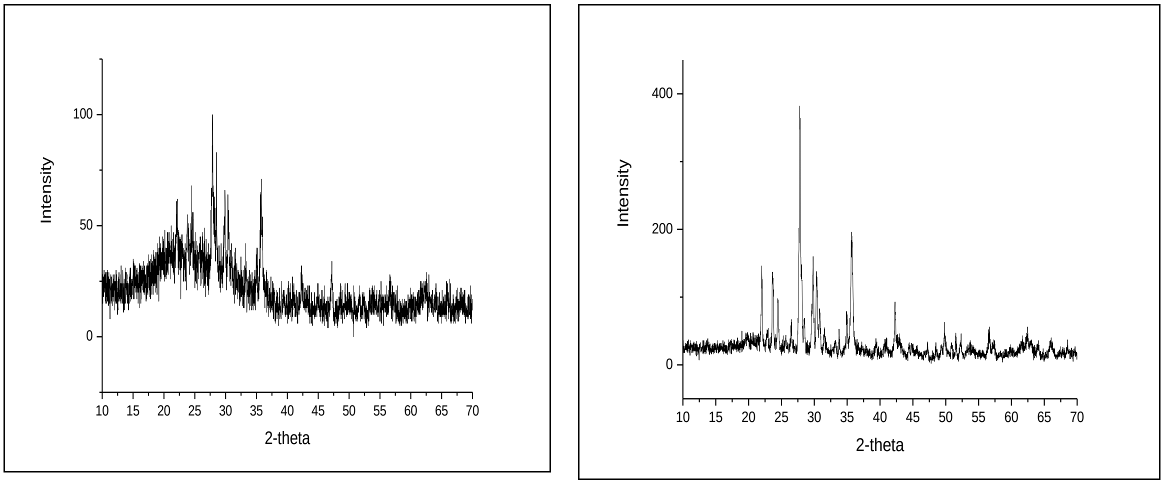

Basalt unleached glass

Basalt leached glass

Figure 1.1: Basalt glass XRD leaching at 200°C temperature and pressure 17 bar

As shown in Figure 5-1, the basalt glass gets further leached under high temperature and pressure.

5.4 Hot spring study

The water springs are observed over earth's surface. The water comes from below earth's surface where water tables are stored. The water springs are categorised based on the temperature which is observed when it touches to earth surface so there are cold springs (<25°C), tepid springs (25°C-34°C), warm springs (34°C-42°C) and hot springs (>42°C). The hot springs are like ordinary springs except they are hot in nature, as they take away heat from earth core. Many hot springs are observed near volcanic activities. The water which touches hot rocks in the earth's crust and emerges out before cooling forms hot springs over the earth surface.

Such geothermal (hot) springs in India are observed in different geological environments and are distributed into seven provinces: Himalaya, Sohana, Cambay, West Coast, Son-Narmada-Tapti (SONATA), Godavari and Mahanadi [10]. In all 18 hot spring areas are spread over the west coast of Maharashtra which is occupied by thick basaltic lava flows [11], these 18 areas contain 60 hot springs.

5.5 Vajreshwari hot springs

The Vajreshwari hot water springs located in the Bhivandi taluka of district Thane in Maharashtra State, India. Vajreshwari is known for its hot water springs and the temple of Goddess Vajreshwari. There are around 21 hot water springs, in a five-kilometer radius of the Vajreshwari temple. The hot springs stretching about 7 km in the bed of the river Tansa are mainly situated at Akloli, Vajreshwari, Ganeshpuri, and Satvalli. The temperature of the water in the springs ranges from 43°C to 49°C. The springs have high sulphur content and are believed to cure many skin ailments.

Vajreshwari is at the foot of Mandakini Mountain, which was formed out of a volcanic eruption and it is this proximity that accounts for the many hot springs in this region. There exist several hot springs here. There are even more hot springs further afield. It is reported that there are around twenty-one hot water springs, just within a five-kilometer radius of the temple. The first one is Akloli Kund, From Vajeshwari one can walk easily to Akloli village, about a kilometre ahead. Then comes Ganeshpuri hot spring, it is about 2 km away from Vajreshwari. Three of the springs are in the bed of the Tansa river, near the temple of Shri Bhimeshvar and they have reservoirs built round them. One of them is called Gorakh Machhindar. Two of the hot springs are in natural hollows in the rock. In

Ganeshpuri village just behind the main temple is a small Shiva shrine with tanks in front that hold the water of some of the hot-water springs. The hot water is temperature is 52°C. Then comes Nimboli, Banganga, and Kalbhon hot springs. As the temperature of the water is near 50°C and the hot water is in contact with basalt glass natural analogue of waste glasses. The water and the altered natural basalt samples are collected from the actual site (see Figure 5.2) and the precipitates are studied to correlate the long term leaching behaviour of VWP.

Figure 1.2: The natural basalt sample from vajreshwari

5.6 Petrographic examination

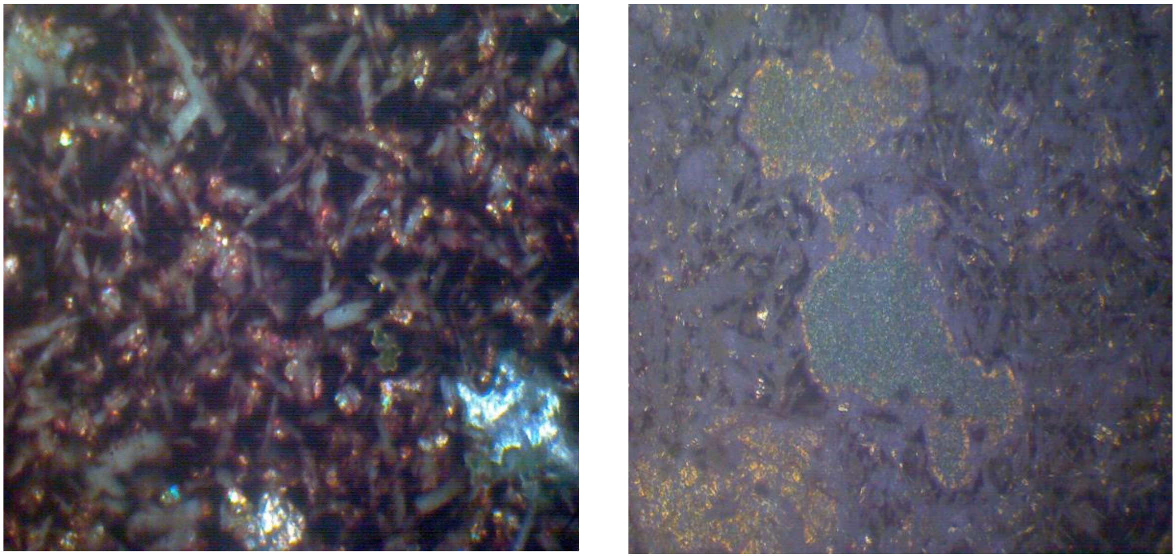

Field of view is 2mm, 4X BCN

Altered glassy basalt showing micro porphyritic texture with amygdales

Field of view is 2mm, 4X BCN

Amygdales filled with fine chert, yellowish glass and having a glassy rim

Figure 1.3: Petrographic examination

The petrographic analysis of vajreshwari leached samples were done (Figure 5-3). It reveals the porphyritic texture, with phenocrysts of plagioclase floating in reddish brown coloured, ferrugionous glassy groundmass. The mineralogical composition consists of pladioclase, clinopyroxene, secondary chalcedony, secondary chert and zeolites. Based on the texture and mineralogical composition, the sample is identified as **Amygdaloidal basalt**.

5.7 XRD examination of natural basalt

As seen from the Figure 5.2 the basalt is already having alterations at the surface in the form of precipitates. The precipitates are studies by XRD (Figure 5.3) and are found to be of sodium aluminum silicate (natrolite) $Na_2Al_2Si_3O_{10}$ $(H_2O)_2$ and aluminum silicate (Mulite)$Al_{(4.56)}Si_{(1.44)}O_{(9.72)}$.

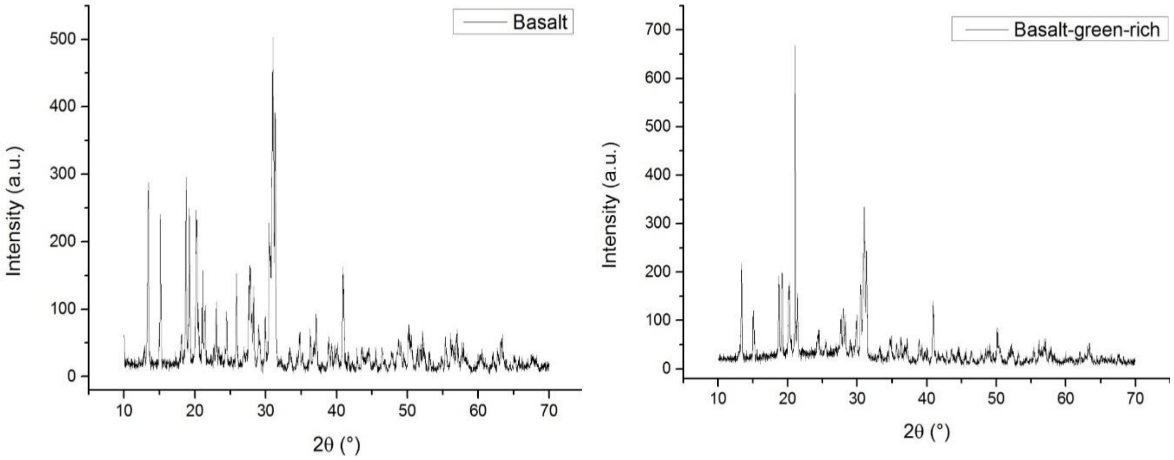

Basalt glass

Basalt glass green phase

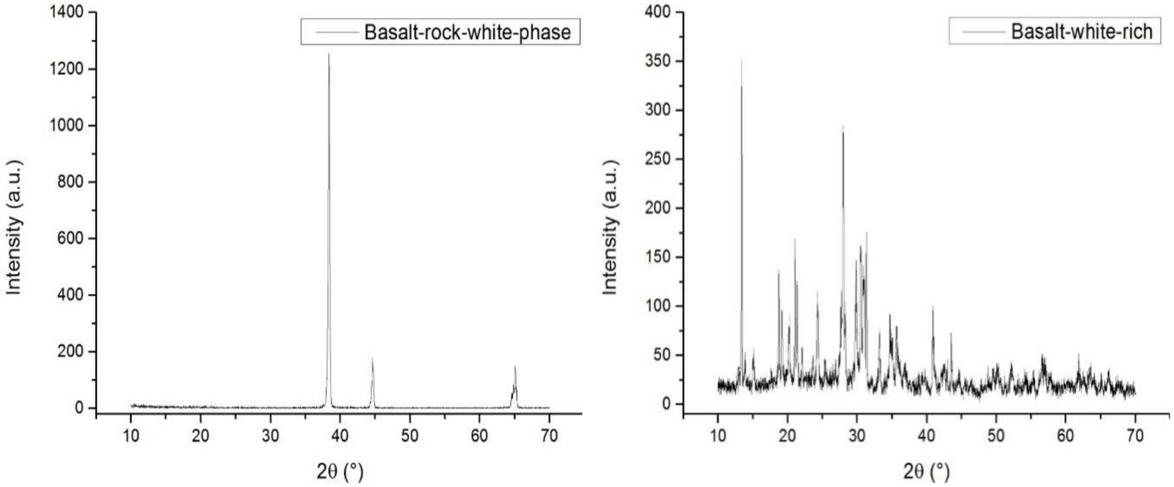

Basalt glass white phase

Basalt glass white phase

Figure 1.4: XRD patters of Vajreshwari basalt glass

5.8 Basalt glass corrosion and naturally altered glass study

The alteration products observed in high temperature and pressure autoclave leaching are somewhat matching with the Vajreshwari sample which is naturally leached under hot water. It shows that the basalt glass altered at hot springs and the basalt glass altered in laboratory at high temperature is giving similar results. The high temperature and pressure results can be extrapolated to get the long term leaching alterations of glass products.

References

---

[1] Ewing et al, Natural glasses: Analogues for radioactive waste forms, Scientific Basis for nuclear waste management Ed, G.J. McCarthy, Plenum Press, New York, (1979) 35-68.

[2] Bates et al, “Waste glass weathering”, Materials Research Society Symposium Proceedings, 333 (1994) 41-54.

[3] Malow, “Alteration effects and leach rates of borosilicate glass implications for the long term stability of nuclear waste form borosilicate glass” Journal of non-crystalline solids, 67 (1984).

[4] Ryan et al, “Glass deterioration in the museum environment” Chemistry and Industry, 5 (1993) 498-501.

[5] Barkatt et al, “Leaching of microtektites, glass compositions in sea water, Advances in ceramic Eds” Clark DE, White WB, Machiels AJ, The Americal Ceramic Society, Westerville,(1986) 661-687.

[6] Isabel Techer, Thierry Advocate, Joel Lancelot, “Basaltic glass: alteration mechanisms and analogy with nuclear waste glasses”, Journal of nuclear materials, volume 282 (2000) 40-46.

[7] Benjamin Parruzot, Patric Jollivet, Diane Rebiscoul, Stephane Gin, "Long term alteration of basaltic glass: Mechanism and rates", Geochimica et Cosmochimica Acta, 154 (2015) 28-48

[8] Hagerty J and Newsom HE, “Hydrothermal alteration at the Lonar impact structure, India: Implications for impact cratering on Mars”, Meteroritics and Plantary Science 38 (2003) 365-381.

[9] Velbel MA, Institute of surface area, surface characteristics an dissolution composition of feldspar weathering rates, Amer. Chem.Soc. Sympo. 323 (1986) 615.

[10] Chandrasekharam.D, Geotheraml resources of India, In IBC Conference, Geothemal Power Asia, Manila, Phillipines, 2000.

---

[11] Ravi Shankar, Status of geothermal exploration in Maharashtra and Madhya Pradesh (Central Region) Geol Surv. India Rec, 115 (1987) 7-29.

Chapter 6 : *Conclusion and Plan of Future Work*

Conclusions and plan of future work

6.1 Glass development work

Sodium borosilicate glass system, containing Al_2O_3 and CaO as additives (GM11 glass) developed for PHWR-HLW and BaO as additive (GM44 glass) was developed for thorium containing high level waste stream. The GM11 and GM44 glasses prepared were characterized for their homogeneity using XRD, SEM/EDS and glass transition temperature using DTA analysis. The glasses prepared were homogeneous in nature. Chemical durability assessment of glasses was done using ASTM (1285-02) PCT test. The leach rate values were comparable with that of International Simple glass (ISG) and natural analogue basalt glass.

6.2 Chemical durability assessment of glasses

Detailed chemical durability assessment of the waste glasses was done using long term leaching study for the duration of one year at three different temperatures viz 50, 70 and 90°C using actual ground water equilibriated with granite powder and clay to simulate repository conditions. Sodium and boron release rates were maximum, then comes silicon. The elemental release rate trend observed is Na~B > Si > Ba> Ca > Al. Leach rates of GM11 and GM44 are higher than ISG. The reason is high silica content of ISG (60 mole%) and also glass formers (75 mole%). Leach rate depends on pH of leaching solution. As alkali metal ion diffuses from the glass to the leachant and is replaced by H_3O^+ ion. Diffusion of the H_3O^+ ion from the water to the glass leaves behind an OH^- ion, which then attacks the silicate structure and increases leaching. The leaching in ground water was slightly more than leaching in demineralised water. Traces of organic materials such as humic acid and tannic acid are often present in actual ground water. These are powerful complexing agents that even in minor quantities can greatly increase leachability, (Therefore use of simulated ground water may give misleading low leachabilities).

For better understanding of the leaching, on mechanism of leaching and kinetics of corrosion products associated with borosilicate glasses, leaching studies were done at high temperature (200^{o}C) and pressures (16bar). The leaching of glass gets accelerated, due to increased reactivity of water molecules with glass. The surface alteration studies it indicates presence of crystalline aluminosilicate (zeolite P) phase forms as alteration product in GM11 glass, which is insoluble phase and further retards leach rate leaving the basic glass structure unaffected. Unlike this, for barium borosilicate glass, GM44, leaching leads to formation of silica rich species with change in the residual glass structure.The alteration products, zeolites, do form in laboratory autoclave leaching studies as well as naturally altered basalt glass with hot springs leaching which are stable for millions of years so the waste glass durability also can be predicted to be stable.

Chemical durability assessments of the selected waste glasses by and large are comparable with ISG and thus are suitable for the immobilisation of high level radioactive waste.

6.3 Comparison with naturally altered basalt glass

The naturally leached basalt glass samples were collected from hot water springs located in Vajreshwari at Bhivandi taluka of district Thane in Maharashtra State, India. The temperature of the hot water was around 50-60 °C and the basalt is leached in the natural environment. The altered phases formed over the basalt were investigated using XRD and were found to be of sodium aluminum silicate (natrolite) $Na_2Al_2Si_3O_{10}$ $(H_2O)_2$ zeolite phase.

Thus, it is seen that after millions of years of continuous leaching zeolite phases do form over basalt glass. These phases are stable and further retards the leach rate. The zeolite phases were formed in nuclear waste glasses as well under aggressive hydrothermal leach test conditions within short test durations in laboratory. Thus, these test conditions can be extrapolated for long term leach durations.

6.4 Future scope

Long term leaching studies of the nuclear waste glasses to be continued for at least three years. Also, long term leaching studies to be done in pellet form to study the altered glass profiling using SEM/EDS to understand mechanism of leaching. To improve the chemical durability, development of new glass systems will be carried out. Dynamic leaching studies of the glasses using soxhlet leaching system can be done, where fresh leachant will be in contact with the glass surface.

Based on the experimental studies carried out in the present investigations, it is felt prudent to develop database on the dependence of elemental leaching on the valence states of polyvalent ions especially actinides, minor actinides and lanthanides. It is proposed to examine the coordination environment using Synchrotron Radiation facility. It is also planned to carry out the study pertaining to damage of glass because of irradiation and its effects on long term chemical durability.